Role of SLC4A11 in Corneal Dystrophies

by

Sampath Kumar Loganathan

A thesis submitted in partial fulfillment of the requirements for the degree of

Doctor of Philosophy

Department of Biochemistry
University of Alberta

ABSTRACT

Congenital hereditary endothelial corneal dystrophy type 2 (CHED2), Harboyan Syndrome (HS) and Fuchs endothelial corneal dystrophy (FECD) are caused by *SLC4A11* mutations. The majority of *SLC4A11* point mutations cause SLC4A11 misfolding and retention in the endoplasmic reticulum (ER). This impairs the ability of SLC4A11 to facilitate water flux across membranes. To develop treatments for the patients with corneal dystrophies caused by *SLC4A11* mutations, we tested the feasibility to rescue misfolded SLC4A11 protein to the plasma membrane as a therapeutic approach. Functional activity assays were carried out in transfected HEK293 cells expressing SLC4A11 variants in combinations representing the state found in CHED2 carriers, CHED2 affected individuals, FECD individuals and unaffected individuals. These cells manifest respectively about 60%, 5%, and 25% of water flux activity, relative to the unaffected (WT alone). ER-retained CHED2 mutant SLC4A11 protein could be rescued to the plasma membrane, where it conferred 25-30% of WT water flux level. Further, cells expressing some ER-retained CHED2 mutants cultured at 30 °C supported increased water flux compared to 37 °C cultures. Caspase activation and cell vitality assays revealed that expression of SLC4A11 mutants in HEK293 cells does not induce cell death. Hence it can be concluded that therapeutics able to increase cell surface localization of ER-retained SLC4A11 mutants hold promise to treat CHED2 and FECD patients. About one third of all reported SLC4A11 mutants are found in the cytoplasmic domain (residues 1-370), indicating an important role in function, yet the role of the cytoplasmic domain is unknown. Interestingly, a catalytically inactive CHED2 mutant R125H resides in the cytoplasmic domain, indicating a role of this domain in SLC4A11

membrane transport activity. While testing the presence of a possible transport pore that transverses through the membrane domain and extends into cytoplasmic domain of SLC4A11, we found that the cytoplasmic domain is essential for the stability of the membrane domain. Fusion of soluble proteins, including green fluorescent protein or mNectarine failed to rescue the SLC4A11 membrane domain to the cell surface. Homology modeling studies show that the SLC4A11 cytoplasmic domain has a similar structural fold as AE1 (SLC4A1) cytoplasmic domain. Fusion of AE1 cytoplasmic domain to SLC4A11 membrane domain assisted the protein in maturing to the cell surface, yet with no functional activity, indicating a role of the cytoplasmic domain in the transport function of SLC4A11. Further, we found that the SLC4A11 cytoplasmic domain and membrane domain specifically associate when co-expressed separately in HEK293 cells. The monomers of SLC4A11 cytoplasmic domain dimerize independently of the membrane domain. Overall, we conclude that the cytoplasmic domain is essential for the function, stabilization and dimerization of SLC4A11 protein.

“I do not know what I may appear to the world, but to myself I seem to have been only like a boy playing on the seashore, and diverting myself in now and then finding a smoother pebble or a prettier shell than ordinary, whilst the great ocean of truth lay all undiscovered before me”.

- Sir Isaac Newton

To Janani and Sivam, who always continue to inspire me.

Also to Jaya, Appa (Dad) and Amma (Mom) for their unconditional support.

ACKNOWLEDGEMENTS

"At times our own light goes out and is rekindled by a spark from another person. Each of us has cause to think with deep gratitude of those who have lighted the flame within us." — Albert Schweitzer

I am thankful to a lot of people that I have known during my Ph.D. studies. I would like to thank my supervisor Dr. Joseph Casey for his continuous support and guidance through out my Ph.D. program. He gave me independence to explore the road less travelled but with focus on the goal and steered me in the right direction. I learned a lot from him and glad to take those lessons with me. It has been a journey that I have been very happy to experience. He is a good mentor, great scientist, and an excellent skier!

I would like to thank my committee members Dr. Ordan Lehmann and Dr. Larry Fliegel for helping me with their valuable guidance. I am happy to know Dr. Todd Alexander who has been a great collaborator and guided me during various times. They are great scientists and I am glad to get their continued support. I would also like to thank Dr. Joachim Deitmer from University of Kaiserslautern, Germany who let me to work in his lab as a part of International Research Training Group in Membrane Biology. I am also thankful to Dr. Nicolas Touret and Dr. Paul M. Schnetkamp for agreeing to be my internal and external examiners. I am glad to get the support of Dr. Rachel Wevrick, Dr. Howard Young, Dr. Emmanuelle Cordat, Dr. Joanne Lemieux, Dr. Yves Sauve and Dr. Richard Fahlmann during various times of my Ph.D.

I am indebted to Dr. Gonzalo Vilas for all the help he provided. He is a great friend who shared my happiness and frustrations and an excellent colleague to work with. I am happy to be friends with Dr. Arghya Basu who taught me the importance of being

patient and I am happy about having a lot of excellent conversations with him. I would like to thank Dr. Pamela Bonar, Jake Mandziuk, Darpan Malhotra who are good friends and colleagues. Thanks to the former lab members Anita Quon, Dr. Danielle Johnson, Phil Quon and Brittany Brown for all the help and support they provided me. I would like to thank Chris Lukowski for all his help and my current lab members Mike Chiu, Nada Alshumaimeri, Katie Badior and Dr. Alka Kumari for their support. I am thankful to the fellow graduate students, staffs and members of Department of Biochemistry and Physiology, members of Membrane Protein Research Disease Group and German colleagues from International Research Training Group in Membrane Biology and Prof. Deitmer's lab. I am unable to mention a lot of names from the department, MPDRG and IRTG group because of limited space. It was a great experience working with all of them and I thank them for their support and for keeping me cheered up.

Special thanks to my friend Sam Joshva for being there whenever I needed. I would like to thank a lot of people who are life long friends from India and Canada for their support, love and affection they showered on me.

I acknowledge the privilege of conducting research at the University of Alberta and thank funding agencies CIHR, NSERC and the unknown Canadian taxpayers.

Special thanks to my parents, grandparents and uncle for their encouragement to follow my dreams and for their indefinite love. Most importantly, I have no words to thank my wife Dr. Jayalakshmi Caliaperumal for her unlimited love and support she showered on me.

Table of Contents

CHAPTER 1: GENERAL INTRODUCTION 1

1.1 THESIS OVERVIEW 2

1.2 HUMAN CORNEA 3

1.3 ANATOMY OF HUMAN CORNEA 3

1.3.1 Epithelium 4

1.3.2 Bowman's membrane 4

1.3.3 Stroma 5

1.3.4 Descemet's membrane 5

1.3.5 Endothelium 6

1.4 CORNEAL TRANSPARENCY AND PHYSIOLOGICAL REGULATION 6

1.4.1 Endothelial pump-leak mechanism 9

1.4.2 Possible models for endothelial pump function 10

1.5 CORNEAL DYSTROPHIES 13

1.5.1 Posterior corneal dystrophies 13

1.5.2 Congenital corneal endothelial dystrophy 13

1.5.3 Fuchs endothelial corneal dystrophy 17

1.5.4 Harboyan syndrome 19

1.6 SLC4A11 MUTATIONS 19

1.7 SLC4 FAMILY OF BICARBONATE TRANSPORTERS 22

1.8 SLC4A11 26

1.8.1 Expression Pattern 26

1.8.2 Structure 27

1.8.3 Oligomerization 28

1.8.4 Function 30

1.8.5 MIP family of Water transporters 32

1.8.6 Mouse models of SLC4A11 34

1.9 THESIS OBJECTIVES 35

1.10 REFERENCES 36

CHAPTER 2: MATERIALS AND METHODS 49
2.1 MATERIALS 50
2.2 DNA CONSTRUCTS 51
2.2.1 Mammalian Expression constructs 51
2.2.2 Bacterial expression constructs 57
2.3 CELL CULTURE 58
2.4 ASSAYS OF OSMOTICALLY DRIVEN WATER FLUX 58
2.5 EXPRESSION OF SLC4A11 CYTOPLASMIC DOMAIN 59
2.6 IMMUNOPRECIPITATION 60
2.7 IMMUNOBLOTS 61
2.8 ENZYMATIC DEGLYCOSYLATION 61
2.9 CELL SURFACE PROCESSING ASSAYS 62
2.10 cDNA SYNTHESIS AND REAL-TIME QUANTITATIVE REVERSE TRANSCRIPTION POLYMERASE CHAIN REACTION (qRT-PCR) 63
2.11 CELL SORTING-BASED VITALITY ASSAYS 63
2.12 STATISTICAL ANALYSIS 64
2.13 REFERENCES 65

CHAPTER 3: CORNEAL DYSTROPHY-CAUSING SLC4A11 MUTANTS: SUITABILITY FOR FOLDING-CORRECTION THERAPY 67
3.1 INTRODUCTION 68
3.2 RESULTS 70
3.2.1 Benchmarks for SLC4A11 functional activity 70
3.2.2 Heterodimerization with R125H-SLC4A11 rescues CHED2-SLC4A11 to the cell surface 80
3.2.3 Co-expression with R125H-SLC4A11 increases cell surface processing of ER-retained CHED2 mutants 85
3.2.4 Some CHED2 mutants are functional when trafficked to the cell surface 86
3.2.5 Increased cell surface processing and functional activity of CHED2-SLC4A11 grown at 30 °C 92
3.2.6 Expression of SLC4A11 mutants does not induce apoptosis or cell death 98

3.3 DISCUSSION 104
3.4 REFERENCES 109

CHAPTER 4: ROLE OF CYTOPLASMIC DOMAIN IN STABILIZATION AND DIMERIZATION OF SLC4A11, A PROTEIN MUTATED IN CORNEAL DYSTROPHIES 114
4.1 INTRODUCTION 115
4.2 RESULTS 117
4.2.1 Role of SLC4A11 cytoplasmic domain 117
4.2.2 GFP and mNectarine fusion proteins to cover hydrophobic surface 122
4.2.3 AE1 cytoplasmic domain and SLC4A11 membrane domain chimera 125
4.2.4 Bacterial over-expression of SLC4A11 cytoplasmic domain 135
4.2.5 Cytoplasmic domain and membrane domain of SLC4A11 strongly associate 138
4.2.6 SLC4A11 cytoplasmic domain dimerizes independently of the membrane domain 142
4.3 DISCUSSION 142
4.3.1 Role of the cytoplasmic domain in SLC4A11 membrane domain stabilization 143
4.3.2. Role of SLC4A11 in membrane transport activity 145
4.3.3 Dimerization of SLC4A11 cytoplasmic domain 148
4.4 CONCLUSIONS 149
4.5 REFERENCES 150

CHAPTER 5: SUMMARY AND FUTURE DIRECTIONS 155
5.1 SUMMARY 156
5.1.1 Rescuing ER-retained SLC4A11 mutants to plasma membrane 156
5.1.2 Role of cytoplasmic domain in SLC4A11 structure and function 157
5.2 FUTURE DIRECTIONS 158
5.3 REFERENCES 163
BIBLIOGRAPHY 168

List of Figures

Figure 1.1 Schematic representation of the human cornea.……...…7

Figure 1.2 The corneal endothelial pump.....14

Figure 1.3 Clinical presentations of FECD and CHED2 patient's eyes.……..…….20

Figure 1.4 Phylogenetic dendrogram of SLC4 family of bicarbonate transporters……...25

Figure 1.5 Topology model of SLC4A11……..29

Figure 1.6 Schematic representation of SLC4A11 and AQP1 in human cornea……...33

Figure 3.1 SLC4A11 expression in transfected HEK293 cells and cornea lysate…….72

Figure 3.2 RT-qPCR to quantify the level of SLC4A11 mRNA in HEK293 cells……...73

Figure 3.3 Representative images of HEK293 cells from water flux assay……..75

Figure 3.4 Osmotically driven water flux in cells expressing CHED2 or FECD SLC4A11 mutants……...77

Figure 3.5 Water flux in cells expressing CHED2 or FECD SLC4A11 mutants……..79

Figure 3.6 Expression of SLC4A11 variants and immunoprecipitation of CHED2 SLC4A11 heterodimers…….....81

Figure 3.7 Association between functionally inactive R125H-SLC4A11 and CHED2-SLC4A11 mutants…….…….83

Figure 3.8 Cell surface processing efficiency of CHED2 mutants of SLC4A11 with or without R125H-SLC4A11…….87

Figure 3.9 Effect of R125H-SLC4A11 on cell surface processing efficiency of CHED2-SLC4A11……...88

Figure 3.10 Osmotically driven water flux in cells expressing ER-retained CHED2 mutants, with or without R125H-SLC4A11……..89

Figure 3.11 Osmotically driven water flux in cells expressing ER-retained CHED2 mutants, with or without R125H-SLC4A11……..91

Figure 3.12 Cell surface processing of SLC4A11 mutants grown at 30 °C……..93

Figure 3.13 Osmotically driven water flux in cells expressing CHED2 SLC4A11 mutants grown at 37 °C and 30 °C……..95

Figure 3.14 Water flux in cells expressing CHED2 SLC4A11 mutants grown at 37 °C and 30 °C……...97

Figure 3.15 Expression of full length Caspase-3 and cleaved Caspase-3……..99

Figure 3.16 Quantification of live and dead HEK293 cells, stably expressing SLC4A11 variants, using flow cytometry……100

Figure 3.17 Cleaved Caspase-3 activity and vitality of HEK293 cells stably expressing SLC4A11 variants……102

Figure 4.1 Substrate translocation pore along the cytoplasmic and membrane domains of dimeric SLC4A11……118

Figure 4.2 Expression and plasma membrane localization of SLC4A11 membrane domain constructs……120

Figure 4.3 Glycosylation state of the various membrane domain constructs of SLC4A11…….....123

Figure 4.4 Expression and plasma membrane localization of enhanced Green fluorescent protein (GFP) and mNectarine protein (mNect) fused variants of MD SLC4A1...…….126

Figure 4.5 Homology modeling of SLC4A11 cytoplasmic domain.....129

Figure 4.6 Phyre2 alignment of SLC4A11 and AE1 cytoplasmic domains.....131

Figure 4.7 Expression, plasma membrane localization and functional activity of AE1 cytoplasmic domain (CD-AE1) fused to MD-SLC4A11.....133

Figure 4.8 Bacterial expression of SLC4A11 cytoplasmic domain.....136

Figure 4.9 Association between SLC4A11 cytoplasmic and membrane domains.....139

Figure 4.10 Association of SLC4A11 cytoplasmic and membrane domains.....140

Figure 4.11 SLC4A11 cytoplasmic domains are dimeric.....141

Figure 4.12 Possible salt bridges on the SLC4A11 cytoplasmic domain homology model.....…….. 147

List of Tables

Table 1.1 List of corneal dystrophies associated with different layers of cornea……..…15

Table 1.2 List of all reported SLC4A11 point mutations…….…..23

Table 1.3 Tissue distribution and Transport mechanisms of SLC4 family of bicarbonate transporters…….…....24

Table 2.1 Oligonucleotides used in cloning of WT, membrane domain and cytosolic domain variants of SLC4A11 and AE1……..…52

Table 2.2 Mutagenic oligonucleotides to clone CHED2/FECD/HS *SLC4A11* point mutations……....54

Table 2.3 Oligonucleotides used in cloning of GFP, mNectarine and AE1 cytoplasmic domain fusion variants of SLC4A11…….……55

List of Abbreviations

AE1; Cl^-/HCO_3^- anion exchanger

AE1-MD; AE1 membrane domain

AQP1; Aquaporin 1

BCA; bicinchoninic acid

cDNA; complementary deoxyribonucleic acid

CD-AE1; cytoplasmic domain of AE1

CD-SLC4A11; cytoplasmic domain of SLC4A11

CHED2; congenital hereditary endothelial dystrophy type 2

DMEM; Dulbecco's modified Eagle media

DMSO; dimethyl sulfoxide

DNA; deoxyribonucleic acid

EDTA; ethylenediaminetetraacetic acid

Endo H; Endoglycosidase H

ER; endoplasmic reticulum

FACS; Fluorescence-activated cell sorting

FECD; Fuchs endothelial corneal dystrophy

GAPDH; glyceraldehyde 3-phosphate dehydrogenase

GFP; green fluorescent protein

GST; glutathione S-transferase

IP; Immunoprecipitation

HA; hemagglutinin

HEK293 cells; human embryonic kidney 293 cells

HEPES; 4-(2-hydroxyethyl)-1-piperazineethanesulfonic acid

HRP; horseradish peroxidase

HS; Harboyan syndrome

IPTG; isopropyl β-D-1-thiogalactopyranoside

MD-SLC4A11; Membrane domain of SLC4A11

MIP; Major intrinsic protein

mNect; mNectarine

Myc; Myc epitope tag

NI; non-immune serum

PCR; polymerase chain reaction

PNGase F; Peptide-N-glycosidase F

PHYRE2; Protein Homology/AnalogY Recognition Engine 2

SDS; sodium dodecyl sulfate

SDS-PAGE; sodium dodecyl sulfate polyacrylamide gel electrophoresis

SEM; standard error of mean

SLC; solute carrier

SLC4A11; solute carrier family 4 member 11

SNSB; N-Hydroxysulfosuccinimide -SS-Biotin

T; total

TEV; tobacco etch virus protease

U; unbound

UV; ultraviolet

WT; wild-type

Chapter 1: General Introduction

1.1 Thesis Overview

The objective of this thesis is to explore the role of a membrane protein, SLC4A11, in corneal eye diseases. Mutations in *SLC4A11* gene cause three distinct posterior corneal dystrophies. As a result of point mutations, SLC4A11 protein is either retained in the endoplasmic reticulum (ER) or catalytically inactive. We tested whether the ER-retained mutants can be rescued to the plasma membrane surface and if rescued, whether they are functional? Several approaches were also used to examine the transport mechanism and structure of SLC4A11 cytoplasmic domain.

SLC4A11 is widely expressed in human tissues, including cornea, kidney, salivary gland, testis, thyroid and trachea [1-3]. The focus of the thesis is on human cornea and the introduction begins with a brief description of the human eye, with emphasis on cornea in detail. To understand the physiological role of SLC4A11 in corneal dystrophies, a large part of the introduction discusses physiological regulation of corneal transparency and the symptoms and effects of some of the posterior corneal dystrophies on human vision. The introductory chapter then continues with details about SLC4A11 mutations and the SLC4 family of bicarbonate transporters. The expression, topological structure and oligomerization of SLC4A11 are then discussed to highlight the importance of SLC4A11 and its role in causing both dominant and recessive corneal diseases. To underscore the physiological significance of SLC4A11 in corneal transparency, the function of SLC4A11 is closely examined. The introductory chapter concludes with a discussion of knock-out mouse models of SLC4A11 that recapitulate the key aspects of human corneal dystrophies.

1.2 Human Cornea

The human eye is one of the most complex organs of the body; vision, a function, which the eye supports, is also a complicated process. The eye has three main layers; the outer layer consists of the transparent cornea and opaque sclera. The middle layer, called the uvea, is made up of the choroid, the ciliary body and the iris. The inner layer consists of retina, the sensory part of the eye (Inset, Fig. 1.1) [4]. Of all the ocular structures, cornea, being placed in front of the eye, has the greatest number of encounters with the environment and hence acts as the primary infectious and structural barrier of the eye. Cornea is the principal refractive element in the eye, contributing ~45 diopters of the total ~60 diopters of unaccommodated ocular power [5].

1.3 Anatomy of Human Cornea

"*About the size of a postage stamp and less than half the thickness of a United States dime, the human cornea is one of the marvels of the human body. Transparent and refractive, it offers us a clear view of the world around us while protecting the delicate contents of the human visual system*" [6].

Human cornea is transparent, avascular and mostly aspheric in shape at the macroscopic scale, however, different ocular dimensions exists in the normal population [5]. Variations in corneal shape arise from the intrinsic biomechanical structure and extrinsic environment of cornea. Anatomically, cornea is approximately 520 μm thick at the center and it can reach 650 μm at the periphery [7]. When examined closely, human cornea is made up of five different layers: three cellular layers (epithelium, stroma and

endothelium) and two interface layers (Bowman's membrane and Descemet's membrane) (Fig. 1.1) [6].

1.3.1 Epithelium

The first barrier between the outside environment and inner cornea is the epithelial cell layer. It is composed of non-keratinized, stratified squamous epithelium that is 4 to 6 cell layers thick (40 μm to 50 μm) [8] and firmly attached to the underlying stroma. The corneal epithelium is covered with a tear film, which supplies immunological and growth factors that are critical for epithelial health, proliferation, and repair [6]. The air–tear film interface, together with the underlying cornea, provides two thirds of the total refractive power of the eye [6]. The underlying basal layer of the epithelium consists of stem cells [9], which are important for the regenerative abilities of corneal epithelium. This is a very important differentiating factor when compared to corneal endothelium, which does not have such regenerative capabilities. Interestingly, corneal epithelial cells have an average lifespan of 7 to 10 days and the epithelial surface continually sheds cells to the environment. This strategy obstructs the progress of pathogens into underlying stroma, which is relatively immuno-deficient [5].

1.3.2 Bowman's membrane

Bowman's membrane (or Bowman's layer) is located immediately posterior to the corneal epithelium and it is not a true membrane. It is an acellular condensate of the most anterior portion of the stroma [10]. Bowman's membrane is approximately 15 μm thick and structurally composed of collagen fibrils, smaller in diameter and randomly oriented. It helps the cornea to maintain its shape and serves as a barrier that protects the corneal

stroma from traumatic injury. When disrupted, it will not regenerate and can form a scar [11].

1.3.3 Stroma

The corneal stroma is an important structural and optical component of human cornea and comprises roughly 80% to 85% of human corneal thickness [12]. Keratocytes are the only cell types found in stroma and are responsible for synthesizing collagen and extracellular matrix of stroma. Corneal stroma is mostly made of collagen fibrils bound by proteoglycans and extracellular matrix arranged in a precise architecture. The major collagen of the stroma is collagen type I, but collagen type V is also required to initiate assembly of this collagen into fibrils [13]. The collagen fibrils are packed in parallel layers called lamellae and the human stroma contains 200 to 250 distinct lamellae. Anatomically, collagen fibrils are highly mono-disperse in diameter (30.8 ± 0.8 nm) and arranged in a pseudohexagonal lattice with ~ 60 nm uniform inter-fibrillar spacing [5]. This precise organization of stroma facilitates corneal transparency and gives the ability for the human cornea to transmit approximately 95% of incident light [5, 12, 14].

1.3.4 Descemet's membrane

Immediately beneath the stroma is Descemet's membrane, which has an amorphous structure [6]. It is secreted by the underlying endothelial cell layer and can accumulate up to 10 μm in thickness with age [8]. The anterior 3 μm, secreted prior to birth, has a distinctive banded appearance when viewed by electron microscopy, but Descemet's membrane produced after birth is unbanded [6]. Descemet's membrane separates the stroma and endothelium and forms an adhesive layer between them. It is important for the health of endothelial cells as they provide a surface for the endothelial

cells to attach [6]. Descemet's membrane injury and detachment is a serious complication that has the potential to lead to significant endothelial cell loss in some cases [6].

1.3.5 Endothelium

The corneal endothelium is a monolayer of approximately 400,000 avascular cells arranged in a hexagonal mosaic shape and up to 4-6 μm in thickness [15]. A human endothelial cell measures 5 μm in height, between 18 and 20 μm in width and has a round nucleus of 7 μm in diameter [9]. Endothelium maintains the nutrition of the corneal cells and keeps the stroma properly dehydrated [16]. At birth, the typical corneal endothelial cell density is 7500 cells/mm^2 and it declines with age at rate of 0.6% per year, as the endothelial cells are arrested in G1 phase of cell cycle and do not regenerate [5, 17]. Any damage or other environmental stress that causes endothelial cell loss is compensated by polymegathism (enlargement of cells) and pleomorphism (alteration in shape or size) of the surrounding cells [15]. However, there is a limit to this compensatory ability of the endothelium. Any substantial loss of cells can lead to corneal swelling, opacity and blindness [16]. Hence endothelial function is critical for maintaining relatively dehydrated state of stroma and overall transparency of cornea [16]. SLC4A11 protein, which is the focus of this thesis, is localized to the basolateral side of the corneal endothelium [1] and critical for regulating corneal transparency. Sections 1.4-1.8 will describe the SLC4A11 protein and its role in corneal diseases in detail.

1.4 Corneal Transparency and Physiological Regulation

Cornea is the major refractive element of the human eye and maintaining the corneal transparency by strict physiological regulation is essential for acute vision.

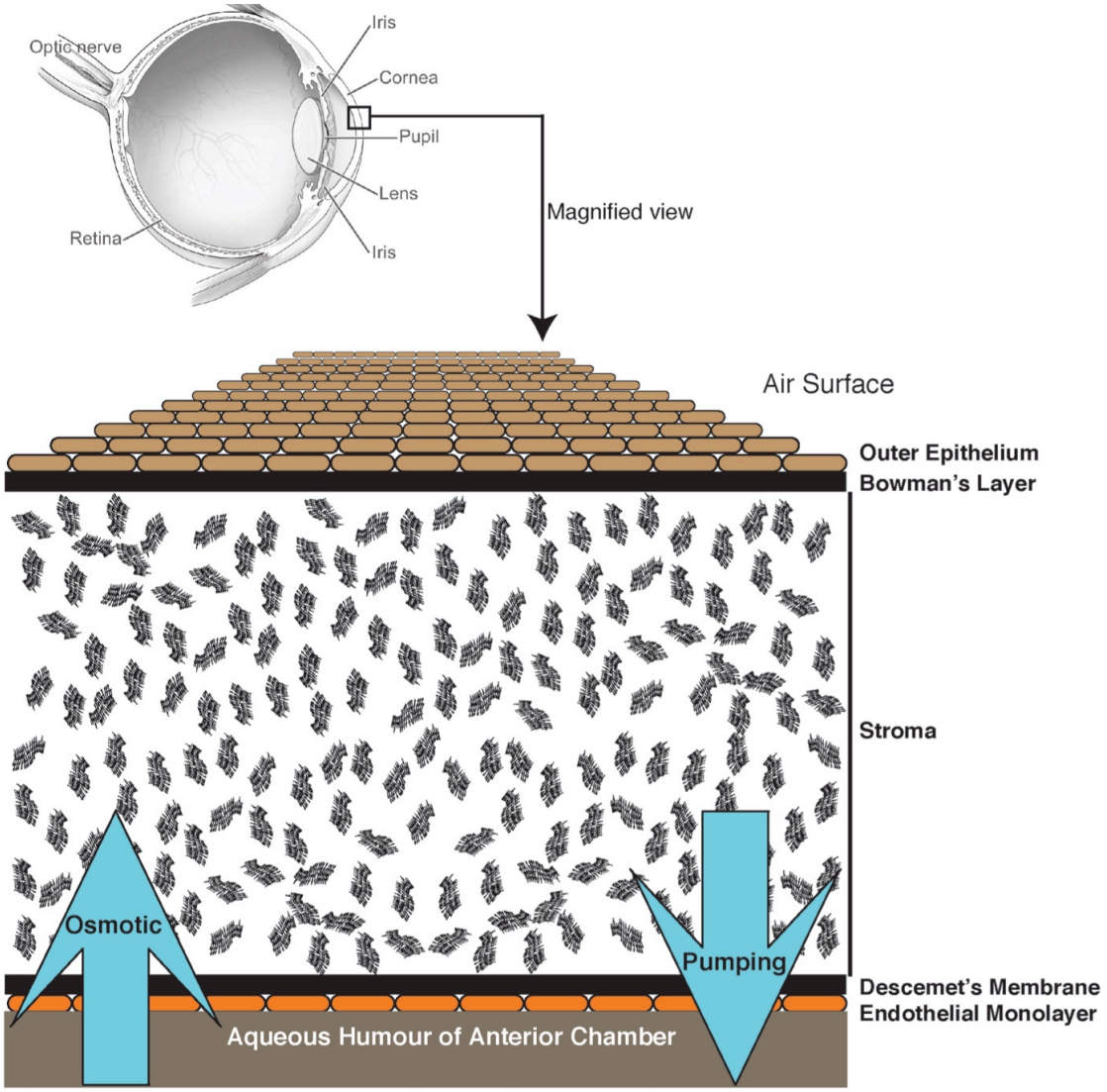

Figure 1.1 Schematic representation of the human cornea (after Pepose and Ubels, 1992). Upper part illustrates an eye in cross section (courtesy of NIH). The lower panel shows a region of the eye that is magnified. The upper image has the outside of the eye on the right, while the lower diagram shows the outside on top. Cornea has five layers. The outer most layer is 1) epithelium followed by 2) Bowman's layer. 3) Stroma is composed largely of proteoglycans and collagen. 4) Descemet's membrane forms an adhesive layer between the endothelial layer and the stroma. 5) The corneal endothelial cell monolayer

is avascular, but highly metabolically active and forms a barrier between stroma and aqueous humor. The high concentration of dissolved proteoglycans accumulates fluid osmotically in the stroma. This is balanced by the fluid reabsorption function of endothelial cell layer.

Corneal endothelium has a major role in maintaining the corneal transparency. While the corneal endothelium is covered by Descemet's membrane and stroma on the one side, it is exposed to aqueous humor on the posterior side (Fig. 1.1). The aqueous is the thin, watery fluid that fills the space between the cornea and the iris (anterior chamber). This fluid nourishes the cornea and is composed of 98% water, amino acids, electrolytes, glucose and immunoglobulins [18]. All the nutrients for cornea come from the aqueous humor and through the corneal endothelium except for oxygen [16]. Hence, the movement of solutes/fluids from aqueous humor to stroma and back to aqueous humor is handled by endothelium.

1.4.1 Endothelial pump-leak mechanism

The corneal endothelium serves two functions to maintain the transparency of the cornea: 1) It controls the hydration state of the stroma. Stroma is composed of a high concentration of proteoglycans and collagen, resulting in a strong osmotic driving force to accumulate fluid. 2) Endothelium must be permeable to nutrients and other molecules from the aqueous humor because these are not supplied by blood vessels like in other tissues [16]. To perform both the functions, the endothelium has a 'pump-leak' mechanism, a combination of leaky barrier and fluid pump, which is a poorly understood complex process [19].

Endothelial cells have a leaky tight junction between adjacent cells accounting for the weak endothelial barrier function that allows nutrients and other molecules (water follows osmotically) from aqueous humor to enter stroma. At the same time, the endothelium acts as an active pump that moves ions and water, from the stroma into the aqueous humor [18]. The fluid movement into and out of the stroma is balanced perfectly

by the endothelial layer to regulate stromal thickness and pressure, without excessive fluid accumulation. As a result, stromal transparency is maintained. To perform the energy-consuming task of moving water efficiently, the endothelial cells have large number of mitochondria and are metabolically very active. Hence the role of the corneal endothelium is to move ions from the stroma to the aqueous humor, resulting in osmotic fluid movement countering the movement into the stroma through a "pump-leak" mechanism.

1.4.2 Possible models for endothelial pump function

The anion secretion model (bicarbonate and chloride), electro-osmosis model, facilitated lactate transport model and fluid transport agonists model are proposed to understand the endothelial function, however, none of them can clearly explain the complex physiological process behind the endothelial pump-leak mechanism and each model has its own drawbacks [20]. The complex process of endothelial pump-leak mechanism is mediated by several membrane proteins like Na^+/K^+-ATPase, Cl^-/HCO_3^- Anion exchanger 2 (SLC4A2 or AE2), a $1Na^+$: $2HCO_3^-$ cotransporter SLC4A4 (NBCe1), Na^+/H^+ exchanger (NHE1), Na^+:K^+:$2Cl^-$ cotransporter (NKCC1), cystic fibrosis transmembrane conductance regulator (CFTR), Calcium activated chloride channels (ClCA1), Monocarboxylate transporters (MCT1) and Aquaporins (AQPs) [20].

According to anion secretion model, a net anion flux generated by active transport mechanism of bicarbonate and chloride ions could produce local osmotic gradients that move water across the endothelial layer. Membrane proteins Na^+/K^+-ATPase, AE2, NBCe1, NHE1 and NKCC1 are localized to basolateral side of endothelium and cause influx of bicarbonate and chloride ions into the endothelium (Fig. 1.2). Carbonic

anhydrases (CAII and CAIV), CFTR and ClCA1 are involved in the efflux of chloride and bicarbonate (as carbon dioxide) ions out of the endothelium. Bonanno J proposed that Na^+/K^+-ATPase, localized at the basolateral side of corneal endothelium, creates a low intracellular [Na^+], high intracellular [K^+], and a negative membrane potential of about -55 mV in conjunction with K^+ channels. NBCe1 can directly load HCO_3^- into the cell whereas Na^+/H^+ exchanger can indirectly load HCO_3^- into the cell because removal of protons favors formation of HCO_3^- from CO_2, catalyzed by carbonic anhydrase II. Conversely, the Cl^-/HCO_3^- exchanger can remove HCO_3^- from the cell and add Cl^-. Moreover, a basolateral NKCC1 helps load intracellular chloride to ~40 mM, above electrochemical equilibrium of ~12 mM. On the apical side, CFTR and CaCC favors an anion permeability of Cl^- vs. HCO_3^- by ~4:1. There is no evidence for apical Cl^-/HCO_3^- exchange. Taken together, the model predicts that HCO_3^- is taken up on the basolateral side and efflux of HCO_3^- across the apical side is through anion channels driven by the negative membrane potential. Because the influx mechanisms for HCO_3^- exceed direct efflux mechanisms and the differential must be converted to CO_2 and the CO_2 can diffuse in any direction and some will diffuse across the apical membrane where carbonic anhydrase IV could catalyze the conversion back to HCO_3^-. These contribute to a local buildup of osmotic pressure at the apical membrane [20].

However, according to this model, influx of bicarbonate and chloride ions far exceeds the efflux and there is no evidence of any other apical bicarbonate transporters in corneal endothelium except CFTR, which is a HCO_3^- conductive channel [20]. There is no direct evidence for the generation of net anion flux that could produce local osmotic gradient and movement of water. In addition, none of these proteins are implicated in

corneal endothelial dystrophies and knock-down studies of NBCe1 further revealed that the anion secretion model is not an integral part of the "pump" [20]. Further, AQP1, a water channel protein is localized at apical side of the corneal endothelium and AQP1 knockout mouse models show corneal thickness, but no corneal edema implicating that the AQP1 is present only as a passive water pathway [21, 22].

According to electro-osmosis model, the generation of trans-epithelial potential through the apical anion channels could draw counter ions (Na^+) through a paracellular pathway [20]. This produces electro-osmotic fluid coupling leading to water movement across the endothelial layer. The drawback of this model is that the reduction in endothelial density due to aging would reduce the paracellular area. This would lead to reduced water movement across the endothelium, which should cause corneal edema. But when individuals age, they do not automatically develop corneal edema. Further experiments and alternative mechanisms are needed to explain this model [20].

The facilitated lactate transport model proposes that due to high amount of lactate produced in stroma, there is a large gradient for lactate flux (though monocarboxylate transporters MCT1 and MCT4) from cornea to aqueous humor [20]. But there is no direct evidence supporting the facilitated lactate transport model exists in the literature. The fluid transport agonists model (by increased cyclic adenosine monophosphate) does not explain the endothelial function convincingly [20]. Hence all the four models need significant experimental testing to explain the endothelial pump-leak mechanism.

Interestingly, a relatively unknown integral membrane protein, SLC4A11 (belonging to SLC4 transporter family), was recently identified as causing some corneal dystrophies when mutated [23-25] and could potentially be involved in the endothelial

pump-leak function. Before looking into the details about SLC4A11, a brief description of corneal dystrophies is discussed to appreciate the importance of SLC4A11.

1.5 Corneal dystrophies

Corneal dystrophies are a heterogeneous group of genetically determined corneal diseases. Depending on the layer of the cornea involved, they can be divided into three groups clinically (Table 1.1) [26]. Abnormalities associated with corneal epithelium, Bowman's membrane and anterior stroma are grouped under superficial corneal dystrophies whereas stromal corneal dystrophies are associated with stroma. Diseases associated with Descemet's membrane and corneal endothelium are classified as posterior corneal dystrophies [27].

1.5.1 Posterior corneal dystrophies

Posterior corneal dystrophies are characterized by a defect in the active fluid transport by the corneal endothelium, causing corneal edema. This results in loss of corneal transparency and reduced visual acuity [26]. Posterior corneal dystrophies include Fuchs corneal dystrophy (FECD), posterior polymorphous corneal dystrophy (PPCD), congenital hereditary endothelial corneal dystrophy (CHED) and X-linked endothelial corneal dystrophy (XECD). This thesis focuses particularly on CHED (MIM # 217700) and FECD (MIM #136800) in addition to Harboyan syndrome (HS; MIM #217400), which is a combination of CHED and perceptive deafness [25].

1.5.2 Congenital corneal endothelial dystrophy

There are two types of congenital hereditary endothelial dystrophy: CHED1, which is autosomal dominant, and CHED2, which is autosomal recessive. Clinically,

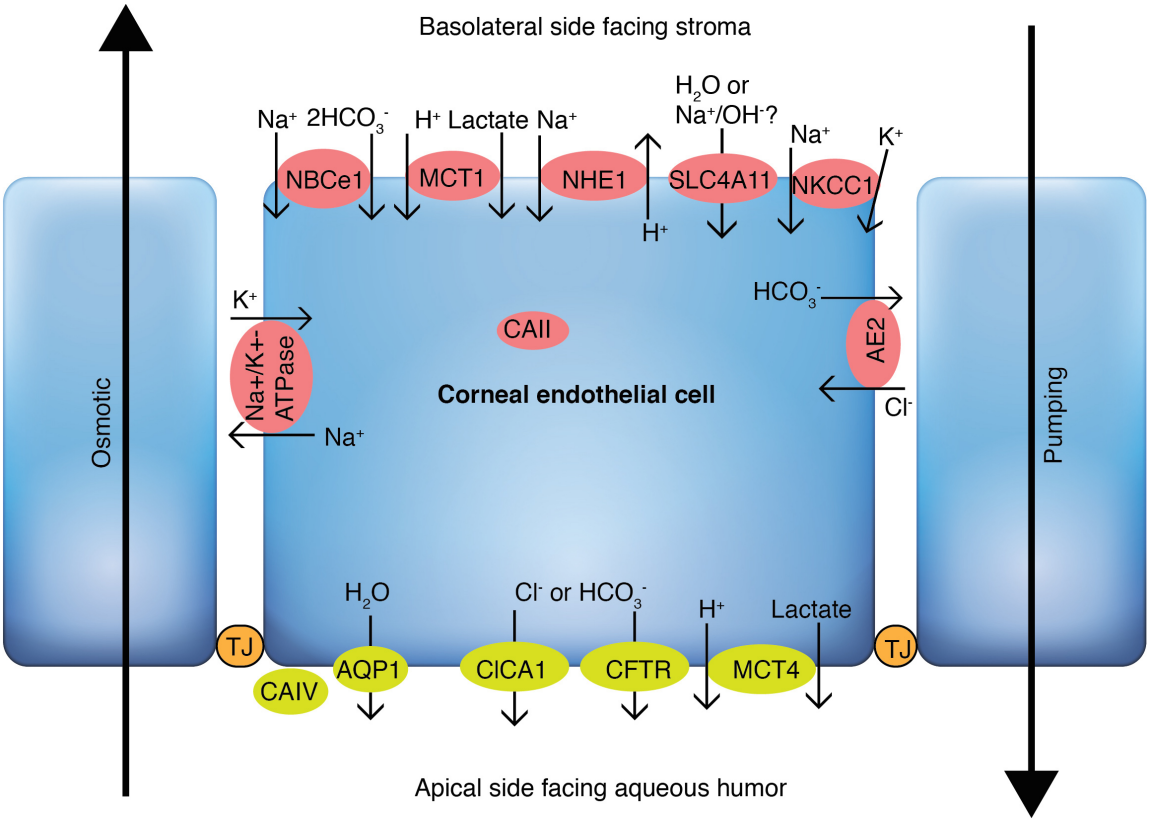

Figure 1.2 The Corneal endothelial pump. NBCe1, NHE1, NKCC1, AE2 and the Na^+/K^+-ATPase localize at the basolateral surface of corneal cells while CFTR, ClCA1 and CAIV localize at the apical side facing the aqueous humor. CAII is localized intracellularly. According to anion secretion model, the movement of bicarbonate and chloride ions is used to explain the fluid secretion. Monocarboxylate transporters (MCT1 and MCT4) localize to the basolateral and apical surfaces of the corneal endothelium. The facilitated lactate transport model proposes that movement of lactic acid contributes to net fluid movement. AQP1 and SLC4A11, a potential water permeation pathway, are localized at the apical and basolateral sides respectively could be involved in fluid movement across corneal endothelium. TJ represents tight junction (modified from [20] and [1]).

Table 1.1 Dystrophies associated with different corneal layers (after Klintworth GK) [26].

Superficial Corneal dystrophies

Name	Mode of Inheritance	Gene
Meesmann dystrophy	Dominant	*KRT3* and *KRT12*
Stocker-Holt dystrophy	Dominant	*KRT12*
Granular corneal dystrophy type III	Dominant	*TGFBI*
Thiel-Behnke dystrophy	Dominant	*TGFBI*
Gelatinous drop-like corneal dystrophy	Recessive	*TACSTD2*
Subepithelial mucinous corneal dystrophy	Dominant	Unknown
Lisch epithelial dystrophy	X-linked	Unknown
Epithelial recurrent erosion dystrophy	Dominant	Unknown

Corneal stromal dystrophies

Name	Mode of Inheritance	Gene
Macular corneal dystrophy	Recessive	*CHST6*
Granular corneal dystrophy type I &II	Dominant	*TGFBI*
Lattice corneal dystrophy type I	Dominant	*TGFBI*
Lattice corneal dystrophy type II	Dominant	*GSN*
Fleck dystrophy	Dominant	*PIP5K3*
Schnyder corneal dystrophy	Dominant	*UBIADI*
Posterior amorphous corneal dystrophy	Dominant	Unknown
Congenital stromal dystrophy	Dominant	*DCN*

Posterior dystrophies

Name	Mode of Inheritance	Gene
Fuchs dystrophy (early onset)	Dominant	*COL8A*
Fuchs dystrophy (late onset)	Dominant	*SLC4A11, TCF8* and various other chromosome locations (unknown gene)
Posterior polymorphous dystrophy type 1	Dominant	Unknown
Posterior polymorphous dystrophy type 2	Dominant	*COL8A2*
Posterior polymorphous dystrophy type 3	Dominant	*TCF8*
Congenital endothelial dystrophy type 1	Dominant	Unknown
Congenital endothelial dystrophy type 2	Recessive	*SLC4A11*
X-linked endothelial corneal dystrophy	X-linked	Unknown

diffuse bilateral ground-glass appearance and markedly thickened corneas characterize both disorders (Fig. 1.3) and the corneal thickness is up to three times greater than normal [26, 28]. The major differences between CHED1 and CHED2 are onset of presentation, mode of inheritance, genetic mutations, and associated conditions. Vision tends to be better in CHED1 patients than in those with CHED2 [28]. Due to its similarity to PPCD, CHED1 is generally not considered a separate dystrophy [29]. For the interest of the thesis, only CHED2 will be further discussed.

The manifestation of CHED2 is more common and more severe than CHED1. CHED2 is an early onset disease that manifests at birth or shortly thereafter, usually within the first decade of life. The symptoms of CHED2 include edematous cornea and diffuse ground glass appearance of cornea that is evident at birth or in the neonatal period. Nystagmus (involuntary movement of eyes) is often present due to early and severe loss of vision [28]. The endothelium is usually attenuated and absent. As CHED2 remains stationary throughout life and if bilateral corneal opacification is severe, then the patient's experience poor quality of life. Corneal transplantation is the only hope for improved vision [26].

Until now, only mutations of the gene *SLC4A11* located on the chromosome 20p12 are found to cause CHED2 [23, 30-40].

1.5.3 Fuchs endothelial corneal dystrophy

FECD is the most common endothelial dystrophy with 4% prevalence in North American adult population [26]. There are two types of FECD: early onset FECD and late onset FECD. Mutations in *Col8A2* have been implicated in early onset FECD [41].

However, in the interest of the thesis focus and simplicity, from here on FECD refers to only the late-onset FECD.

FECD manifests in the fourth to fifth decade of life and is characterized by markedly opaque cornea caused by extensive edema due to a loss of endothelial cells (Fig. 1.3) [26, 42]. Genetic factors combined with oxidative stress and post mitotic arrest of corneal endothelium lead to a combination of oxidative mitochondrial damage, endothelial morphological changes and apoptosis in FECD. Ultimately this results in endothelial cell loss and reduced cell density in the endothelium [28]. Clinically, the disease progresses in four stages: In stage 1, collagenous warts extending from the Descemet's membrane called "guttae" reduce visual acuity, but the patient is asymptomatic. In stage 2, the deposition of guttae progresses accompanied by loss of corneal endothelial cells, followed by mild corneal stromal edema and painless reduction in vision. In stage 3, sustained loss of endothelial cells cause reduced endothelial pump function. The severity of corneal stromal edema increases and is associated with epithelial and sub-epithelial bullae, and painful loss of vision. In stage 4, severe edema is associated with opacification, vascularisation and scarring of the cornea [43]. At this stage, corneal transplantation is the only viable treatment option. In fact, 47% of all corneal transplants performed in United States are in patients suffering from FECD [42]. Mutations in the genes *LOXHD1, TCF4* and *TCF8* are implicated in FECD and it is also associated with chromosomal loci FCD1, 2, 3 & 4 (chromosomes 13, 18, 5 & 9 respectively) [28, 44-46].

Apart from these, mutations in *SLC4A11* are also found in a few FECD patients [24, 47-50].

1.5.4 Harboyan syndrome

Harboyan syndrome combines the corneal symptoms found in CHED2 with perceptive deafness [25]. While vision loss is common at birth or shortly after birth as in CHED2, hearing loss in Harboyan syndrome is not reported at birth [25]. It is sensorineural, slowly progressive, with typical deficits in the 20–50 db range (mild to moderate) at ages 10–25 years, and mainly affects the higher frequencies. In families with Harboyan syndrome, hearing loss has been found as early as age four years [25]. Mutations in gene SLC4A11 have been implicated in Harboyan syndrome as well [50].

1.6 SLC4A11 mutations

Mutations in *SLC4A11* gene cause three different diseases: CHED2, FECD and HS. The first novel report implicating SLC4A11 in CHED2 patients was published in 2006 [23], while two years later, SLC4A11 mutations were also found in FECD patients [24]. The first report of *SLC4A11* mutations in Harboyan syndrome was published in 2007 [50]. After these three reports, several groups reported additional mutations in the *SLC4A11* gene, causing CHED2, FECD and HS. These were found in patients from all over the world, and include missense, nonsense, frame-shift, insertion and deletion mutations [23-25, 30-40, 47-50]. To date, more than 60 point mutations have been identified (Table 1.2) that cause single amino acid substitutions in the SLC4A11 protein. *SLC4A11* gene encodes for SLC4A11 protein, which belongs to solute carrier 4 (SLC4) family of bicarbonate transporters.

A

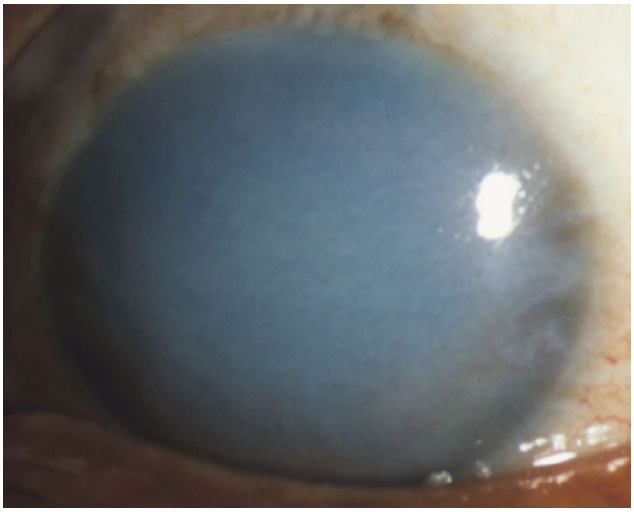

B

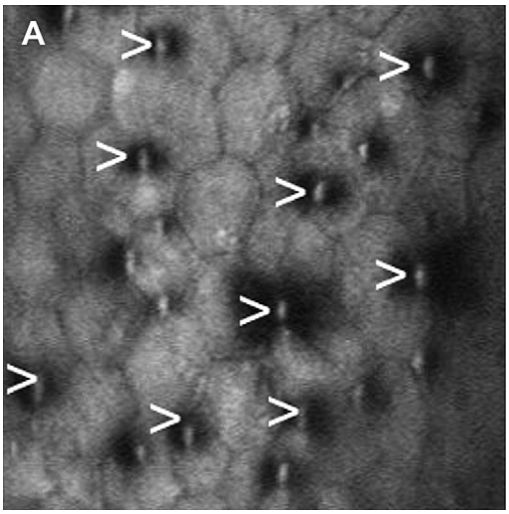

C

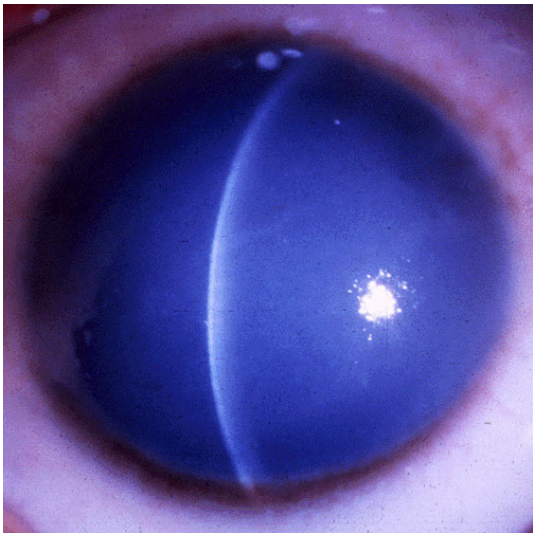

Figure 1.3 Clinical presentations of FECD and CHED2 patient's eyes. A) In FECD patients, the cornea is opaque caused by extensive edema due to a loss of endothelial cells [26]. B) Confocal microscopy examination of a patient with FECD shows corneal guttae (arrowheads) that are scattered in between corneal endothelial cells, disrupting a normally continuous layer of hexagonally shaped cells [28]. C) In CHED2 patients, a markedly opaque cornea due to stromal edema is found during slit lamp examination (modified and reproduced from [26] under Creative Commons Attribution License).

1.7 SLC4 family of bicarbonate transporters

The Human Genome Organization has termed the proteins that transport substances across plasma membranes as SoLute Carriers (SLC) [51]. The SLC4 family of bicarbonate transporters contains 10 members that include sodium independent chloride bicarbonate exchangers (AE1, AE2, and AE3), sodium bicarbonate co-transporters (SLC4A9, NBCn1, NBCe2, and NBCe1), sodium dependent chloride bicarbonate exchangers (NDCBE and NCBE) and relatively unknown SLC4A11 [52]. They have wide range of tissue distribution (Table 1.3) in the human body. Phylogenetic analysis places SLC4A11 as distantly related to all other members (Fig. 1.4).

The SLC4 family of bicarbonate transporters plays important roles in the maintenance of physiological pH, cell volume regulation and acid/base secretion [52, 53]. Cl^-/HCO_3^- exchangers (both electroneutral and electrogenic) move bicarbonate either into or out of the cell in exchange for chloride, whereas Na^+/HCO_3^- co-transporters move bicarbonate along with sodium into or out of the cell, thereby either alkalinizing or acidifying the cell, respectively. As CO_2/HCO_3^- acts as an important buffering system in the body, SLC4 protein family members are implicated in various diseases. A few examples include cardiac hypertrophy [79-81], hereditary spherocytosis of the erythrocyte [82-86], proximal and distal renal tubular acidosis [84, 87-94], epilepsy [95, 96], cataract and glaucoma [97], mental retardation [91, 98] and autism [99]. Apart from these, SLC4A11 is implicated in corneal dystrophies as discussed above [52, 97].

While SLC4A11 has received little attention, decades of research has explored AE1 (SLC4A1) to understand the structure and transport mechanism of the protein [52]. Mutations in *AE1* cause distal renal tubular acidosis [52]. Using the knowledge gained

Table 1.2 All reported SLC4A11 point mutations. The position of amino acids is based on the variant 2 of SLC4A11 (891 amino acids long, NP_114423.1).

FECD [24, 47-50]

N72T	M91V	E167D	W240S	R282P	A327V	E399K	T434I
V507I	Y526C	T561M	S565L	V575M	G583D	G709E	G742R
T754M	G834S						

CHED2 [23, 30-40]

R125C	R125H	E143K	A160T	R209W	S213L	S213P	S232N
R233C	K260E	T262I	A269V	T271M	C386R	G394R	T401K
G417R	G418D	G464D	L473R	R488K	S489L	T584K	C611R
H724D	R755Q	R755W	P773L	R804H	V824M	T833M	M856V
R869C	R869H	L873P					

HS [25, 50]

S213P	R488K	V824M	L843P	M856V			

Table 1.3 Tissue distribution and Transport mechanisms of SLC4 family of bicarbonate transporters (modified from [52]).

Protein	Tissue distribution	Function	Reference
AE1 (SLC4A1)	Red blood cells, kidney, heart	Electroneutral Cl^-/HCO_3^- exchanger	[54]
AE2 (SLC4A2)	Widespread (mostly basolateral)	Electroneutral Cl^-/HCO_3^- exchanger	[55]
AE3 (SLC4A3)	Brain, heart, retina, smooth muscle, kidney, GI tract, adrenal and pituitary gland	Electroneutral Cl^-/HCO_3^- exchanger	[56]
NBCe1 (SLC4A4)	Kidney, heart, prostate, colon, pancreas, stomach, thyroid and brain	Electrogenic Na^+-coupled HCO_3^-cotransporter	[57-60]
NBCe2 (SLC4A5)	Brain, epididymis, liver, spleen, testis, cardiac muscle, smooth muscle, kidney, spleen, and choroid plexus	Electrogenic Na^+-coupled HCO_3^-cotransporter	[61-66]
NBCn1 (SLC4A7)	Heart, kidney, spleen, skeletal muscle, smooth muscle, liver, lungs, submandibular gland, pancreas, and stomach	Electroneutral Na^+-coupled HCO_3^-cotransporter	[67-69]
NDCBE (SLC4A8)	Cardiac myocytes, prefrontal cortex, testis, oocytes and kidney	Electroneutral Na^+-coupled Cl^-/HCO_3^-exchanger	[70-72]
AE4 (SLC4A9)	Kidney, testis and pancreas	Electroneutral Na^+/HCO_3^- cotransporter	[2, 73-75]
NCBE (SLC4A10)	Choroid plexus, neurons, kidney, uterus, adrenal cortex, and cardiac myocytes	Electroneutral Na^+-dependent Cl^-/HCO_3^- exchanger or HCO_3^- dependent Cl^-/ Cl^- exchanger	[76-78]
SLC4A11	Cornea, kidney, salivary gland, testis, thyroid and trachea	Osmotic transmembrane water movement facilitator	[1, 3]

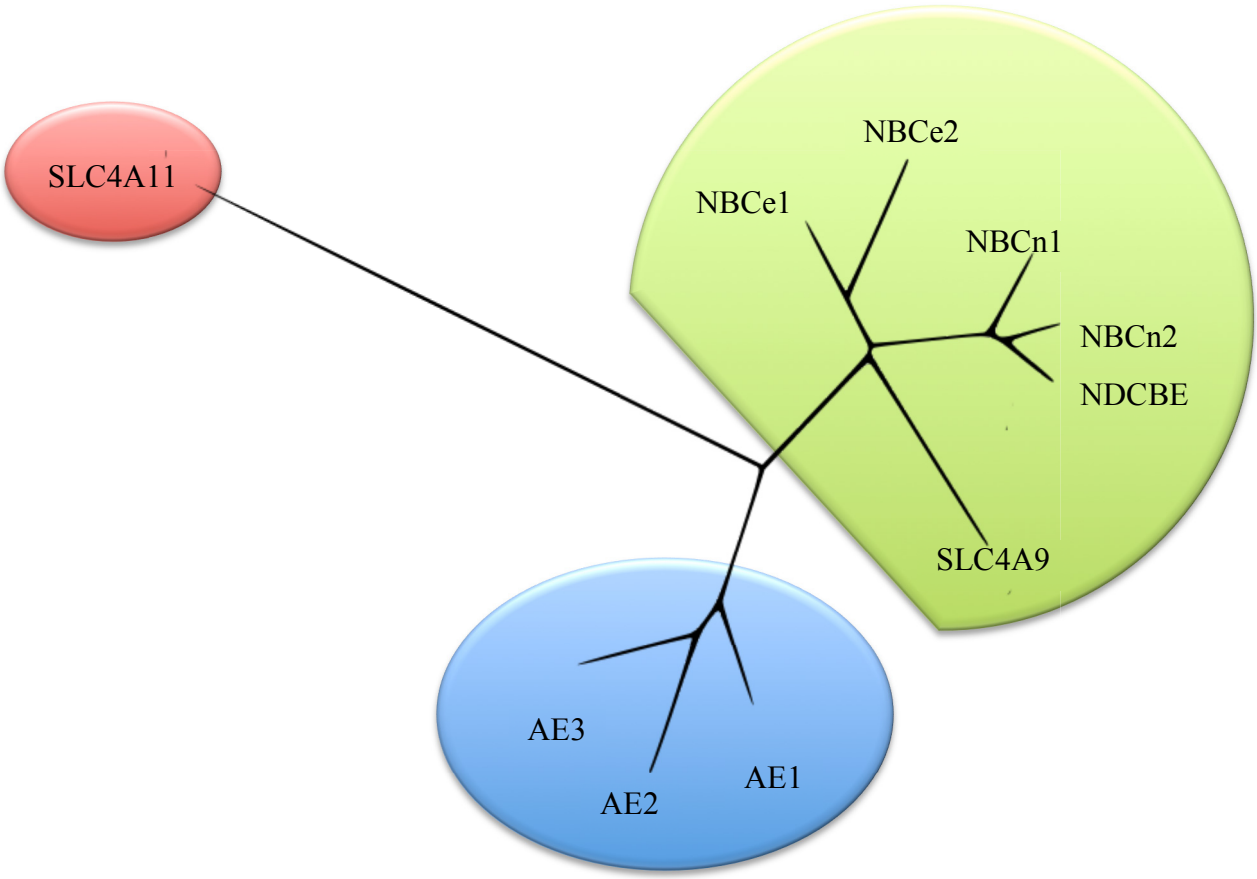

Figure 1.4 Phylogenetic dendrogram of SLC4 family of bicarbonate transporters. Amino acid sequences of the indicated SLC4 family members were aligned using Clustal W2 software (http://www.ebi.ac.uk/Tools/msa/clustalw2/). The length of each line denotes the relative evolutionary distance between transporters. SLC4 family of bicarbonate transporters comprised of three sub-families: electroneutral Cl^-/HCO_3^- exchangers (blue oval)), Na^+ coupled bicarbonate transporters (green oval) and SLC4A11, which is an osmotically driven water transporter or OH^- permeation pathway (red oval).

from AE1 studies, research over the past few years has led to some understanding of the topology and functional role of SLC4A11 [1, 100, 101].

1.8 SLC4A11

1.8.1 Expression Pattern

SLC4A11 is expressed in cornea, blood cells, ovary, tongue, lung, skin, colon kidney, salivary glands, testis, thyroid, and trachea [2, 3]. Other tissues such as the cerebellum, esophagus, and mammary gland also express SLC4A11 to a lesser extent [2]. Immunohistochemistry studies show that SLC4A11 was particularly expressed in the basolateral side of corneal endothelium, podocytes of renal corpuscules, basolateral membranes in inner medullary collecting ducts and choroid plexus epithelial cells [1, 102]. Based on National Center for Biotechnology Information UniGene expression profile, SLC4A11 is also expressed in some tumours, including gastrointestinal, oral, ovarian, respiratory and skin tumours, as well as in leukaemia and retinoblastoma [32].

Human SLC4A11 has three known NH_2-terminal variants arising from differential splicing of the mRNA: SLC4A11-Variant 1, which is 918 amino acids long (NP_001167561.1); SLC4A11-Variant 2, which is 891 amino acids long (NP_114423.1); and SLC4A11-Variant 3, which is 875 amino acids long (NP_001167560.1). The last 861 amino acids in all the three variants are identical. Out of these, variant 2 was cloned initially from human cornea [2] and subsequently used to study the function of the protein and corneal dystrophy causing mutations [1, 3, 23, 24, 100, 101, 103, 104]. A recent report shows that at the mRNA transcript level, variant 3 is expressed in human corneal endothelium [105]. This raises the possibility that both variant 2 and variant 3 could be

expressed in human cornea. However, there is no evidence in the literature about which variant is expressed at the protein level. All the experiments carried out in this thesis used the SLC4A11-variant 2, which is 891 amino acids long.

1.8.2 Structure

Understanding SLC4A11 structure is pertinent in studying the disease-causing mutants and to develop viable treatments for SLC4A11-caused CHED2, FECD and HS. When *SLC4A11* mutations were first implicated in corneal dystrophies [23, 24, 50], there was no topological or structural information available other than the fact that on immunoblots, it migrates at 100 kDa [2, 3, 102]. Expression studies in HEK293 cells showed that SLC4A11 was immuno-detected as two bands on western blot of approximately 90 and 110 kDa [23, 24]. The upper band corresponds to the complex glycosylated (post-ER associated) form of the protein, while the lower band corresponds to core glycosylated (endoplasmic reticulum associated) form of the protein. The 110 kDa complex glycosylated form targets to the plasma membrane, while 90 kDa immature form is retained in the endoplasmic reticulum [23, 24].

SLC4A11 has only 19% amino acid identity with AE1 and thus any investigation of SLC4A11 structure based on AE1 studies has to be ascertained through biochemical experiments. Hydropathy analysis of SLC4A11 suggested a two domain topology: a cytosolic N-terminal domain spanning residues 1−374, and a membrane domain containing residues 375−873 organized as 14 transmembrane segments, with a short cytosolic C-terminal tail, encompassing residues 874−891 (Fig. 1.5). Confocal microscopy confirmed the cytosolic orientation of both N- and C-terminal domains

proposed in the SLC4A11 topology model. Limited proteolysis studies provided additional evidence in support of the proposed topology model [101].

1.8.3 Oligomerization

Investigating the oligomeric state of SLC4A11 is important to explain the difference in inheritance and age of onset between CHED2/HS and FECD even though they both were caused by SLC4A11 mutations. The missense mutations in SLC4A11 from all three diseases might either represent sites in the protein important for transport function or for proper protein folding. When these particular sites are mutated, it could either compromise transport function or cause misfolding and ER-retention. When SLC4A11 mutant proteins are ER-retained, it leads to decreased levels of accumulation at the plasma membrane compared to wild-type (WT) protein. Indeed the majority of SLC4A11 mutant proteins characterized so far have the ER-retention phenotype [1, 23, 24, 47, 48, 100, 101].

SLC4A11 exists as a dimer when expressed in HEK293 cells [100]. Multiple biochemical experiments including non-denaturing perfluoro-octanoic acid PAGE, extracellular cross-linking and co-immunoprecipitation have shown that SLC4A11 forms dimers when expressed in HEK293 cells [100]. Dimerization of SLC4A11 at the protein level explains the dominant and recessive inheritance of FECD and CHED2 diseases caused by *SLC4A11* mutations.

In HEK293 cells expressing WT SLC4A11, WT/WT homodimers are formed and process normally to the plasma membrane. In the case of cells expressing recessive CHED2 SLC4A11 mutants, the mutant proteins form CHED2/CHED2 homodimers and do not reach the cell surface due to its retention in ER, thereby causing the disease.

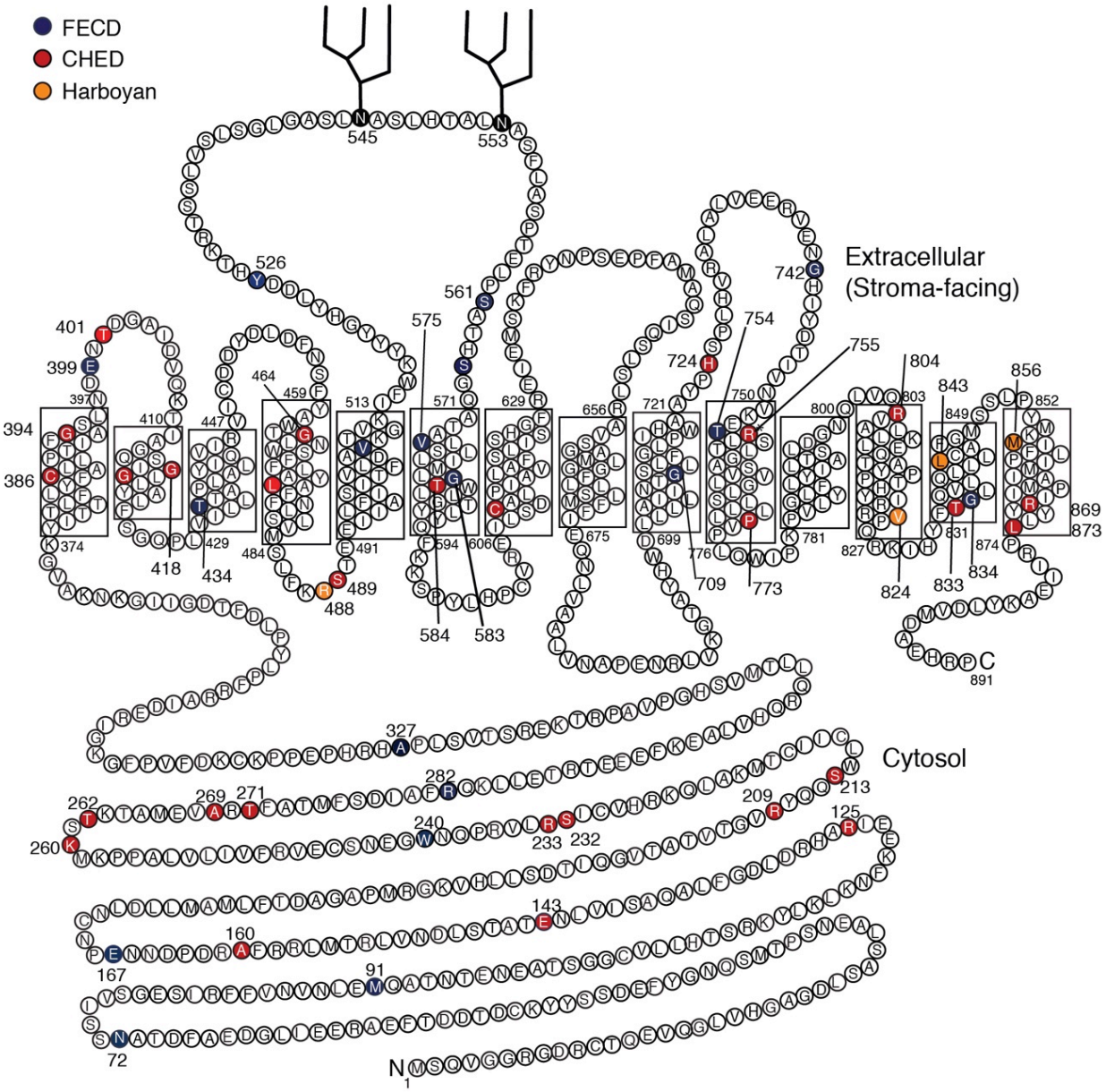

Figure 1.5 Topology model of SLC4A11. Boxes indicate the transmembrane segments. Inset legend indicates colors associated with disease mutations of Fuchs endothelial corneal dystrophy (FECD), congenital hereditary endothelial dystrophy (CHED2) and Harboyan syndrome [23-25, 30-40, 47-50]. Position 545 and 553 indicates putative N-linked glycosylation sites [101].

HEK293 cells co-expressing WT and CHED2 mutants form WT/CHED2 heterodimers. The presence of CHED2 SLC4A11 mutant protein in the dimer did not affect the ability of WT to move to the cell surface, which shows that ER-retained CHED2 mutant phenotype is recessive to the plasma membrane localized WT phenotype. As a result, individuals with heterozygous CHED2 *SLC4A11* mutations act as a carrier for CHED2 disease and do not manifests any early onset disease symptoms unlike CHED2 patients. On the other hand, FECD mutant proteins behave differently from CHED2 mutants. Cells co-expressing WT and FECD mutants form WT/FECD heterodimers and the presence of FECD mutant protein reduces the cell surface processing of WT SLC4A11 in heterodimers. The delay in the onset of symptoms in FECD is explained by the sufficient WT/WT dimer that reaches cell surface, despite the dominant-negative effects exerted by the mutant protein on WT. Thus FECD disease caused by *SLC4A11* mutations is inherited dominantly in patients [100]. This mechanism of inheritance is similar to AE1, whose mutations cause diseases with both recessive and dominant inheritance patterns. The formation of WT/mutant AE1 heterodimers explains the pattern of inheritance [52, 94, 106-108]. Taken together, SLC4A11 exists as a dimer and the oligomerization explains the difference in inheritance of CHED2 and FECD.

1.8.4 Function

As SLC4A11 is localized to the basolateral side of corneal endothelium, facing the stroma, and its mutations are implicated in corneal dystrophies, deciphering the functional role of SLC4A11 is important to understand the endothelial pump-leak mechanism. The transport function of SLC4A11 has been controversial during the past decade. The plant orthologue of SLC4A11, BOR1, was convincingly characterized as a

borate transporter [109]. Later, human SLC4A11 was reported as a sodium-coupled borate transporter [3]. Borate stabilizes the structure of cell walls by cross-linking vicinal diols in bacteria, plants and fungi [110]. Mammals do not have any cell walls and borate transport by SLC4A11 does not provide an apparent explanation for the corneal diseases. One of the drawbacks of the report on borate transport by human SLC4A11 is that in experiments, Na^+ was substituted with *N*-methyl-d-glucamine ($NMDG^+$). This compound is used as a borate chelator (forms a 1:1 complex with $B[OH]_4^-$) [111]. Several studies confirmed that indeed human SLC4A11 is not a borate transporter [104, 105, 111]. Even though SLC4A11 belongs to SLC4 family of bicarbonate transporters, no bicarbonate activity was observed in HEK293 cells expressing human SLC4A11 [104, 105, 111]. While human SLC4A11 variant 2 has EIPA-sensitive Na^+-OH^- (H^+) and NH_4^+ permeability [104] and bovine SLC4A11 has Na^+-coupled OH^-transport [111], a recent report suggests that human SLC4A11 variant 3 functions as an Na^+ independent electrogenic H^+ (OH^-) permeation pathway that can be stimulated by disulfonic stilbenes [105]. In all these studies, only HEK293 expression system was used.

In addition to reports of ion transport by SLC4A11, it also mediates water flux osmotically across plasma membrane [1]. SLC4A11 variant 2, when expressed in HEK293 or in *Xenopus laevis* oocytes, mediates water flux when cells are hypo-osmotically challenged. This function can occur in two ways: a) SLC4A11 can form a pathway that facilitates water movement (as in aquaporins) or b) SLC4A11 can induce solute entry into the cell driving parallel osmotic water accumulation [1]. Experiments carried out in the absence of Na^+ showed that the water flux activity of SLC4A11 is Na^+

independent [1]. Hence SLC4A11 can form a transport pore that facilitates water movement, which is examined more closely in chapter 4 of this thesis.

Patients with *SLC4A11* mutations accumulate fluid in their cornea resulting in loss of corneal transparency. SLC4A11 localized at the basolateral surface of corneal endothelium (Fig. 1.6) and mediating water flux would better explain the corneal symptoms [1]. SLC4A11 is the only protein localized at the basolateral surface of corneal endothelium that mediates water flux as no aquaporins have been reported there [22]. Interestingly, SLC4A11 is the only protein that mediates osmotic trans-membrane water flux apart from proteins of the Major Intrinsic Protein (MIP) family, which includes the aquaporins [1].

1.8.5 MIP family of Water transporters

Prior to the discovery of SLC4A11 mediating osmotic water flux, the MIP family of water transporters that comprises Aquaporins (AQP0-12) and plant intrinsic proteins (NIP5;1, PIP2.2 and TIP2.2) were found to mediate trans-membrane water flux. In human cornea, AQP1 localizes apically in corneal endothelium, facing the aqueous humor (Fig. 1.5) [1]. Localization of AQP1 on the apical side and SLC4A11 on the basolateral side of endothelial cells suggests they may work cooperatively to provide a water conductive pathway across the endothelial layer [1]. Interestingly, SLC4A11 carries a lower water-flux per protein molecule than AQP1 (10^7 vs. 10^9 $.s^{-1}$ molecules). If the endothelial cell reabsorbs more water at its basolateral surface than it can efflux at its apical surface, it will result in cell swelling and destruction of corneal endothelium. Hence it is safe to function with regulated water flux at the basolateral side in endothelial cells and with excess water-flux capacity at their apical surface. The evidence that

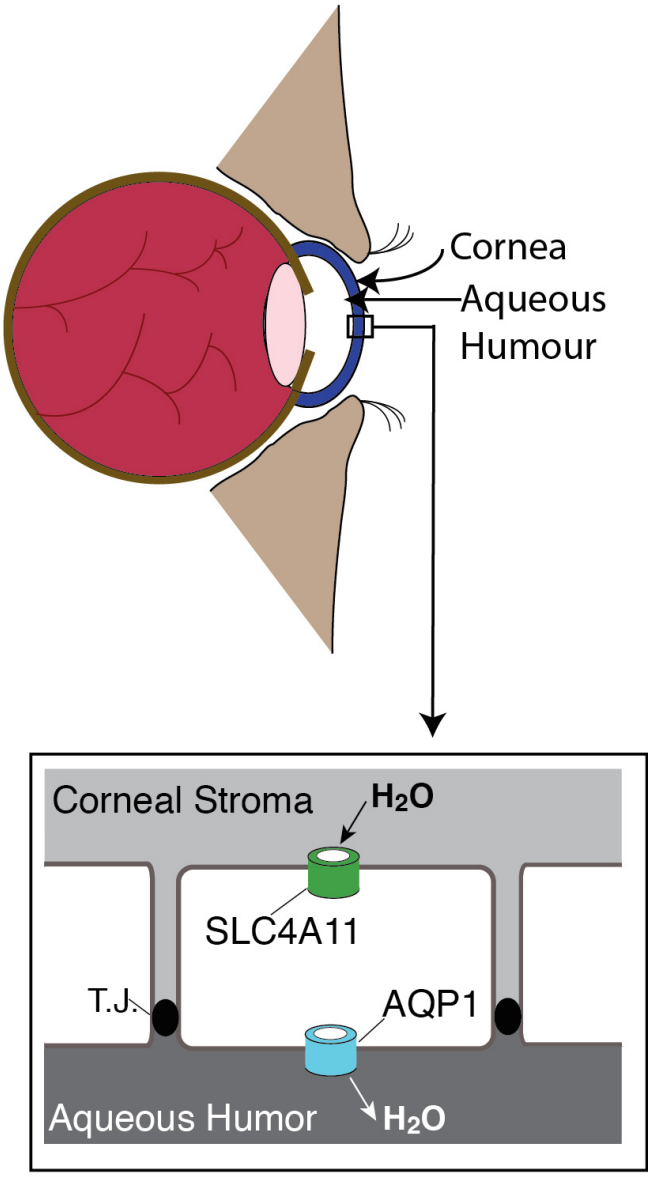

Figure 1.6 Schematic representation of SLC4A11 and AQP1 in human cornea. SLC4A11 is localized to basolateral side of corneal endothelium facing the stroma whereas AQP1 is localized to apical side facing aqueous humor. SLC4A11 and AQP1 localization in endothelial cells suggests they may work cooperatively to provide a water conductive pathway through the endothelial layer. T.J. represents the tight junction that connects cells of the endothelium [1].

basolateral water flux is important in regulating corneal transparency comes from the fact that SLC4A11 mutants cause corneal dystrophies whereas there are no known reports of severe endothelial corneal dystrophies caused by AQP1 mutations [1].

1.8.6 Mouse models of SLC4A11

Three independent mouse models of SLC4A11 have been reported [1, 112-114]. The first model was generated, using injection of retroviral vector into embryonic stem cells to perform insertional deletion of *slc4a11* gene. These mice had a mild corneal phenotype but significant hearing abnormalities [112]. The second model was generated by inserting a β-galactosidase reporter gene in frame resulting in truncation of the *slc4a11*gene before the first predicted transmembrane domain. Mice generated by this method exhibited thickening of the corneal stroma and Descement's membrane, impaired urinary concentration, increased urinary volume and stress-induced morphological changes of fibrocytes of the inner ear resulting in deafness [113]. The third model was generated using *Cre-lox* system in which exons 9 to 13 of *slc4a11* gene were modified by lox P elements and *Cre* mediated deletion. The knock out mouse has hazy corneas indicating corneal oedema and a progressive increase in corneal thickness. At 32 weeks, membrane ruffling, indicative of cell swelling was observed. Decreased urine osmolarity and electrolyte concentrations were also found in the knock out mouse [1, 114]. Although there are phenotypic differences owing to their method of gene modification, *slc4a11* knock out mouse models recapitulate the key aspects of human corneal dystrophies and hearing abnormalities caused by *SLC4A11* mutations. The mouse models also indicate some kidney related abnormalities, although nothing similar is found in patients [115].

1.9 Thesis objectives

The objectives of the thesis are to examine the feasibility of folding correction therapy as an approach to treat mis-sense mutations of SLC4A11 and ultimately to understand the structure-function relationships of SLC4A11 protein. Until the last decade, SLC4A11 was a relatively unknown protein and the discovery that its mutations cause corneal dystrophies made studying this protein more important than ever. The preliminary studies helped us to understand the role of SLC4A11 in the context of corneal dystrophies. The thesis work sheds more light on the SLC4A11 protein so that effective therapeutic strategies can be developed in future to treat the corneal diseases caused by *SLC4A11* mutations.

Chapter 2 of the thesis lists all the experimental materials and methods used to carry out the research studies. Chapter 3 of the thesis focuses on the endoplasmic reticulum-retained SLC4A11 mutants and the feasibility of rescuing them to the plasma membrane surface. Chapter 4 of the thesis focuses on testing the role of SLC4A11 membrane and cytoplasmic domains in the function of the protein with the ultimate goal of deciphering structure-function relationship in SLC4A11. Chapter 5 summarizes the key findings of the thesis and postulates future directions towards examining SLC4A11 role in healthy corneal endothelium.

1.10 References

1. Vilas, G. L., Loganathan, S. K., Liu, J., Riau, A. K., Young, J. D., Mehta, J. S., Vithana, E. N. and Casey, J. R. (2013) Transmembrane water-flux through SLC4A11: a route defective in genetic corneal diseases. Human Molecular Genetics. **22**, 4579-4590
2. Parker, M. D., Ourmozdi, E. P. and Tanner, M. J. (2001) Human BTR1, a New Bicarbonate Transporter Superfamily Member and Human AE4 from Kidney. Biochem. Biophys. Res. Commun. **282**, 1103-1109
3. Park, M., Li, Q., Shcheynikov, N., Zeng, W. and Muallem, S. (2004) NaBC1 is a ubiquitous electrogenic Na^+ -coupled borate transporter essential for cellular boron homeostasis and cell growth and proliferation. Mol. Cell. **16**, 331-341
4. Scott, R. L. P. and Cannon, B. D. P. (2015) Ophthalmology. Magill's Medical Guide (Online Edition)
5. Ruberti, J. W., Sinha Roy, A. and Roberts, C. J. (2011) Corneal Biomechanics and Biomaterials. Annual Review of Biomedical Engineering. **13**, 269-295
6. DelMonte, D. W. and Kim, T. (2011) Anatomy and physiology of the cornea. Journal of Cataract & Refractive Surgery. **37**, 588-598
7. Beuerman, R. W. and Pedroza, L. (1996) Ultrastructure of the human cornea. Microscopy Research and Technique. **33**, 320-335
8. Farjo A, M. M., Soong HK. (2008) Corneal anatomy, physiology, and wound healing. In: Yanoff M, Duker JS, eds, Ophthalmology, 3rd ed. St. Louis, MO, Mosby, 203–208
9. Wiley, L., SundarRaj, N., Sun, T. T. and Thoft, R. A. (1991) Regional heterogeneity in human corneal and limbal epithelia: an immunohistochemical evaluation. Investigative Ophthalmology & Visual Science. **32**, 594-602
10. Hayashi, S., Osawa, T. and Tohyama, K. (2002) Comparative observations on corneas, with special reference to bowman's layer and descemet's membrane in mammals and amphibians. Journal of Morphology. **254**, 247-258
11. Germundsson, J., Karanis, G., Fagerholm, P. and Lagali, N. (2013) Age-Related Thinning of Bowman's Layer in the Human Cornea In VivoAge-Related Thinning

of Bowman's Layer. Investigative Ophthalmology & Visual Science. **54**, 6143-6149

12. Chen, S., Mienaltowski, M. J. and Birk, D. E. (2015) Regulation of corneal stroma extracellular matrix assembly. Experimental Eye Research. **133**, 69-80
13. Hassell, J. R. and Birk, D. E. (2010) The molecular basis of corneal transparency. Experimental Eye Research. **91**, 326-335
14. Meek, K. M. and Leonard, D. W. (1993) Ultrastructure of the corneal stroma: a comparative study. Biophysical Journal. **64**, 273-280
15. Tuft, S. J. and Coster, D. J. (1990) The corneal endothelium. Eye. **4**, 389-424
16. Bourne, W. M. (2003) Biology of the corneal endothelium in health and disease. Eye (Lond). **17**, 912-918
17. Bourne, W. M., Nelson, L. R. and Hodge, D. O. (1997) Central corneal endothelial cell changes over a ten-year period. Investigative Ophthalmology & Visual Science. **38**, 779-782
18. Brubaker, R. F. (1991) Flow of aqueous humor in humans [The Friedenwald Lecture]. Investigative Ophthalmology & Visual Science. **32**, 3145-3166
19. Bonanno, J. A. (2003) Identity and regulation of ion transport mechanisms in the corneal endothelium. Prog Retin Eye Res. **22**, 69-94
20. Bonanno, J. A. (2012) Molecular mechanisms underlying the corneal endothelial pump. Exp Eye Res. **95**, 2-7
21. Fischbarg, J. (2012) Water channels and their roles in some ocular tissues. Molecular Aspects of Medicine. **33**, 638-641
22. Schey, K. L., Wang, Z., L. Wenke, J. and Qi, Y. (2014) Aquaporins in the eye: Expression, function, and roles in ocular disease. Biochimica et Biophysica Acta (BBA) - General Subjects. **1840**, 1513-1523
23. Vithana, E. N., Morgan, P., Sundaresan, P., Ebenezer, N. D., Tan, D. T., Mohamed, M. D., Anand, S., Khine, K. O., Venkataraman, D., Yong, V. H., Salto-Tellez, M., Venkatraman, A., Guo, K., Hemadevi, B., Srinivasan, M., Prajna, V., Khine, M., Casey, J. R., Inglehearn, C. F. and Aung, T. (2006) Mutations in sodium-borate cotransporter SLC4A11 cause recessive congenital hereditary endothelial dystrophy (CHED2). Nature Genetics. **38**, 755-757

24. Vithana, E. N., Morgan, P. E., Ramprasad, V., Tan, D. T., Yong, V. H., Venkataraman, D., Venkatraman, A., Yam, G. H., Nagasamy, S., Law, R. W., Rajagopal, R., Pang, C. P., Kumaramanickevel, G., Casey, J. R. and Aung, T. (2008) SLC4A11 Mutations in Fuchs Endothelial Corneal Dystrophy (FECD). Hum. Mol. Genet. **17**, 656-666

25. Desir, J. and Abramowicz, M. (2008) Congenital hereditary endothelial dystrophy with progressive sensorineural deafness (Harboyan syndrome). Orphanet J Rare Dis. **3**, 28-36

26. Klintworth, G. K. (2009) Corneal dystrophies. Orphanet. J. Rare Dis. **4**, 7

27. Vincent, A. L. (2014) Corneal dystrophies and genetics in the International Committee for Classification of Corneal Dystrophies era: a review. Clinical & Experimental Ophthalmology. **42**, 4-12

28. Schmedt, T., Silva, M. M., Ziaei, A. and Jurkunas, U. (2012) Molecular bases of corneal endothelial dystrophies. Experimental Eye Research. **95**, 24-34

29. Aldave, A. J., Han, J. and Frausto, R. F. (2013) Genetics of the corneal endothelial dystrophies: an evidence-based review. Clinical Genetics. **84**, 109-119

30. Puangsricharern, V., Yeetong, P., Charumalai, C., Suphapeetiporn, K. and Shotelersuk, V. (2014) Two novel mutations including a large deletion of the SLC4A11 gene causing autosomal recessive hereditary endothelial dystrophy. British Journal of Ophthalmology. **98**, 1460-1462

31. Hemadevi, B., Veitia, R. A., Srinivasan, M., Arunkumar, J., Prajna, N. V., Lesaffre, C. and Sundaresan, P. (2008) Identification of mutations in the SLC4A11 gene in patients with recessive congenital hereditary endothelial dystrophy. Arch Ophthalmol. **126**, 700-708

32. Jiao, X., Sultana, A., Garg, P., Ramamurthy, B., Vemuganti, G. K., Gangopadhyay, N., Hejtmancik, J. F. and Kannabiran, C. (2007) Autosomal recessive corneal endothelial dystrophy (CHED2) is associated with mutations in SLC4A11. J Med Genet. **44**, 64-68.

33. Ramprasad, V. L., Ebenezer, N. D., Aung, T., Rajagopal, R., Yong, V. H., Tuft, S. J., Viswanathan, D., El-Ashry, M. F., Liskova, P., Tan, D. T., Bhattacharya, S. S., Kumaramanickavel, G. and Vithana, E. N. (2007) Novel SLC4A11 mutations in

patients with recessive congenital hereditary endothelial dystrophy (CHED2). Mutation in brief #958. Online. Hum. Mutat. **28**, 522-523

34. Sultana, A., Garg, P., Ramamurthy, B., Vemuganti, G. K. and Kannabiran, C. (2007) Mutational spectrum of the SLC4A11 gene in autosomal recessive congenital hereditary endothelial dystrophy. Mol Vis. **13**, 1327-1332
35. Park, S. H., Jeong, H. J., Kim, M. and Kim, M. S. (2013) A Novel Nonsense Mutation of the SLC4A11 Gene in a Korean Patient With Autosomal Recessive Congenital Hereditary Endothelial Dystrophy. Cornea. **32**, e181-e182
36. Paliwal, P., Sharma, A., Tandon, R., Sharma, N., Titiyal, J. S., Sen, S., Nag, T. C. and Vajpayee, R. B. (2010) Congenital hereditary endothelial dystrophy - mutation analysis of SLC4A11 and genotype-phenotype correlation in a North Indian patient cohort. Mol Vis. **16**, 2955-2963
37. Aldahmesh, M., Khan, A., Meyer, B. and Alkuraya, F. (2009) Mutational Spectrum of SLC4A11 in Autosomal Recessive CHED in Saudi Arabia. Invest Ophthalmol Vis Sci. **50**, 4142-4145
38. Shah, S. S., Al-Rajhi, A., Brandt, J. D., Mannis, M. J., Roos, B., Sheffield, V. C., Syed, N. A., Stone, E. M. and Fingert, J. H. (2008) Mutation in the SLC4A11 gene associated with autosomal recessive congenital hereditary endothelial dystrophy in a large Saudi family. Ophthalmic Genet. **29**, 41-45
39. Aldave, A. J., Yellore, V. S., Bourla, N., Momi, R. S., Khan, M. A., Salem, A. K., Rayner, S. A., Glasgow, B. J. and Kurtz, I. (2007) Autosomal Recessive CHED Associated With Novel Compound Heterozygous Mutations in SLC4A11. Cornea. **26**, 896-900
40. Kumar, A., Bhattacharjee, S., Prakash, D. R. and Sadanand, C. S. (2007) Genetic analysis of two Indian families affected with congenital hereditary endothelial dystrophy: two novel mutations in SLC4A11. Mol Vis. **13**, 39-46.
41. Biswas, S., Munier, F. L., Yardley, J., Hart-Holden, N., Perveen, R., Cousin, P., Sutphin, J. E., Noble, B., Batterbury, M., Kielty, C., Hackett, A., Bonshek, R., Ridgway, A., McLeod, D., Sheffield, V. C., Stone, E. M., Schorderet, D. F. and Black, G. C. (2001) Missense mutations in COL8A2, the gene encoding the

alpha2 chain of type VIII collagen, cause two forms of corneal endothelial dystrophy. Hum. Mol. Genet. **10**, 2415-2423.

42. Iliff, B. W., Riazuddin, S. A. and Gottsch, J. D. (2012) The genetics of Fuchs' corneal dystrophy. Expert Rev Ophthalmol. **7**, 363-375

43. Zhang, J. and Patel, D. V. (2015) The pathophysiology of Fuchs' endothelial dystrophy – A review of molecular and cellular insights. Experimental Eye Research. **130**, 97-105

44. Riazuddin, S. A., McGlumphy, E. J., Yeo, W. S., Wang, J., Katsanis, N. and Gottsch, J. D. (2011) Replication of the TCF4 intronic variant in late-onset Fuchs corneal dystrophy and evidence of independence from the FCD2 locus. Invest. Ophthalmol. Vis. Sci. **52**, 2825-2829

45. Riazuddin, S. A., Parker, D. S., McGlumphy, E. J., Oh, E. C., Iliff, B. W., Schmedt, T., Jurkunas, U., Schleif, R., Katsanis, N. and Gottsch, J. D. (2012) Mutations in LOXHD1, a recessive-deafness locus, cause dominant late-onset Fuchs corneal dystrophy. Am. J. Hum. Genet. **90**, 533-539

46. Riazuddin, S. A., Zaghloul, N. A., Al-Saif, A., Davey, L., Diplas, B. H., Meadows, D. N., Eghrari, A. O., Minear, M. A., Li, Y. J., Klintworth, G. K., Afshari, N., Gregory, S. G., Gottsch, J. D. and Katsanis, N. (2010) Missense mutations in TCF8 cause late-onset Fuchs corneal dystrophy and interact with FCD4 on chromosome 9p. Am. J. Hum. Genet. **86**, 45-53

47. Riazuddin, S. A., Vithana, E. N., Seet, L. F., Liu, Y., Al-Saif, A., Koh, L. W., Heng, Y. M., Aung, T., Meadows, D. N., Eghrari, A. O., Gottsch, J. D. and Katsanis, N. (2010) Missense mutations in the sodium borate co-transporter SLC4A11 cause late onset Fuchs corneal dystrophy. Hum. Mutat. **31**, 1261-1268

48. Soumittra, N., Loganathan, S. K., Madhavan, D., Ramprasad, V. L., Arokiasamy, T., Sumathi, S., Karthiyayini, T., Rachapalli, S. R., Kumaramanickavel, G., Casey, J. R. and Rajagopal, R. (2014) Biosynthetic and functional defects in newly identified SLC4A11 mutants and absence of COL8A2 mutations in Fuchs endothelial corneal dystrophy. J Hum Genet. **59**, 444-453

49. Minear, M. A., Li, Y.-J., Rimmler, J., Balajonda, E., Watson, S., Allingham, R. R., Hauser, M. A., Klintworth, G. K., Afshari, N. A. and Gregory, S. G. (2013)

Genetic screen of African Americans with Fuchs endothelial corneal dystrophy. Molecular Vision. **19**, 2508-2516

50. Desir, J., Moya, G., Reish, O., Van Regemorter, N., Deconinck, H., David, K. L., Meire, F. M. and Abramowicz, M. (2007) Borate transporter SLC4A11 mutations cause both Harboyan syndrome and non-syndromic corneal endothelial dystrophy. J. Med. Genet. **44**, 322-326
51. Wain, H. M., Lush, M. J., Ducluzeau, F., Khodiyar, V. K. and Povey, S. (2004) Genew: the Human Gene Nomenclature Database, 2004 updates. Nucleic Acids Res. **32**, D255-257
52. Alka, K. and Casey, J. R. (2014) Bicarbonate transport in health and disease. IUBMB Life. **66**, 596-615
53. Cordat, E. and Casey, J. R. (2009) Bicarbonate transport in cell physiology and disease. The Biochemical Journal. **417**, 423-439
54. Kopito, R. R. and Lodish, H. F. (1985) Primary structure and transmembrane orientation of the murine anion exchange protein. Nature. **316**, 234-238
55. Alper, S. L., Kopito, R. R., Libresco, S. M. and Lodish, H. F. (1988) Cloning and characterization of a murine Band 3-related cDNA from kidney and a lymphoid cell line. J. Biol. Chem. **263**, 17092-17099
56. Kudrycki, K. E., Newman, P. R. and Shull, G. E. (1990) cDNA cloning and tissue distribution of mRNAs for two proteins that are related to the Band 3 Cl^-/HCO_3^- exchanger. J. Biol. Chem. **265**, 462-471
57. Pushkin, A., Abuladze, N., Newman, D., Lee, I., Xu, G. and Kurtz, I. (2000) Cloning, characterization and chromosomal assignment of NBC4, a new member of the sodium bicarbonate cotransporter family. Biochim Biophys Acta. **1493**, 215-218
58. Sassani, P., Pushkin, A., Gross, E., Gomer, A., Abuladze, N., Dukkipati, R., Carpenito, G. and Kurtz, I. (2002) Functional characterization of NBC4: a new electrogenic sodium-bicarbonate cotransporter. Am J Physiol Cell Physiol. **282**, C408-416

59. Virkki, L. V., Wilson, D. A., Vaughan-Jones, R. D. and Boron, W. F. (2002) Functional characterization of human NBC4 as an electrogenic Na^+-HCO_3^- cotransporter (NBCe2). Am J Physiol Cell Physiol. **282**, C1278-1289

60. Xu, J., Wang, Z., Barone, S., Petrovic, M., Amlal, H., Conforti, L., Petrovic, S. and Soleimani, M. (2003) Expression of the Na^+-HCO_3^- cotransporter NBC4 in rat kidney and characterization of a novel NBC4 variant. Am J Physiol Renal Physiol. **284**, F41-50

61. Burnham, C. E., Amlal, H., Wang, Z., Shull, G. E. and Soleimani, M. (1997) Cloning and functional expression of a human kidney Na^+:HCO_3^- cotransporter. J. Biol. Chem. **272**, 19111-19114

62. Romero, M. F., Hediger, M. A., Boulpaep, E. L. and Boron, W. F. (1997) Expression cloning and characterization of a renal electrogenic Na^+/HCO_3^- cotransporter. Nature. **387**, 409-413

63. Abuladze, N., Lee, I., Newman, D., Hwang, J., Boorer, K., Pushkin, A. and Kurtz, I. (1998) Molecular cloning, chromosomal localization, tissue distribution, and functional expression of the human pancreatic sodium bicarbonate cotransporter. J. Biol. Chem. **273**, 17689-17695

64. Choi, I., Romero, M. F., Khandoudi, N., Bril, A. and Boron, W. F. (1999) Cloning and characterization of a human electrogenic Na^+-HCO_3^- cotransporter isoform (hhNBC). Am. J. Physiol. **276**, C576-584

65. Bevensee, M. O., Schmitt, B. M., Choi, I., Romero, M. F. and Boron, W. F. (2000) An electrogenic Na^+-HCO_3^- cotransporter (NBC) with a novel COOH-terminus, cloned from rat brain. Am. J. Physiol. **278**, C1200-C1211

66. Sun, X. C. and Bonanno, J. A. (2003) Identification and cloning of the Na/HCO_3^- cotransporter (NBC) in human corneal endothelium. Exp Eye Res. **77**, 287-295

67. Ishibashi, K., Sasaki, S. and Marumo, F. (1998) Molecular cloning of a new sodium bicarbonate cotransporter cDNA from human retina. Biochem. Biophys. Res. Commun. **246**, 535-538

68. Pushkin, A., Abuladze, N., Lee, I., Newman, D., Hwang, J. and Kurtz, I. (1999) Cloning, tissue distribution, genomic organization, and functional characterization

of NBC3, a new member of the sodium bicarbonate cotransporter family. J. Biol. Chem. **274**, 16569-16575

69. Choi, I., Aalkjaer, C., Boulpaep, E. L. and Boron, W. F. (2000) An electroneutral sodium/bicarbonate cotransporter NBCn1 and associated sodium channel. Nature. **405**, 571-575

70. Grichtchenko, II, Choi, I., Zhong, X., Bray-Ward, P., Russell, J. M. and Boron, W. F. (2001) Cloning, characterization, and chromosomal mapping of a human electroneutral Na^+-driven Cl^- /HCO_3^- exchanger. J Biol Chem. **276**, 8358-8363

71. Romero, M. F., Henry, D., Nelson, S., Harte, P. J., Dillon, A. K. and Sciortino, C. M. (2000) Cloning and characterization of a Na^+ driven anion exchanger (NDAE1): a new bicarbonate transporter. J. Biol. Chem. **275**, 24552-24559

72. Wang, Z., Conforti, L., Petrovic, S., Amlal, H., Burnham, C. E. and Soleimani, M. (2001) Mouse Na^+: HCO_3^- cotransporter isoform NBC-3 (kNBC-3): cloning, expression, and renal distribution. Kidney Int. **59**, 1405-1414

73. Parker, M. D., Boron, W. F. and Tanner, M. J. (2002) Characterization of human "AE4" as an electroneutral sodium bicarbonate cotransporter. FASEB J. **16**, A796

74. Romero, M. F., Fulton, C. M. and Boron, W. F. (2004) The SLC4 family of HCO_3^- transporters. Pflugers Arch. **447**, 496-509

75. Tsuganezawa, H., Kobayashi, K., Iyori, M., Araki, T., Koizumi, A., Watanabe, S. I., Kaneko, A., Fukao, T., Monkawa, T., Yoshida, T., Kim, D. K., Kanai, Y., Endou, H., Hayashi, M. and Saruta, T. (2001) A new member of the HCO_3^- transporter superfamily is an apical anion exchanger of beta-intercalated cells in the kidney. J Biol Chem. **276**, 8180-8189

76. Wang, C. Z., Yano, H., Nagashima, K. and Seino, S. (2000) The Na^+-driven Cl^- /HCO_3^- exchanger: Cloning, tissue distribution, and functional characterization. J Biol Chem. **275**, 35486-35490

77. Parker, M. D., Musa-Aziz, R., Rojas, J. D., Choi, I., Daly, C. M. and Boron, W. F. (2008) Characterization of human SLC4A10 as an electroneutral Na/HCO_3 cotransporter (NBCn2) with Cl^- self-exchange activity. J Biol Chem. **283**, 12777-12788

78. Praetorius, J., Nejsum, L. N. and Nielsen, S. (2004) A SLC4A10 gene product maps selectively to the basolateral plasma membrane of choroid plexus epithelial cells. Am J Physiol Cell Physiol. **286**, C601-610

79. Perez, N. G., Alvarez, B. V., Camilion de Hurtado, M. C. and Cingolani, H. E. (1995) pHi regulation in myocardium of the spontaneously hypertensive rat. Compensated enhanced activity of the Na^+-H^+ exchanger. Circ Res. **77**, 1192-1200

80. Alvarez, B. V., Fujinaga, J. and Casey, J. R. (2001) Molecular Basis for angiotensin II-induced increase of chloride/bicarbonate exchange in the myocardium. Circ. Research. **89**, 1246-1253

81. Alvarez, B. V., Xia, Y., Sowah, D., Soliman, D., Light, P., Karmazyn, M. and Casey, J. R. (2007) A Carbonic Anhydrase Inhibitor Prevents and Reverts Cardiomyocyte Hypertrophy. J. Physiol. **579**, 127-145

82. Eber, S. a. L., S. E. (2004) Hereditary spherocytosis--defects in proteins that connect the membrane skeleton to the lipid bilayer. Semin Hematol. **41**, 118-141

83. Alloisio, N., Texier, P., Vallier, A., Ribeiro, M. L., Morle, L., Bozon, M., Bursaux, E., Maillet, P., Goncalves, P., Tanner, M. J., Tamagnini, G. and Delaunay, J. (1997) Modulation of clinical expression and band 3 deficiency in hereditary spherocytosis. Blood. **90**, 414-420

84. Ribeiro, M. L., Alloisio, N., Almeida, H., Gomes, C., Texier, P., Lemos, C., Mimoso, G., Morle, L., Bey-Cabet, F., Rudigoz, R. C., Delaunay, J. and Tamagnini, G. (2000) Severe hereditary spherocytosis and distal renal tubular acidosis associated with the total absence of band 3. Blood. **96**, 1602-1604

85. Perrotta, S., Borriello, A., Scaloni, A., De Franceschi, L., Brunati, A. M., Turrini, F., Nigro, V., del Giudice, E. M., Nobili, B., Conte, M. L., Rossi, F., Iolascon, A., Donella-Deana, A., Zappia, V., Poggi, V., Anong, W., Low, P., Mohandas, N. and Della Ragione, F. (2005) The N-terminal 11 amino acids of human erythrocyte band 3 are critical for aldolase binding and protein phosphorylation: implications for band 3 function. Blood. **106**, 4359-4366

86. Toye, A. M., Williamson, R. C., Khanfar, M., Bader-Meunier, B., Cynober, T., Thibault, M., Tchernia, G., Déchaux, M., Delaunay, J. and Bruce, L. J. (2008)

Band 3 Courcouronnes (Ser667Phe): a trafficking mutant differentially rescued by wild-type band 3 and glycophorin A

87. Dinour, D., Chang, M. H., Satoh, J., Smith, B. L., Angle, N., Knecht, A., Serban, I., Holtzman, E. J. and Romero, M. F. (2004) A novel missense mutation in the sodium bicarbonate cotransporter (NBCe1/SLC4A4) causes proximal tubular acidosis and glaucoma through ion transport defects. J Biol Chem. **279**, 52238-52246.

88. Igarashi, T., Inatomi, J., Sekine, T., Seki, G., Shimadzu, M., Tozawa, F., Takeshima, Y., Takumi, T., Takahashi, T., Yoshikawa, N., Nakamura, H. and Endou, H. (2001) Novel nonsense mutation in the Na^+/HCO_3^- cotransporter gene (SLC4A4) in a patient with permanent isolated proximal renal tubular acidosis and bilateral glaucoma. J Am Soc Nephrol. **12**, 713-718

89. Igarashi, T., Inatomi, J., Sekine, T., Cha, S. H., Kanai, Y., Kunimi, M., Tsukamoto, K., Satoh, H., Shimadzu, M., Tozawa, F., Mori, T., Shiobara, M., Seki, G. and Endou, H. (1999) Mutations in SLC4A4 cause permanent isolated proximal renal tubular acidosis with ocular abnormalities. Nat. Genet. **23**, 264-266

90. Inatomi, J., Horita, S., Braverman, N., Sekine, T., Yamada, H., Suzuki, Y., Kawahara, K., Moriyama, N., Kudo, A., Kawakami, H., Shimadzu, M., Endou, H., Fujita, T., Seki, G. and Igarashi, T. (2004) Mutational and functional analysis of SLC4A4 in a patient with proximal renal tubular acidosis. Pflugers Arch. **448**, 438-444

91. Horita, S., Yamada, H., Inatomi, J., Moriyama, N., Sekine, T., Igarashi, T., Endo, Y., Dasouki, M., Ekim, M., Al-Gazali, L., Shimadzu, M., Seki, G. and Fujita, T. (2005) Functional analysis of NBC1 mutants associated with proximal renal tubular acidosis and ocular abnormalities. J Am Soc Nephrol. **16**, 2270-2278.

92. Demirci, F. Y., Chang, M. H., Mah, T. S., Romero, M. F. and Gorin, M. B. (2006) Proximal renal tubular acidosis and ocular pathology: a novel missense mutation in the gene (SLC4A4) for sodium bicarbonate cotransporter protein (NBCe1). Mol Vis. **12**, 324-330.

93. Shayakul, C. and Alper, S. L. (2000) Inherited renal tubular acidosis. Current opinion in nephrology and hypertension. **9**, 541-546

94. Cordat, E. (2006) Unraveling trafficking of the kidney anion exchanger 1 in polarized MDCK epithelial cells. Biochem Cell Biol. **84**, 949-959.

95. Vilas, G. L., Johnson, D. E., Freund, P. and Casey, J. R. (2009) Characterization of an epilepsy-associated variant of the human Cl^-/HCO_3^- exchanger AE3. American Journal of Physiology. Cell physiology. **297**, C526-536

96. Sander, T., Toliat, M. R., Heils, A., Leschik, G., Becker, C., Ruschendorf, F., Rohde, K., Mundlos, S. and Nurnberg, P. (2002) Association of the 867Asp variant of the human anion exchanger 3 gene with common subtypes of idiopathic generalized epilepsy. Epilepsy Res. **51**, 249-255

97. Romero, M. F., Chen, A.-P., Parker, M. D. and Boron, W. F. (2013) The SLC4 Family of Bicarbonate (HCO_3^-) Transporters. Molecular aspects of medicine. **34**, 159-182

98. Krepischi, A. C. V., Knijnenburg, J., Bertola, D. R., Kim, C. A., Pearson, P. L., Bijlsma, E., Szuhai, K., Kok, F., Vianna-Morgante, A. M. and Rosenberg, C. (2010) Two distinct regions in 2q24.2-q24.3 associated with idiopathic epilepsy. Epilepsia. **51**, 2457-2460

99. Sebat, J., Lakshmi, B., Malhotra, D., Troge, J., Lese-Martin, C., Walsh, T., Yamrom, B., Yoon, S., Krasnitz, A., Kendall, J., Leotta, A., Pai, D., Zhang, R., Lee, Y.-H., Hicks, J., Spence, S. J., Lee, A. T., Puura, K., Lehtimäki, T., Ledbetter, D., Gregersen, P. K., Bregman, J., Sutcliffe, J. S., Jobanputra, V., Chung, W., Warburton, D., King, M.-C., Skuse, D., Geschwind, D. H., Gilliam, T. C., Ye, K. and Wigler, M. (2007) Strong Association of De Novo Copy Number Mutations with Autism. Science (New York, N.Y.). **316**, 445-449

100. Vilas, G. L., Loganathan, S., Quon, A., Sundaresan, P., Vithana, E. N. and Casey, J. R. (2012) Oligomerization of SLC4A11 protein and the severity of FECD and CHED2 corneal dystrophies caused by SLC4A11 mutations. Human Mutation. **33**, 419-428

101. Vilas, G. L., Morgan, P. E., Loganathan, S., Quon, A. and Casey, J. R. (2011) Biochemical Framework for SLC4A11, the Plasma Membrane Protein Defective in Corneal Dystrophies. Biochemistry. **50**, 2157-2169

102. Damkier, H. H., Nielsen, S. and Praetorius, J. (2007) Molecular expression of SLC4 derived Na^+ dependent anion transporters in selected human tissues. Am. J Physiol. Regul. Integr. Comp. Physiol. **293**, R2136-2146

103. Liu, J., Seet, L.-F., Koh, L. W., Venkatraman, A., Venkataraman, D., Mohan, R. R., Praetorius, J., Bonanno, J. A., Aung, T. and Vithana, E. N. (2012) Depletion of SLC4A11 Causes Cell Death by Apoptosis in an Immortalized Human Corneal Endothelial Cell Line. Investigative Ophthalmology & Visual Science. **53**, 3270-3279

104. Ogando, D. G., Jalimarada, S. S., Zhang, W., Vithana, E. N. and Bonanno, J. A. (2013) SLC4A11 is an EIPA-sensitive Na^+ permeable pHi regulator. American Journal of Physiology - Cell Physiology. **305**, C716-C727

105. Kao, L., Azimov, R., Abuladze, N., Newman, D. and Kurtz, I. (2015) Human SLC4A11-C functions as a DIDS-stimulatable $H^+(OH^-)$ permeation pathway: partial correction of R109H mutant transport. American Journal of Physiology - Cell Physiology. **308**, C176-C188

106. Cordat, E., Kittanakom, S., Yenchitsomanus, P. T., Li, J., Du, K., Lukacs, G. L. and Reithmeier, R. A. (2006) Dominant and Recessive Distal Renal Tubular Acidosis Mutations of Kidney Anion Exchanger 1 Induce Distinct Trafficking Defects in MDCK Cells. Traffic. **7**, 117-128.

107. Quilty, J. A., Cordat, E. and Reithmeier, R. A. (2002) Impaired trafficking of human kidney anion exchanger (kAE1) caused by hetero-oligomer formation with a truncated mutant associated with distal renal tubular acidosis. Biochem J. **13**, 895-903

108. Alper, S. L. (2009) Molecular physiology and genetics of Na^+-independent SLC4 anion exchangers. J Exp Biol. **212**, 1672-1683

109. Takano, J., Noguchi, K., Yasumori, M., Kobayashi, M., Gajdos, Z., Miwa, K., Hayashi, H., Yoneyama, T. and Fujiwara, T. (2002) Arabidopsis boron transporter for xylem loading. Nature. **420**, 337-340.

110. O'Neill, M. A., Ishii, T., Albersheim, P. and Darvill, A. G. (2004) Rhamnogalacturonan II: structure and function of a borate cross-linked cell wall pectic polysaccharide. Annu. Rev. Plant Biol. **55**, 109-139.

111. Jalimarada, S. S., Ogando, D. G., Vithana, E. N. and Bonanno, J. A. (2013) Ion Transport Function of SLC4A11 in Corneal Endothelium. Investigative Ophthalmology & Visual Science. **54**, 4330-4340

112. Lopez, I. A., Rosenblatt, M. I., Kim, C., Galbraith, G. G., Jones, S. M., Kao, L., Newman, D., Liu, W., Yeh, S., Pushkin, A., Abuladze, N. and Kurtz, I. (2009) Slc4a11 gene disruption in mice: Cellular targets of sensorineuronal abnormalities. J. Biol. Chem. **28**, 26882-26896

113. Groeger, N., Froehlich, H., Maier, H., Olbrich, A., Kostin, S., Braun, T. and Boettger, T. (2010) Slc4a11 prevents osmotic imbalance leading to corneal endothelial dystrophy, deafness, and polyuria. J. Biol. Chem. **285**, 14467-14474

114. Han, S. B., Ang, H.-P., Poh, R., Chaurasia, S. S., Peh, G., Liu, J., Tan, D. T. H., Vithana, E. N. and Mehta, J. S. (2013) Mice With a Targeted Disruption of Slc4a11 Model the Progressive Corneal Changes of Congenital Hereditary Endothelial Dystrophy. Investigative Ophthalmology & Visual Science. **54**, 6179-6189

115. Liskova, P., Dudakova, L., Tesar, V., Bednarova, V., Kidorova, J., Jirsova, K., Davidson, A. E. and Hardcastle, A. J. (2015) Detailed Assessment of Renal Function in a Proband with Harboyan Syndrome Caused by a Novel Homozygous SLC4A11 Nonsense Mutation. Ophthalmic Research. **53**, 30-35

Chapter 2: Materials and Methods

2.1 Materials

Oligonucleotides were from Integrated DNA Technologies (Coralville, IA). T4 DNA ligase, PNGase F and Endo H and restriction enzymes were from New England Biolabs (Ipswich, MA). QuikChange Lightning Site Directed Mutagenesis Kit was from Agilent Technologies (Mississauga, ON, Canada). Pfx DNA Polymerase, Dulbecco's modified Eagle's medium (DMEM), fetal bovine serum (FBS), calf serum (CS), penicillin-streptomycin-glutamine (PSG), Geneticin, LIVE/DEAD Cell Vitality Assay Kit (L34951) and Dynabeads Protein G resin were from Life Technologies (Carlsbad, CA, USA). Infusion cloning system was from Clontech Laboratories Inc. (Mountain View, CA, USA). PCR and restriction digests products were purified by agarose gel electrophoresis and extraction, using the Gel Extraction Kit (Froggabio, Ontario, Canada). Plasmid DNA was purified, using the HiSpeed Plus Plasmid Purification Kit (Qiagen, Mississauga, ON, Canada). Cell culture dishes were from Sarstedt (Montreal, QC, Canada). Complete Protease Inhibitor tablets were from Roche Applied Science (Indianapolis, IN, USA). BCA Protein Assay Kit was from Pierce (Rockford, IL, USA). Immobilized Streptavidin Sepharose resin, sulfo-NHS-SS-biotin and glass coverslips were from Thermo Fisher Scientific (Ottawa, ON, Canada). Poly-L-lysine and staurosporine were from Sigma-Aldrich (Oakville, ON, Canada). Hydrogen peroxide was from Ricca Chemical company (Arlington, TX, USA). Immobilon-P PVDF was from Millipore (Billerica, MA). Monoclonal antibodies against HA (clone 16B12) and GAPDH were from Covance (Princeton, NJ, USA) and Santa Cruz Biotechnology (Santa Cruz, CA, USA), respectively. Mouse (clone 4A6) and rabbit anti-Myc antibodies were from Millipore (Billerica, MA, USA) and Abcam (Cambridge, MA, USA), respectively.

Rabbit anti-caspase-3 and anti-Cleaved caspase-3 were from Cell signaling Technology (Danvers, MA, USA). Mouse anti-AE1 monoclonal antibody (IVF12) was a generous gift from Dr. Michael Jennings, University of Arkansas [1]. Mouse Anti-His and Horseradish peroxidase-conjugated sheep anti-mouse IgG was from GE Healthcare Bio-Sciences Corp. (Piscattaway, NJ, USA). ECL chemiluminescent reagent was from Perkin Elmer Life Sciences (Waltham, MA) or Millipore (Billerica, MA, USA).

2.2 DNA constructs

Integrity of all the clones was confirmed by DNA sequencing (Institute for Biomolecular Design, Department of Biochemistry, University of Alberta).

2.2.1 Mammalian Expression constructs

Eukaryotic-expression construct for splicing variant 2 of human SLC4A11 encoding an 891 amino acid protein (NCBI Reference Sequence: NG_017072.1), N-terminally tagged with the Myc epitope (pGV1), was reported earlier [2]. Amino-terminally Hemagglutinin epitope tagged (HA-tagged) PCR product was prepared using pGV1 as a template and the pSKL1 primers (Table 2.1), that contains a 5' *NheI* and *3' EcoNI* restriction site in forward and reverse primers respectively. The forward primer (Table 2.1) also encodes an N-terminal hemagglutinin (HA) tag (amino acid sequence YPYDVPDYA, underlined). The PCR product was cloned into *NheI/EcoNI* digested pGV1, resulting in pSKL1 that encodes N-terminally HA-tagged wild type SLC4A11. Using a PCR-based strategy with mutagenic oligonucleotides (Table 2.2), Agilent Quik Change Lightning site-directed mutagenesis kit and pGV1 as a template, Myc epitope tagged (Myc-tagged) R125H SLC4A11 [3] cDNA was constructed.

Table 2.1 Oligonucleotides used in cloning of WT, membrane domain and cytosolic domain variants of SLC4A11 and AE1. Underlined bases code for HA or Myc epitope tag as indicated.

Construct	Forward Primer	Reverse Primer
pSKL1 (HA-WT SLC4A11)	5'-CTAGCTAGCGCCACCATGTACCCATACGATGTTCCGGATTACGCTAGCCAGGTCGGGGG-3'	5'-AGCGGCGAAGCA-3'
pSKL2 (HA-353-MD-SLC4A11)	5'-CTAGCTAGCGCCACCATGTACCCATACGATGTTCCGGATTACGCTAGGTTCCCCTTGTACCCCTTG -3'	5'-CCGCTCGAGTCAAGGCCTGTGCTCAGCGTC -3'
pSKL3 (HA-347-MD-SLC4A11)	5'-CTAGCTAGCGCCACCATGTACCCATACGATGTTCCGGATTACGCTCGGGAGGACATCGCACGCAGG -3'	5'-CCGCTCGAGTCAAGGCCTGTGCTCAGCGTC -3'
pSKL4 (HA-329-MD-SLC4A11)	5'-CTAGCTAGCGCCACCATGTACCCATACGATGTTCCGGATTACGCTAGACACCCAGAGCCCCCAAAG -3'	5'-CCGCTCGAGTCAAGGCCTGTGCTCAGCGTC -3'
pSKL5 (HA-307-MD-SLC4A11)	5'-CTAGCTAGCGCCACCATGTACCCATACGATGTTCCGGATTACGCTGTGAGCCACGGTCCAGTGGCG -3'	5'-CCGCTCGAGTCAAGGCCTGTGCTCAGCGTC -3'
pSKL6 (Myc-307-MD-SLC4A11)	5'-CTAGCTAGCGCCACCATGGAACAAAAGCTAATTTCAGAAGAAGACCTAGTGAGCCACGGTCCAGTGGCG -3'	5'-CCGCTCGAGTCAAGGCCTGTGCTCAGCGTC -3'
pSKL7 (HA-CD-SLC4A11)	5'-CTAGCTAGCGCCACCATGTACCCATACGATGTTCCGGATTACGCTAGCCAGGTCGGGGGGCGGGGAGAC-3'	5'-CCGCTCGAGTCATTTCCCAATAATGCCATCAGT -3'
pSKL8 (Myc-CD-SLC4A11)	5'-CTAGCTAGCGCCACCATGGAACAAAAGCTAATTTCAGAAGAAG	5'-CCGCTCGAGTCATTTCCCAATAATGCCATCAGT -

	ACCTAAGCCAGGTCGGGGGGC GGGGAGAC-3’	3’
pSKL9 (340-MD-AE1)	5’ - CTAGCTAGCGCCACCAGGGAGC TACTTCGAAGGC-3’	5’- CCGCTCGAGTCACACA GGCATGGCCAC -3’
pCML1 (Native sequence CD-SLC4A11-His_6)	5’- AAGGAGATATACATATGAGCC AGGTCGGG -3’	5’- GGTGGTGGTGCTCGAG TCCTCCTCCTCCCTGGA AGTACAGGTTCTCTCCT CCTCCTTTCCCAATAAT GC CATCAGTGAAGTCC -3’
pCML1 (Codon optimized CD-SLC4A11-His_6)	5’- GTCGGAGGGCGTGGAGACCGTT GCACTCAGGAGGTCCAG -3’	5’- CTCCTGAGTGCAACGG TCTCCACGCCCTCCGAC CTG -3’
pCML2 (GST-CD-SLC4A11-His_{10})	5’- GGGATCCCCGGAATTCATGAGC CAGGTCGGAGG -3’	5’- TTTCCCAATAATGCCAT CAGTGAAGTCC -3’

Table 2.2 Mutagenic oligonucleotides to clone CHED2/FECD/HS *SLC4A11* point mutations. Positions of the mutated codons are indicated in bold.

Construct	Forward Primer	Reverse Primer
E143K	5'-GCATCGTCCTGAAC**AAG**ACGGCCACCTCC-3'	5'-GGAGGTGGCCGT**CTT**GTTCAGGACGATGC-3'
G709E	5'-GCCATCATCAACACA**GAG**CTGTCTCTGTTTGGG-3'	5'-CCCAAACAGAGACAG**CTC**TGTGTTGATGATGGC-3'
S213L	5'-GCGGTACCAGCAG**TTG**TGGCTCTGCATCA-3'	5'-TGATGCAGAGCCA**CAA**CTGCTGGTACCGC-3'
T401K	5'-GGTCTCTCAATGACGAGAAC**AAA**GACGGGGCCA-3'	5'-TGGCCCCGTC**TTT**GTTCTCGTCATTGAGAGACC-3'
R755W	5'-CGTGAAGGAGACG**TGG**CTGACCTCGCT-3'	5'-AGCGAGGTCAG**CCA**CGTCTCCTTCACG-3'
L843P	5'-CAGCTGCTGCTG**CCG**TGTGCCTTCGGC-3'	5'-GCCGAAGGCACA**CGG**CAGCAGCAGCTG-3'
R125H	5'-CAAGGAAGAGATC**CAT**GCGCACCGCGACC-3'	5'-GGTCGCGGTGCGC**ATG**GATCTCTTCCTTG-3'
A269V	5'-GCGATGGAGGTG**GTG**CGCACGTTTGCC-3'	5'-GGCAAACGTGCG**CAC**CACCTCCATCGC-3'
C386R	5'-CCTCTACTT**CGC**CCGCCTCCTGCCCAC-3'	5'-TGGGCAGGAGGCGG**GCG**AAGTAAGG-3'

Table 2.3 Oligonucleotides used in cloning of GFP, mNectarine and AE1 cytoplasmic domain fusion variants of SLC4A11. Underlined bases code for HA epitope tag as indicated.

Construct	Primer 1	Primer 2	Primer 3
pSKL10 (GFP-368-MD-SLC4A11)/ pSKL11 (mNect-368-MD-SLC4A11)	5'-CTAGCTAGCGCCACCATGGTGAGCAAGGGCGAGGAG -3'	5'-GCCCACAGCCTTGTTTTTAGCGTAATCCGGAACATCGTATGGGTACTTGTACAGCTC -3'	5'-CCGCTCGAGTCAAGGCCTGTGCTCAGCGTC -3'
pSKL12 (GFP-307-MD-SLC4A11)/ pSKL13 (mNect-307-MD-SLC4A11)	5'-CTAGCTAGCGCCACCATGGTGAGCAAGGGCGAGGAG -3'	5'-CACTGGACCGTGGCTCACAGCGTAATCCGGAACATCGTATGGGTACTTGTACAGCTC -3'	5'-CCGCTCGAGTCAAGGCCTGTGCTCAGCGTC -3'
pSKL14 (CD-AE1-MD-SLC4A11)	5'-CTAGCTAGCGCCACCATGTACCCATACGATGTTCCGGATTACGCTGAGGAGCTGCAGGAT -3'	5'-GCGTGCGATGTCCTCCCGGATGCCCTTCCCAAATGGCTTGGCAGGGCTGGACTGATAGCGCCTTCG-3'	5'-CCGCTCGAGTCAAGGCCTGTGCTCAGCGTC -3'

Expression constructs for all other HA-tagged SLC4A11 point mutants, R125H (c.374G>A (p.Arg125His)), E143K (c.427G>A (p.Glu143Lys)), S213L (c.638C>T (p.Ser213Leu)), A269V (c.806C>T (p.Ala269Val)), C386R (c.1156T>C (p.Cys386Arg)), T401K (c.1202C>A (p.Thr401Lys)), G709E (c.2126G>A (p.Gly709Glu)), R755W (c.2263C>T (p.Arg755Trp)) and L843P (c.2528T>C (p.Leu843Pro)) [3-7] were created, using the PCR strategy, with pSKL1 as a template, oligonucleotides (Table 2.2) and the Agilent Quik Change Lightning Site-Directed Mutagenesis Kit.

SLC4A11 membrane domain (MD) variants HA-353-MD (pSKL2), HA-347-MD (pSKL3), HA-329-MD (pSKL4), HA-307-MD (pSKL5), Myc-307-MD-SLC4A11 (pSKL6) and cytoplasmic domain (CD) variants HA-CD (pSKL7) and Myc-CD-SLC4A11 (pSKL8) were prepared using PCR-based strategy with pSKL1 as a template and corresponding primers (Table 2.1) that contains a 5' *NheI* restriction site, an N-terminal HA or Myc tag (underlined) and 3' *XhoI* restriction site. The PCR product was cloned into *NheI/XhoI* digested pSKL1, resulting in variants of SLC4A11, as indicated. To clone 340-MD-AE1 (pSKL9) construct, the same strategy was employed except that pPBAE1-oocyte was used as a template [8] and the corresponding primers (Table 2.1)

The fusion proteins, GFP-368-MD, GFP-307-MD, mNect-368-MD and mNect-307-MD-SLC4A11, were constructed with a three-step mega-primer cloning strategy, and the indicated oligonucleotides (Table 2.3). Using primer 1 and primer 2, peGFP-C1 (Clontech, USA) as a template for GFP-368-MD (pSKL10) and GFP-307-MD (pSKL11), the Green fluorescent protein cDNA was cloned. The resulting first PCR product (~790 bp in size) had a 5' *NheI* restriction site, DNA sequence encoding for GFP and the first 18 bp of MD-SLC4A11 DNA. This first PCR product was purified and diluted 1/50 and

used as a megaprimer for second PCR along with Primer 1 and primer 3 (Table 2.3) and pSKL1 as a template. The second PCR product contains a 5' *NheI* restriction site, DNA sequence encoding for GFP, HA tag and Membrane domain of SLC4A11 (starting at either 368 or 308 amino acid of WT-SLC4A11) and 3' *XhoI* restriction site. *NheI/XhoI* digested pSKL1 and second PCR product were ligated, resulting in pSKL10 and pSKL11. The same procedure was followed to clone mNect-368-MD (pSKL12) and mNect-308-MD-SLC4A11 (pSKL13) except that pDEJ6 [9] was used as a template which contains mNectarine sequence. To construct CD-AE1-MD-SLC4A11 (pSKL14), the same strategy was used again except that pPBAE1-oocyte [8] was initially used as a template to clone CD-AE1 along with Primers 1 and 2 (Table 2.3). Then with purified and diluted first PCR product as megaprimer, pSKL1 as a template and primers 1 and 3 (Table 2.3), pSKL14 fusion construct was made.

2.2.2 Bacterial expression constructs

His-tagged SLC4A11 cytoplasmic domain (CD-SLC4A11-His_6, pCML1) was constructed by sub-cloning the insert (created by PCR using primers from Table 2.1 and pSKL1 as template) into the *NdeI* and *XhoI* sites of pET-12b using the In-Fusion cloning system and following manufacturer's protocol. Primer design facilitated the incorporation of a TEV protease cleavage site between the end of the protein sequence and the HIS_6 tag present in pET-21b. To promote translational stability of the nascent peptide in *E. coli*, the first 20 codons of Human SLC4A11 were examined and were identified to contain several rare codons in *E. coli*. These codons were optimized for expression in a bacterial host. Using the QuikChange Lightning mutagenesis kit (Agilent) and indicated primers (Table 2.1), a partially codon optimized pCML1 (CD-SLC4A11-His_6) was constructed.

To enhance the solubility of the SLC4A11 cytoplasmic domain, a GST fusion construct was created using pGEX-6P1 (GE Health care). The construct was modified to include C-terminal TEV cleavage site and a His_{10} tag. Using the *BamHI/NotI* sites in this modified construct, primers (Table 2.1), codon optimized CD-SLC4A11-His_6 as template and In-Fusion cloning kit, the final construct pCML2 was made which had CD-SLC4A11 with GST tag at N-terminus and His_{10} tag at C-terminus (GST-CD-SLC4A11-His_{10}).

2.3 Cell culture

cDNA encoding HA or Myc-tagged WT SLC4A11 or the indicated mutants were transiently transfected, using the calcium phosphate method [10]. HEK293 cells were grown at 37 °C or 30 °C in 5% CO_2/air environment in complete DMEM (DMEM, supplemented with 5% (v/v) fetal bovine serum, 5% (v/v) calf serum, and 1% (v/v) penicillin-streptomycin-glutamine). All experiments involving transiently transfected cells were carried out 40 to 48 h post-transfection. HEK293 cells stably expressing SLC4A11 variants were monoclonally selected and cultured in complete DMEM, containing Geneticin (0.75 mg/ml).

2.4 Assays of osmotically driven water flux

HEK293 cells were grown on poly-L-lysine-coated 25 mm round glass coverslips and co-transfected with cytosolic enhanced green fluorescent protein (eGFP) (peGFP-C1 vector, Clontech, USA) and, or pcDNA 3.1 (empty vector) or the indicated SLC4A11 plasmid constructs in a 1:8 molar ratio [11]. Forty-eight h later, coverslips were mounted in a 35 mm diameter Attofluor Cell Chamber (Molecular Probes) and washed with

phosphate buffered saline (PBS) (140 mM NaCl, 3 mM KCl, 6.5 mM Na_2HPO_3, 1.5 mM KH_2PO_3, pH 7.4). During experiments, the chamber was perfused at 3.5 ml/min with isotonic MBSS buffer (90 mM NaCl, 5.4 mM KCl, 0.4 mM $MgCl_2$, 0.4 mM $MgSO_4$, 3.3 mM $NaHCO_3$, 2 mM $CaCl_2$, 5.5 mM glucose, 100 mM D-mannitol and 10 mM HEPES, pH 7.4, 300 mOsm/kg) and then with hypotonic (200 mOsm/kg) MBSS buffer, pH 7.4 (same composition as previous but lacking D-mannitol). The chamber was mounted on the stage of a Wave FX Spinning Disc Confocal Microscope (Quorum Technologies, Guelph, Canada), with a Yokogawa CSU10 scanning head. The microscope has a motorized XY stage with Piezo Focus Drive (ASI, MS-4000 XYZ Automated Stage) and a live cell environment chamber (Chamlide, Korea), set to 24 ºC during the duration of the experiment. Acquisition was performed with a Hamamatsu C9100-13 Digital Camera (EM-CCD) and a 20x objective during excitation with laser (Spectral Applied Research, Richmond Hill, ON, Canada) at 491 nm. eGFP fluorescence, collected though a dichroic cube (Quorum Technologies, Guelph, Canada) at wavelengths 520-540 nm, was acquired at 1 point s^{-1} for 4-6 min. Quantitative image analysis was performed by selecting a region of interest for each HEK293 cell with Volocity 6.0 software (PerkinElmer, ON, Canada). Following the switch to hypotonic medium, the rate of fluorescence change was determined from the initial 15 s of linear fluorescence change.

2.5 Expression of SLC4A11 cytoplasmic domain

E. coli were transformed with pCML1 or pCML2 and grown in LB medium containing, 0.1 mg/ml ampicillin. Cultures were grown at 37 °C until an A_{600} of 0.6–0.8 was reached. Protein expression was induced by the addition of isopropyl-β-d-1-

thiogalactopyranoside (IPTG) to a final concentration of 0.1 or 1 mM and incubation for 2-4 h at 37 °C. Cells were harvested by centrifugation at 7500 x *g* for 10 min at 4 °C. Bacterial pellets were lysed in extraction buffer (phosphate buffered saline pH 7.4 with 1 mM PMSF, 2 mM EDTA, 1 µg/mL DNase, 1X Roche protease inhibitor cocktail) by sonication using W185 probe sonifier (Heat systems-Ultrasonic Inc., Plainview, NY) with eight, 10 s pulses, while kept on ice. An aliquot of total lysate was removed (T) and the remaining lysate was centrifuged at 15000 x *g* to isolate the supernatant as the soluble fraction (S).

2.6 Immunoprecipitation

Immunoprecipitation experiments were performed as described earlier [12]. HEK293 cells, transiently transfected with cDNA encoding indicated SLC4A11 variants were grown for 48 h. Cells were lysed in immunoprecipitation buffer (IPB: 1% (v/v) IGEPAL CA-630, 5 mM EDTA, 150 mM NaCl, 0.5% (w/v) sodium deoxycholate, 10 mM Tris, pH 7.5), containing Complete Protease inhibitor Cocktail and incubated at 4 °C for 20 min. Cell lysates were centrifuged at 13,200 x g for 20 min at 4 °C and protein concentration was determined by BCA Assay [13]. A 50 µg aliquot of total protein was taken (T) separately for storage at -20 °C and 300 µg of the remaining lysates was incubated at 4 °C overnight with either 1.5 µl of rabbit polyclonal anti-Myc (IP) or rabbit non-immune serum (NI) along with 50 µl of Dynabeads Protein G resin. Immunocomplexes were washed 18 h later, three times with 4 °C IPB buffer, containing complete protease inhibitors. Dynabeads resin was then resuspended in 40 µl of 2x SDS-

PAGE sample buffer and heated at 65 °C for 5 min. Samples were then processed for immunoblotting, as described.

2.7 Immunoblots

Cell lysates were prepared in 2X SDS-PAGE sample buffer (10% (v/v) glycerol, 2% (w/v) SDS, 0.5% (w/v) bromophenol blue, 75 mM Tris, pH 6.8), containing Complete Protease Inhibitor Cocktail (Roche). Lysates were made to 1% (v/v) 2-mercaptoethanol, heated for 5 min at 65 °C and insoluble material was removed by centrifugation at 16000 x g for 10 min. Samples were then resolved by SDS-PAGE on 7.5% or 10% (w/v) acrylamide gels [14]. Immunoblots were processed as described [2]. Mouse anti-HA or mouse anti-GAPDH or mouse anti-Myc or mouse anti-AE1 or Rabbit anti-caspase-3 or Rabbit anti-Cleaved caspase-3 were used at 1:2000 or 1:5000 or 1:2000 or 1:5000 or 1:1500 or 1:1500 dilution in TBS-TM (5% skim milk powder in TBS-T: 0.1% (v/v) Tween-20, 0.15 M NaCl, 50 mM Tris-HCl, pH 7.5), respectively. After incubation with sheep anti-mouse or donkey anti-rabbit HRP conjugated secondary antibody at 1:5000 dilution, immunoblots were developed, using Western Lightning™ Chemiluminescence Reagent Plus and visualized, using a Kodak Image Station 440CF (Kodak, NY, USA) or GE ImageQuant LAS4000. Quantitative densitometric analyses were performed, using Kodak Molecular Imaging Software v4.0.3 (Kodak, NY, USA) or ImageQuant TL 8.1 software (GE Healthcare).

2.8 Enzymatic deglycosylation

HEK293 cell lysates, containing SLC4A11 membrane domain variants, were prepared in IPB buffer as described and their total protein concentration was measured by BCA assay [4]. Samples (25 µg of protein aliquots) were heated 5 min at 65 °C and then incubated with 5 µl (2500 units) of N-glycosidase F (PNGase F) or 3 µl of Endo H (1500 units) for 2 h at 37°C. SDS–PAGE sample buffer were added to stop the reaction and the samples were processed for immunoblotting.

2.9 Cell surface processing assays

Cell surface processing assays were performed as described earlier [15]. Transfected cells were rinsed with 4 °C PBS, washed with 4 °C Borate buffer (154 mM NaCl, 7.2 mM KCl, 1.8 mM $CaCl_2$, 10 mM boric acid, pH 9.0) and labelled with Sulpho-NHS-SS-Biotin (0.5 mg/ml). After washing three times with 4 °C Quenching buffer (192 mM glycine, 25 mM Tris, pH 8.3), cells were solubilised in 500 µl of IPB buffer, containing Complete Protease Inhibitor. For each sample, half of the recovered supernatant was retained for later SDS-PAGE analysis (T). The remaining half of the recovered supernatants was combined with 100 µl of 50% suspension of immobilized streptavidin Sepharose resin to precipitate the biotinylated proteins and the supernatant collected (Unbound Protein, U). The T and U fractions of each sample were processed for SDS-PAGE analysis and immunoblotting as described above. Densitometry used Kodak Molecular Imaging Software v4.0.3 or ImageQuant TL 1.8 and the formula (T-U)/T x 100% was used to calculate the percentage of biotinylated protein.

2.10 cDNA synthesis and real-time quantitative reverse transcription polymerase chain reaction (qRT-PCR)

HEK293 cell lysates (Vector and WT-SLC4A11 cDNA transfected) were collected using 600 µL buffer RLT (Qiagen). mRNA was extracted from the lysates using an RNeasy Mini Kit (Qiagen #74104) according to the manufacturer's instruction and quantified using a Nanodrop 2000c spectrophotometer (Fisher Scientific). cDNA was synthesized using iScript RT Supermix Kit (Biorad #1708840) as per manufacturer's instructions. Real-time PCR was performed using synthesized cDNA equivalent to 10 pg of mRNA as template, iQ SYBR Green Supermix (Biorad #1708880) on Rotorgene 3000 real time thermal cycler (Corbett Reasearch) and 1 µmol/L of the following primers (GAPDH: 5'- tgtggtcatgagtccttcca-3' and 5'-cagcctcaagatcatcagca-3', SLC4A11: 5'-ggctggtgacctttctgctt-3' and 5'- tcacacttgtagtagcttgaatcc-3'). The differences in mRNA levels were corrected by using Ct values of GAPDH made to be the same and that correction was applied to the Ct values of other samples (n=3). Corrected Ct values were graphed.

2.11 Cell sorting-based vitality assays

HEK293 cells in 100 mm dishes, stably expressing HA-tagged WT, E143K or G709E SLC4A11 or empty vector were either treated with 2 µM H_2O_2 (which induces cell death, [16]), or left untreated for 4 h. Cell viability was quantified, using Live/Dead Cell Vitality Assay kit according to manufacturer's instructions. Briefly, one million live and dead cells from each condition, suspended separately in 100 µl PBS at 37 °C, were stained with 1 µl of 50 µM C_{12}-resazurin and 5 µl of 1 µM SYTOX® Green solution for

15 min at 37 °C in 5% CO_2/air environment. PBS (400 µl) was added to cell suspensions, which were incubated at 4 °C. C_{12}-resazurin was reduced to red-fluorescent C_{12}-resorufin in metabolically active cells, whereas the SYTOX® Green stains cells with compromised plasma membranes (usually late apoptotic and necrotic cells) [17]. Gating parameters to select for individual cells, excluding clusters, were determined in parallel unstained cultures, using fluorescence activated cell sorter (FACSCanto II, BD Biosciences, Mississauga, ON). Stained cells (100,000 cells/run) were sorted, using excitation at 488 nm and emission at 530 nm and 575 nm. Live cells separate into groups with high level of red fluorescence whereas injured and dead cells separate into groups with high level of green fluorescence and low level of red fluorescence.

2.12 Statistical Analysis

Numerical values were represented as mean ± standard error of measurement. Statistical analyses were performed using Prism software (Graphpad v5). Groups were compared with one-way ANOVA and unpaired *t*-test with $p < 0.05$ considered significant.

2.13 References

1. Jennings, M. L., Anderson, M. P. and Monaghan, R. (1986) Monoclonal antibodies against human erythrocyte Band 3 protein: localization of proteolytic cleavage sites and stilbenedisulfonate-binding lysine residues. J. Biol. Chem. **261**, 9002-9010
2. Vilas, G. L., Morgan, P. E., Loganathan, S., Quon, A. and Casey, J. R. (2011) Biochemical Framework for SLC4A11, the Plasma Membrane Protein Defective in Corneal Dystrophies. Biochemistry. **50**, 2157-2169
3. Hemadevi, B., Veitia, R. A., Srinivasan, M., Arunkumar, J., Prajna, N. V., Lesaffre, C. and Sundaresan, P. (2008) Identification of mutations in the SLC4A11 gene in patients with recessive congenital hereditary endothelial dystrophy. Arch Ophthalmol. **126**, 700-708
4. Vithana, E. N., Morgan, P. E., Ramprasad, V., Tan, D. T., Yong, V. H., Venkataraman, D., Venkatraman, A., Yam, G. H., Nagasamy, S., Law, R. W., Rajagopal, R., Pang, C. P., Kumaramanickevel, G., Casey, J. R. and Aung, T. (2008) SLC4A11 Mutations in Fuchs Endothelial Corneal Dystrophy (FECD). Hum. Mol. Genet. **17**, 656-666
5. Ramprasad, V. L., Ebenezer, N. D., Aung, T., Rajagopal, R., Yong, V. H., Tuft, S. J., Viswanathan, D., El-Ashry, M. F., Liskova, P., Tan, D. T., Bhattacharya, S. S., Kumaramanickavel, G. and Vithana, E. N. (2007) Novel SLC4A11 mutations in patients with recessive congenital hereditary endothelial dystrophy (CHED2). Mutation in brief #958. Online. Hum. Mutat. **28**, 522-523
6. Desir, J., Moya, G., Reish, O., Van Regemorter, N., Deconinck, H., David, K. L., Meire, F. M. and Abramowicz, M. (2007) Borate transporter SLC4A11 mutations cause both Harboyan syndrome and non-syndromic corneal endothelial dystrophy. J. Med. Genet. **44**, 322-326
7. Sultana, A., Garg, P., Ramamurthy, B., Vemuganti, G. K. and Kannabiran, C. (2007) Mutational spectrum of the SLC4A11 gene in autosomal recessive congenital hereditary endothelial dystrophy. Mol Vis. **13**, 1327-1332
8. Bonar, P., Schneider, H.-P., Becker, H. M., Deitmer, J. W. and Casey, J. R. (2013) Three-Dimensional Model for the Human Cl^-/HCO_3^- Exchanger, AE1, by

Homology to the *E. coli* ClC Protein. Journal of Molecular Biology. **425**, 2591-2608

9. Johnson, D. E., Ai, H.-W., P., W., Young, J. D., Campbell, R. E. and Casey, J. R. (2009) Red fluorescent protein pH biosensor to detect concentrative nucleoside transport. J. Biol. Chem. **284**, 20499-20511
10. Ruetz, S., Lindsey, A. E., Ward, C. L. and Kopito, R. R. (1993) Functional activation of plasma membrane anion exchangers occurs in a pre-Golgi compartment. J. Cell Biol. **121**, 37-48
11. Vilas, G. L., Loganathan, S. K., Liu, J., Riau, A. K., Young, J. D., Mehta, J. S., Vithana, E. N. and Casey, J. R. (2013) Transmembrane water-flux through SLC4A11: a route defective in genetic corneal diseases. Human Molecular Genetics. **22**, 4579-4590
12. Loganathan, S. K. and Casey, J. R. (2014) Corneal Dystrophy-Causing SLC4A11 Mutants: Suitability for Folding-Correction Therapy. Human Mutation. **35**, 1082-1091
13. Smith, P. K., Krohn, R. I., Hermanson, G. T., Mallia, A. K., Gartner, F. H., Provenzano, M. D., Fujimoto, E. K., Goeke, N. M., Olson, B. J. and Klenk, D. C. (1985) Measurement of protein using bicinchoninic acid. Anal. Biochem. **150**, 76-85
14. Laemmli, U. K. (1970) Cleavage of structural proteins during assembly of the head of bacteriophage T4. Nature. **227**, 680-685
15. Vilas, G. L., Loganathan, S., Quon, A., Sundaresan, P., Vithana, E. N. and Casey, J. R. (2012) Oligomerization of SLC4A11 protein and the severity of FECD and CHED2 corneal dystrophies caused by SLC4A11 mutations. Human Mutation. **33**, 419-428
16. Whittemore, E. R., Loo, D. T., Watt, J. A. and Cotmans, C. W. (1995) A detailed analysis of hydrogen peroxide-induced cell death in primary neuronal culture. Neuroscience. **67**, 921-932
17. White, M. J., DiCaprio, M. J. and Greenberg, D. A. (1996) Assessment of neuronal viability with Alamar blue in cortical and granule cell cultures. Journal of Neuroscience Methods. **70**, 195-200

Chapter 3: Corneal Dystrophy-causing SLC4A11 Mutants: Suitability for Folding-Correction Therapy

A version of this chapter has been published as Loganathan, S. K. and Casey, J. R. (2014) Corneal Dystrophy-Causing SLC4A11 Mutants: Suitability for Folding-Correction Therapy. Human Mutation. **35**, 1082-1091. (Reproduced with permission).

3.1 Introduction

In human cornea, the high solute concentration in the stromal layer induces osmotic accumulation of water, countered by water reabsorption by the endothelial cell layer [1, 2]. Posterior corneal dystrophies arise from dysfunction of endothelial cells, which disrupt the fluid reabsorption process, resulting in the corneal stromal fluid accumulation and abnormal deposition of material (guttae) on the Descemet's membrane that underlies the corneal endothelial layer [1]. The density of endothelial cells declines and eventually, posterior corneal dystrophies result in serious deterioration of vision.

The *SLC4A11* gene (MIM# 610206) encodes an 891 amino acid membrane protein [3], whose mutations cause three posterior corneal dystrophies: recessive congenital hereditary endothelial dystrophy type 2 (CHED2) (MIM# 217700) [4-8], recessive Harboyan syndrome (HS) (MIM# 217400) [9] (a combination of corneal dystrophy and perceptive deafness) and dominant late-onset Fuchs endothelial corneal dystrophy (FECD) (MIM# 136800) [8-10]. Hearing deficits also have been observed with an increased frequency in individuals with FECD [11]. At present, corneal transplantation is the only effective treatment for these inherited corneal dystrophies [1]. Lengthy waiting times for corneal transplantation, coupled with the risk of graft rejection [1], underscore the need for non-invasive therapeutic options for genetic corneal dystrophies.

Therapies that target the molecular defect in mutated SLC4A11 require a deeper understanding of the SLC4A11 role in human cornea. Phylogenetically SLC4A11 is a member of SLC4 family of bicarbonate transporters [12], yet has no reported bicarbonate transport activity [13]. Neither does SLC4A11 have Na^+ coupled borate transport [13] as reported earlier [14]. Bovine SLC4A11, however, displays Na^+ coupled OH^- transport

[13]. Interestingly, human SLC4A11 was recently found to facilitate trans-membrane water movement, which makes it the first such protein that is not a member of the major intrinsic protein family [15]. SLC4A11 localizes to the basolateral surface of human corneal endothelial cells [15]. Biochemical data and similarity to AE1 (SLC4A1) led to an SLC4A11 structural model, featuring an N-terminal 370 amino acid cytoplasmic domain, a 500 amino acid integral membrane domain with 14 transmembrane segments, and a very short cytoplasmic C-terminal tail [3].

SLC4A11 exists as dimers, and heterodimerization of WT and diseased monomers of SLC4A11 provides a molecular explanation for the recessive and dominant inheritance of CHED2 and FECD respectively [16]. To date, close to 50 SLC4A11 point mutations have been identified [4, 6-8, 10, 17]. When expressed homozygously, most CHED2 and FECD mutants of SLC4A11 are retained intracellularly [8]. When co-expressed with WT SLC4A11, CHED2/WT heterodimers target to the plasma membrane but FECD/WT heterodimers do not [16].

A pharmacological strategy to ameliorate ER-retained SLC4A11 mutants would target compounds that enable the release of the protein from the ER. Such an approach is being used for ΔF508 CFTR, a recessive ER-retained mutation of cystic fibrosis transmembrane regulatory protein (CFTR) that causes cystic fibrosis disease [18, 19]. ΔF508 CFTR rescued to the cell surface retains function [20, 21]. Some small molecule protein folding correctors have proven successful in rescuing ΔF508 CFTR protein to the cell surface, and are undergoing clinical trials [21].

For plasma membrane rescue of SLC4A11 to be a viable therapeutic strategy three conditions must be met: 1) ER-retained SLC4A11 must be able to move to the

plasma membrane, 2) Rescued SLC4A11 would need to retain sufficient functional activity to correct the functional defect and 3) Expression of mutant SLC4A11 in itself (perhaps arising from its ER retention phenotype) should not induce cell death. Here we tested the amount of functional activity required to either delay or avoid the onset of disease symptoms, explored the idea of rescuing the ER-retained SLC4A11 mutants to the cell surface, using a unique co-expression strategy and determined whether the rescued protein retains function. We also tested whether the expression of mutant SLC4A11 in HEK293 cells induced cell death.

3.2 Results

3.2.1 Benchmarks for SLC4A11 functional activity

Therapies for genetic corneal dystrophies have as their goal the restoration functional activity in excess of the minimum needed to avoid symptoms. Benchmark values for SLC4A11 activity associated with normal and diseased eyes are thus required. CHED2 patients manifest disease symptoms shortly after birth, whereas heterozygous FECD patients develop disease in the 4-5th decades of life [1, 2]. Thus, CHED2 homozygous state, FECD heterozygous state and CHED2 heterozygous state define the level of SLC4A11 functional activity associated with early-onset, late-onset and no disease, respectively.

Since it is unfeasible to assess SLC4A11 functional activity in human eyes, HEK293 cells, transfected to mimic the genotype of humans, provide a tractable model. In this study cells were transfected with a single SLC4A11 variant, or co-transfected with two variants (i.e. mutant and WT). Formally these do not represent the homozygous and

heterozygous states, as the genes are not genomically-encoded, but rather are introduced exogenously. To simplify these data for the reader, however, this manuscript uses the terms “homozygous state” (expressing a single SLC4A11 variant) and “heterozygous state” (co-expressing two SLC4A11 variants), with the understanding that these are limited cell culture models, representing the complexity of the cornea.

In using HEK293 cells as a model to study SLC4A11, we characterized the cells for their expression of the protein. SLC4A11 expression was undetectable in lysates from vector-transfected HEK293 cells [15], whereas the protein was readily detectable in cells transfected with WT-SLC4A11 cDNA (Fig. 3.1). Transfected HEK293 cells also seem to be a reasonable model system in which to study SLC4A11, as the level of SLC4A11 expression in corneal cells is similar to that in transfected HEK293 cells (Fig. 3.1). The lysate was prepared from whole cornea. In the corneal endothelial cell layer (the predominant site of expression in the cornea), the relative abundance of SLC4A11 would be higher than indicated here. In the human corneal lysate sample, the prominent 63 kDa band likely represents a proteolytic fragment.

Since immunoblots could not detect endogenous SLC4A11 in HEK293 cells, we further assessed expression by reverse transcription PCR (Fig. 3.2). Following 30 cycles of amplification, a PCR product was observed in samples from SLC4A11-transfected cells, but not in untransfected cells (Fig. 3.2A). Quantitative RT-PCR revealed cycle thresholds (Ct) for SLC4A11 message amplification was 10 cycles higher for untransfected cells than SLC4A11-transfected cells. This indicates that mRNA for SLC4A11 is 2^{10} (1024) fold higher in SLC4A11 transfected cells than in untransfected cells. If we assume that SLC4A11 protein expression levels are proportional to mRNA

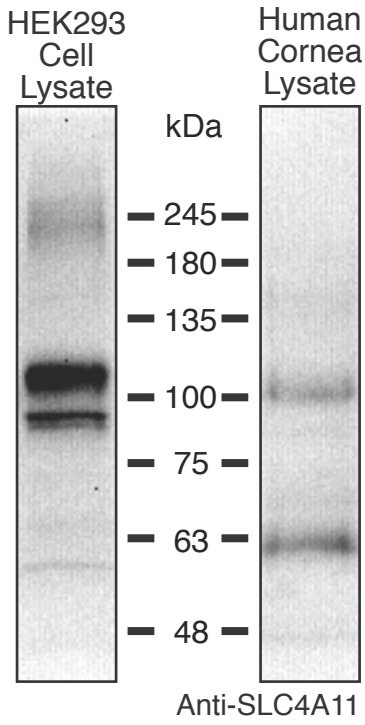

Figure 3.1 SLC4A11 expression in transfected HEK293 cells and human cornea lysate. HEK293 cells were transiently transfected with cDNA encoding WT SLC4A11. Cells were lysed and probed on immunoblots, using anti-SLC4A11 antibody to detect the expression of SLC4A11 variants. Human corneal tissue, unfit for transplantation, were snap froze in liquid nitrogen and homogenized. Tissue lysate was probed on immunoblots using anti-SLC4A11 antibody.

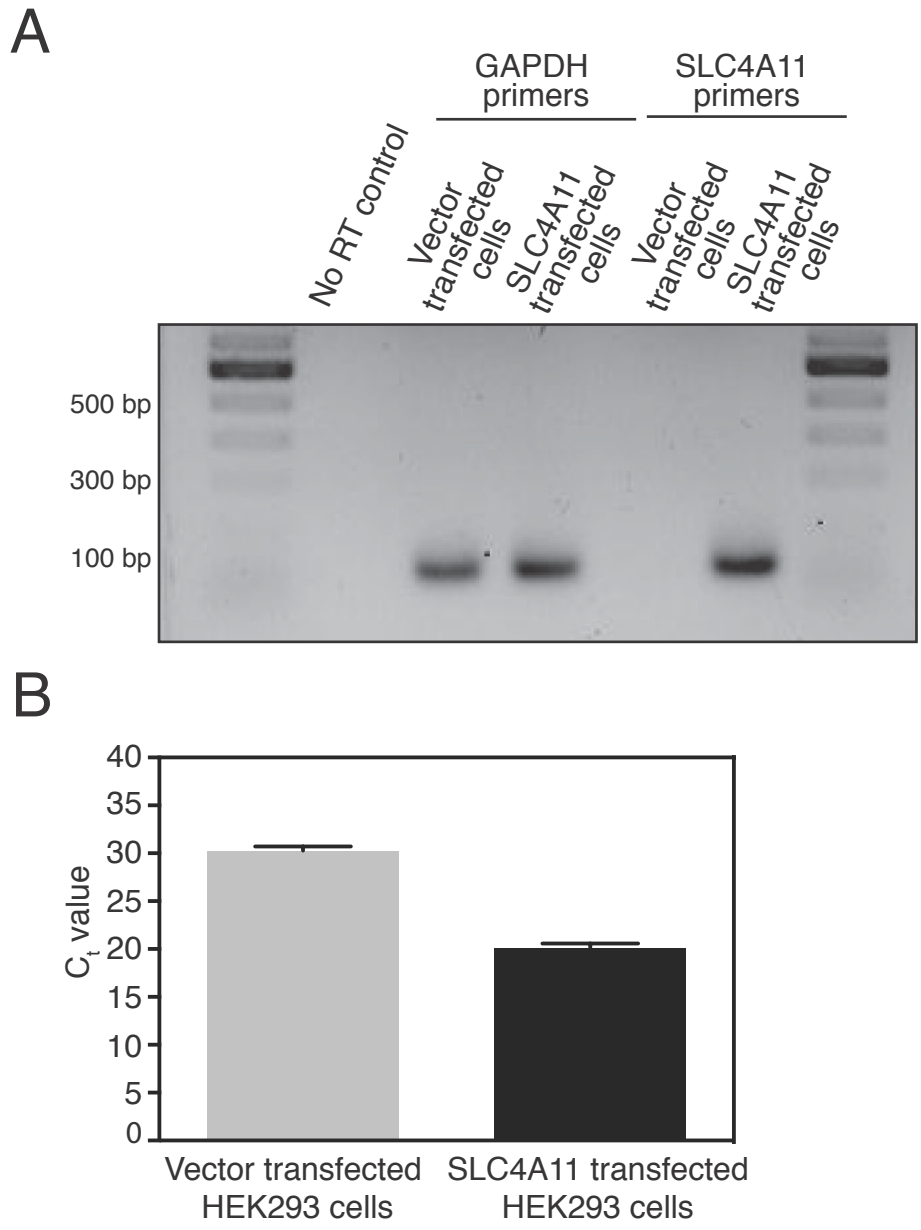

Figure 3.2 RT-qPCR to quantify the level of SLC4A11 mRNA in HEK293 cells. Cells were transfected with WT-SLC4A11 cDNA or vector alone. **(A)** mRNA was isolated from HEK293 cell lysates and cDNA was synthesized. Using the cDNA as template, 30 cycles of PCR were performed with primers specific for GAPDH and SLC4A11. Amplified products were loaded onto a 1.2 % agarose gel. **(B)** Using the synthesized

cDNA as template, quantitative RT-PCR was performed for GAPDH and SLC4A11. SLC4A11 Ct values were corrected by GAPDH Ct values.

abundance, it suggests that endogenous WT-SLC4A11 in HEK293 cells is about 1000 fold lower than the level arising from transfection. Endogenous SLC4A11 protein will thus little affect the analysis of SLC4A11 in transfected HEK293 cells.

We tested the relative functional activity of CHED2 and FECD-SLC4A11 mutants that are ER-retained [10, 16] in both homozygous and heterozygous conditions. Water flux activity of SLC4A11 variants was assessed in HEK293 cells exposed to hypotonic medium, by monitoring the rate of dilution of cytosolic eGFP [15]. HEK293 cells were co-transfected with cDNA encoding eGFP and WT-SLC4A11 (representing the unaffected state), WT/E143K-SLC4A11 (representing a CHED2 carrier), WT/G709E-SLC4A11 (representing a FECD patient), E143K/E143K-SLC4A11 (representing a CHED2 patient), or G709E-SLC4A11 (representing homozygous FECD state, although no homozygous FECD patients have been reported). Coverslips were perfused alternately with isotonic and hypotonic media (Fig. 3.4A, black and white bars) and eGFP fluorescence was monitored, as a measure of cytosolic eGFP concentration (Figure 3.3). Rate of fluorescence change, which is a surrogate for cell volume change, was determined and corrected for the rate observed in vector-transfected cells (Fig. 3.5). HEK293 cells expressing WT-SLC4A11 alone provide a model for unaffected individuals and were defined as having 100% activity. Cells expressing E143K/WT-SLC4A11 (modeling CHED2 carriers) had 53 ± 6% of WT rate of function (Fig. 1B). Heterozygously expressed G709E-SLC4A11 (mimicking FECD patients) had only 27 ± 2% of WT rate of cell swelling. Cells homozygously expressing E143K-SLC4A11 (modeling CHED2 patients) had less than 5% of WT water flux activity (Fig. 3.4B).

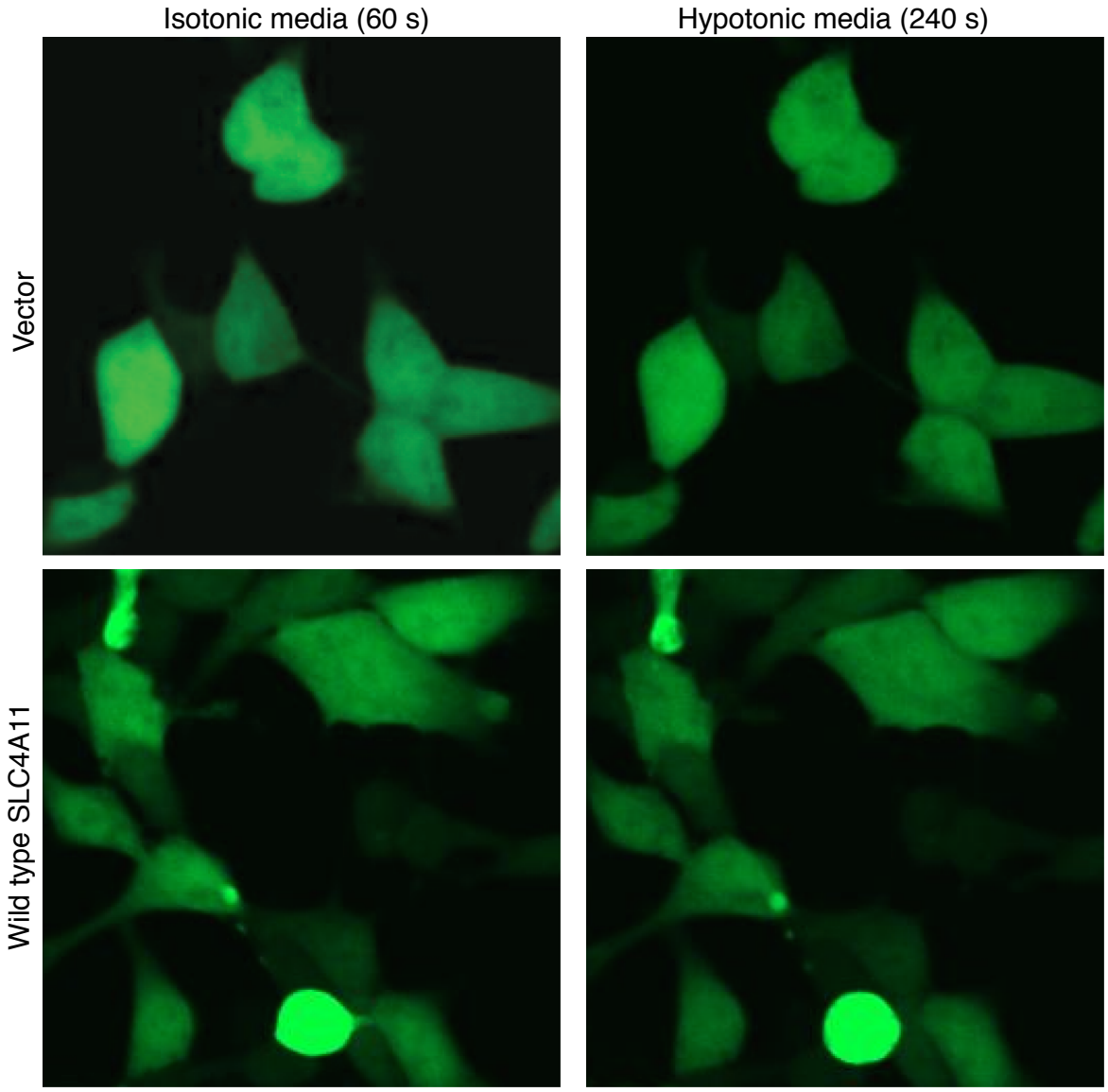

Figure 3.3 Representative images of HEK293 cells from water flux assay. HEK293 cells were co-transfected with cDNA encoding eGFP and WT SLC4A11 or pcDNA 3.1. 48 h later, cells were perfused with isotonic media for the first 120 s and then with hypotonic media for the next 240 s. Representative snapshots show the cells perfused with isotonic media at 60 s and hypotonic media at 240 s (Row 1: Vector and Row 2: WT SLC4A11 co-transfected with eGFP)

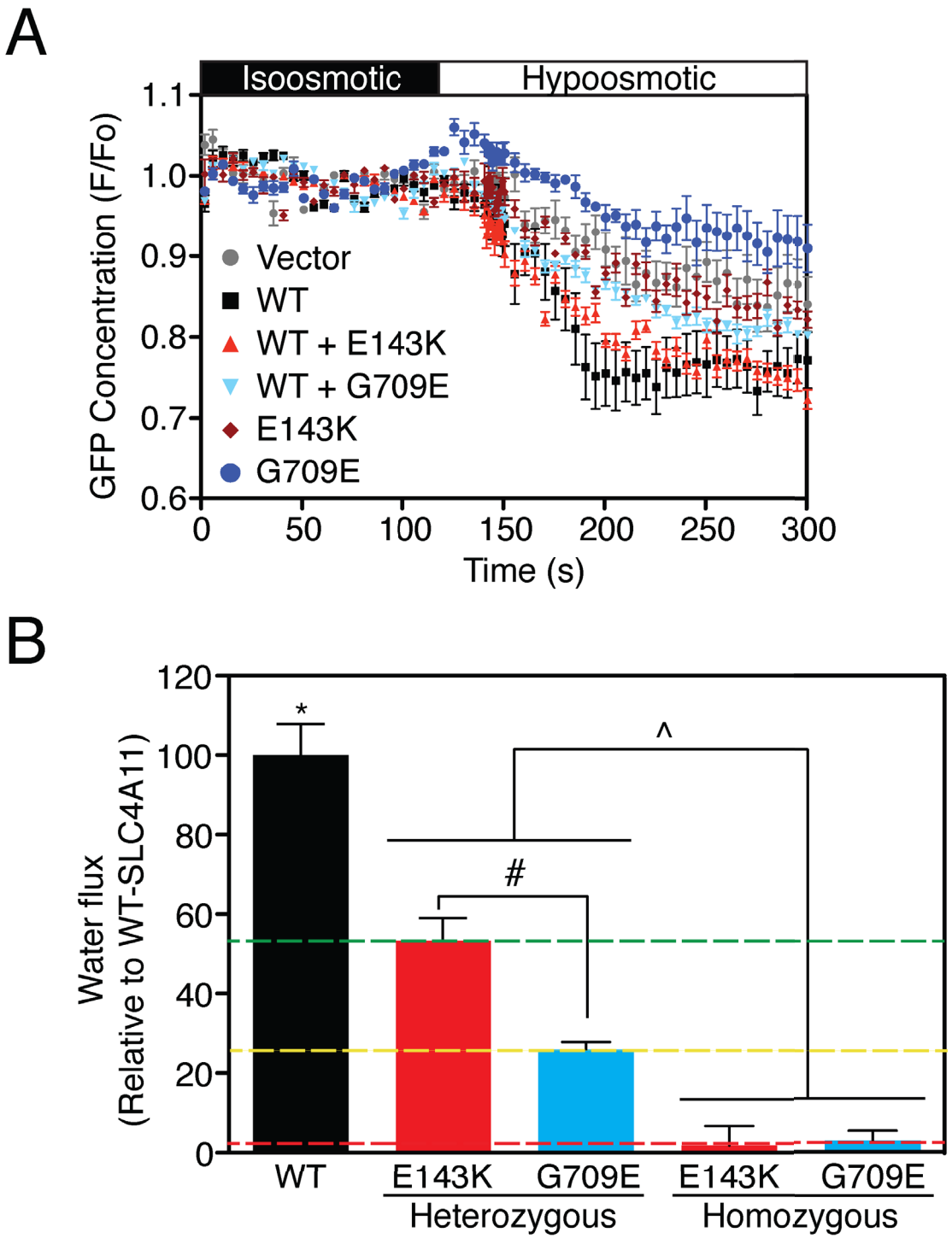

Figure 3.4 Osmotically driven water flux in cells expressing CHED2 or FECD SLC4A11 mutants. HEK293 cells were transiently transfected with cDNA encoding eGFP along

with empty vector, or HA-tagged WT SLC4A11 alone (homozygous) or HA-WT along with HA-tagged SLC4A11 mutants (heterozygous). The HA-tagged SLC4A11 mutants were also expressed alone (homozygous). **(A)** Cells were perfused alternately with isosmotic (black bar) and hypoosmotic (white bar) media. eGFP fluorescence (F) was normalized to F averaged for time 0-120 seconds (F_0) and F/F_0 plotted. **(B)** Rate of fluorescence change (a surrogate for cell volume change) was calculated, corrected for activity in vector-transfected cells and normalized to the rate found for homozygous WT-SLC4A11. Data represent the mean ± SEM of water flux in cells from 9 independent coverslips with 8-10 cells measured per coverslip. *: Significant difference ($P<0.05$) when compared to homozygous or heterozygous E143K and G709E SLC4A11. #: Significant difference ($P<0.05$) between heterozygous E143K and heterozygous G709E and ^: Significant difference ($P<0.05$) when compared between indicated heterozygous and homozygous SLC4A11 mutants. Dashed lines indicate the level of activity found in cells mimicking CHED2 patients (red), FECD patients (yellow) and CHED2 carriers (green).

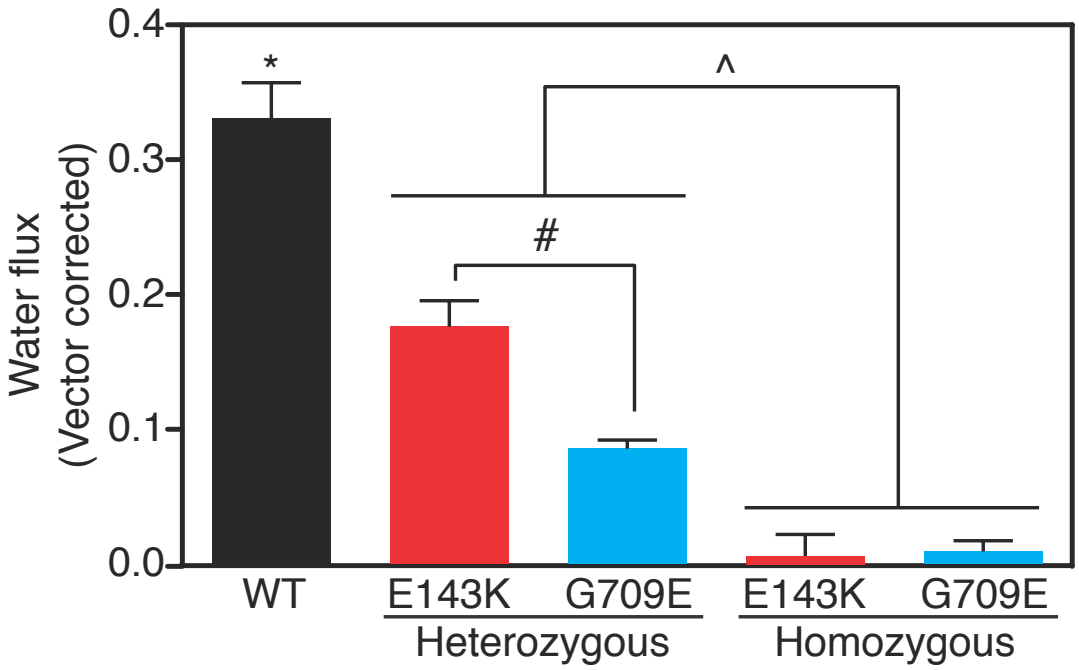

Figure 3.5 Water flux in cells expressing CHED2 or FECD SLC4A11 mutants. HEK293 cells were transiently transfected with cDNA encoding eGFP along with empty vector, or HA-tagged WT SLC4A11 alone (homozygous) or HA-WT along with HA-tagged SLC4A11 mutants (heterozygous). The HA-tagged SLC4A11 mutants were also expressed alone (homozygous). Cells were perfused alternately with isosmotic and hypoosmotic media. Rate of fluorescence change (a surrogate for cell volume change) was calculated and corrected for activity in vector-transfected cells ($0.20 \pm 0.03\ s^{-1}$). Data from 9 independent coverslips with 8-10 cells measured per coverslip were represented as mean ± SEM. *: Significant difference ($P<0.05$) when compared to homozygous or heterozygous E143K and G709E SLC4A11. #: Significant difference ($P<0.05$) between heterozygous E143K and heterozygous G709E and ^: Significant difference ($P<0.05$) when compared between indicated heterozygous and homozygous SLC4A11 mutants.

Immunoblots confirmed expression of SLC4A11 in cells used for water flux assays (Fig. 3.6A). In particular, SLC4A11 variants expressed as a mature upper band and an immature lower band, previously attributed to plasma membrane and ER-retained forms [8]. Also evident is the reduced steady-state accumulation of the mutant proteins, which is partially corrected when they are co-expressed with WT-SLC4A11.

3.2.2 Heterodimerization with R125H-SLC4A11 rescues CHED2-SLC4A11 to the cell surface

We next sought to develop a model that enabled rescue of mutant SLC4A11 to the cell surface, followed by assays of the functional activity of the rescued protein. While co-expression with WT-SLC4A11 would move mutant SLC4A11 to the cell surface in WT/mutant heterodimers [15], the drawback would be a high background activity arising from the WT-SLC4A11. R125H-SLC4A11, which processes to the cell surface like WT, but has a defect which prevents it from supporting water flux [15], held potential to rescue other SLC4A11 mutants to the cell surface, in heterodimers, without conferring background water flux on cells.

To the explore the utility of R125H-SLC4A11 in rescuing mutant SLC4A11 to the cell surface, N-terminally Myc-tagged R125H-SLC4A11 was co-expressed with HA-tagged CHED2 mutants. SLC4A11 migrates as two bands on immunoblots: a 110 kDa mature band (corresponding to plasma membrane protein) and a 90 kDa immature band (corresponding to intracellularly retained protein) (Fig. 3.7A and B, grey and black arrows) [8]. The absence of mature SLC4A11 on immunoblots indicates that all five representative CHED2-SLC4A11 mutants were ER-retained when expressed

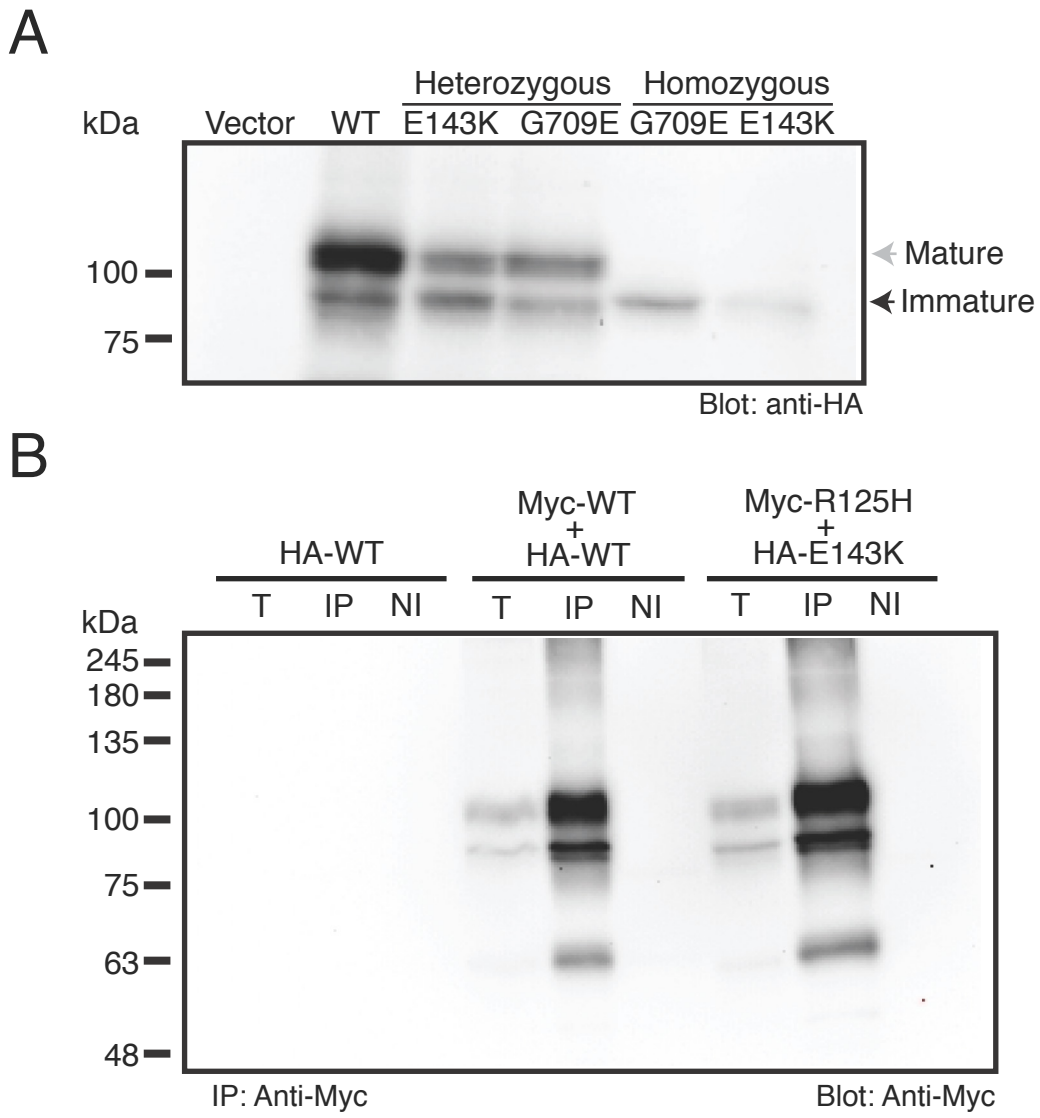

Figure 3.6 Expression of SLC4A11 variants and Immunoprecipitation of CHED2 SLC4A11 heterodimers. **(A)** HEK293 cells were transiently co-transfected with cDNA encoding eGFP and empty vector or HA-tagged WT SLC4A11 alone (homozygous) or HA-WT along with HA-tagged SLC4A11 mutants (heterozygous). HA-tagged SLC4A11 mutants were also expressed alone (homozygous). Cells were lysed and probed on immunoblots, using anti-HA antibody to detect the expression of SLC4A11 variants. Grey and black arrows mark the presence of mature and immature bands respectively. **(B)**

HEK293 cells were co-transfected with HA-tagged and Myc tagged WT SLC4A11 or HA-tagged E143K and Myc-tagged R125H. Cells were also transfected only with HA-tagged WT SLC4A11. Cells were lysed and 300 μg of total protein lysate was incubated either with rabbit polyclonal anti-MYC antibody (IP) or rabbit non-immune serum (NI). 50 μg of total protein from cell lysate (T) and immunoprecipitation of Myc-tagged proteins in the complex was detected on immunoblots using mouse monoclonal anti-Myc antibody.

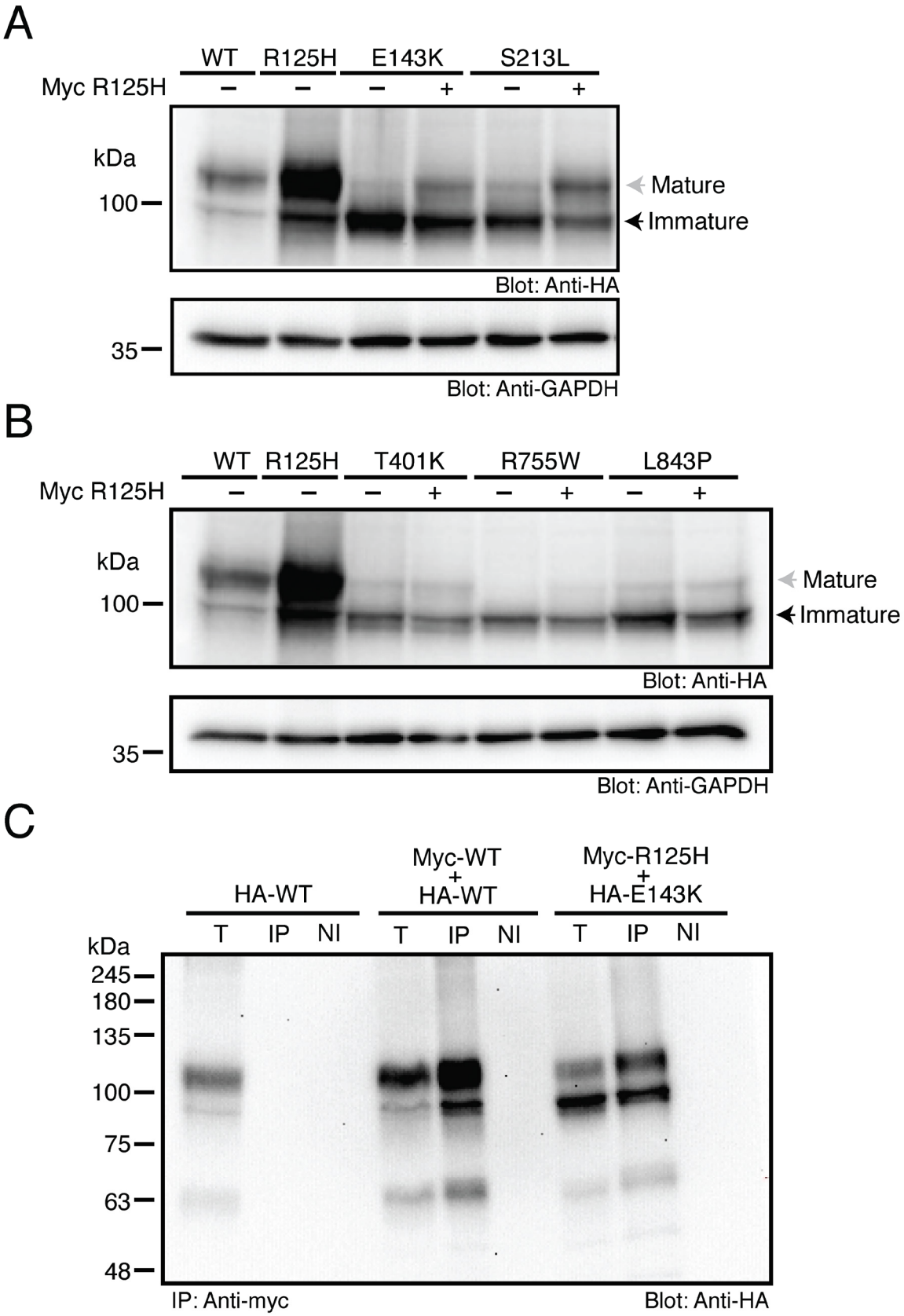
A
WT
R125H
E143K
S213L
Myc R125H
–
–
–
+
–
+
kDa
100
Mature
Immature
Blot: Anti-HA
35
Blot: Anti-GAPDH
B
WT
R125H
T401K
R755W
L843P
Myc R125H
–
–
–
+
–
+
–
+
kDa
100
Mature
Immature
Blot: Anti-HA
35
Blot: Anti-GAPDH
C
HA-WT
Myc-WT
+
HA-WT
Myc-R125H
+
HA-E143K
T
IP
NI
T
IP
NI
T
IP
NI
kDa
245
180
135
100
75
63
48
IP: Anti-myc
Blot: Anti-HA

Figure 3.7 Association between functionally inactive R125H-SLC4A11 and CHED2-SLC4A11 mutants. **(A & B)** HEK293 cells were either transfected with HA-tagged SLC4A11 (WT or CHED2 mutant cDNAs) or co-transfected with Myc-tagged R125H SLC4A11 and HA-tagged CHED2 SLC4A11 mutants as shown. Cell lysates were probed on immunoblots with anti-HA and anti-GAPDH antibodies. Grey and black arrows mark the presence of mature and immature bands. **(C)** For immunoprecipitation experiments, cells were co-transfected with HA-tagged and Myc-tagged WT SLC4A11 or HA-tagged E143K and Myc-tagged R125H. As a control for the specificity, the cells were also transfected only with HA-tagged WT-SLC4A11. Cell lysates (300 μg of total protein) were incubated either with rabbit polyclonal anti-Myc antibody (IP) or rabbit non-immune serum (NI). Immunoprecipitates and 50 μg of total protein cell lysate (T) were probed on immunoblots with anti-HA antibody.

homozygously (Fig. 3.7A and B). Co-expression with Myc-R125H-SLC4A11, however, led to the appearance of mature HA-tagged (CHED2 mutant) SLC4A11. In particular, E143K and S213L showed a strong presence of mature band when co-expressed with Myc-R125H (Fig. 3.7A). These data indicate the R125H-SLC4A11 expression induces cell surface maturation of co-expressed CHED2 mutants.

To test whether R125H exerts its effects on CHED2 mutants through heterodimerization, we performed co-immunoprecipitation studies. Myc antibody did not immunoprecipitate HA-tagged WT-SLC4A11, when expressed alone (Fig. 3.7C), indicating specificity of the immunoprecipitation. HA-probed immunoblots of cells co-transfected with Myc-WT and HA-WT SLC4A11 had SLC4A11 bands in both total and IP lanes, demonstrating dimerization of Myc and HA-WT SLC4A11. Similarly, co-expressed Myc-R125H and HA-E143K formed heterodimers, which was evident from the signal in the IP lane (Fig. 3.7C). SLC4A11 bands in total and IP lanes, when probed with anti-Myc antibody, confirmed pull down of the Myc-tagged proteins in these experiments (Fig. 3.6B). Taken together, these experiments reveal that ER-retained CHED2-SLC4A11 mutants can be rescued to the cell surface when heterodimerized with R125H-SLC4A11.

3.2.3 Co-expression with R125H-SLC4A11 increases cell surface processing of ER-retained CHED2 mutants

Next, we quantified the level of surface expression of CHED2 mutants when expressed homozygously (mimicking CHED2 patients), compared to co-expression with Myc-R125H-SLC4A11. When expressed alone, all of the CHED2 mutants tested have less than 50% of the cell surface processing level of WT-SLC4A11 (Figs. 3.8 and 3.9).

Remarkably, CHED2 SLC4A11 mutants co-expressed with Myc-R125H SLC4A11 had cell surface expression that increased significantly; some even had similar cell surface expression to WT (Figs. 3.8 and 3.9). Plasma membrane localization of HA-tagged R125H-SLC4A11 was not affected by the presence or absence of Myc-tagged R125H-SLC4A11 (Fig. 3.9). We conclude that the plasma membrane trafficking of most ER-retained CHED2 mutants increased when co-expressed with Myc-R125H-SLC4A11.

3.2.4 Some CHED2 mutants are functional when trafficked to the cell surface

We next assessed the functional activity of CHED2 mutant SLC4A11, following rescue to the cell surface by co-expression with R125H-SLC4A11. Cell swelling assays were performed for CHED2 mutants E143K, S213L, R755W and L843P and controls, R125H and WT-SLC4A11 (Figs. 3.10A and 3.11). Assays were also performed on cells co-expressing these SLC4A11 variants and R125H-SLC4A11 (Fig. 3.10B). Rates of swelling of cells expressing R125H-SLC4A11 was 4.2 ± 6.1% of WT level (Fig. 3.10C), consistent with the previous finding that this mutant is non-functional [15]. Water fluxes of cells homozygously expressing CHED2 mutants E143K, S213L, R755W and L843P were similar to background levels (Fig. 3.10C). Interestingly, three CHED2 mutants (E143K, S213L and L843P) co-expressed with R125H-SLC4A11 had significant functional activity (33-41% of WT). In contrast, functional activity of R755W did not increase upon co-expression with R125H-SLC4A11. Taken together, these experiments reveal that some CHED2 mutants confer water flux function upon cells when they are processed to the cell surface.

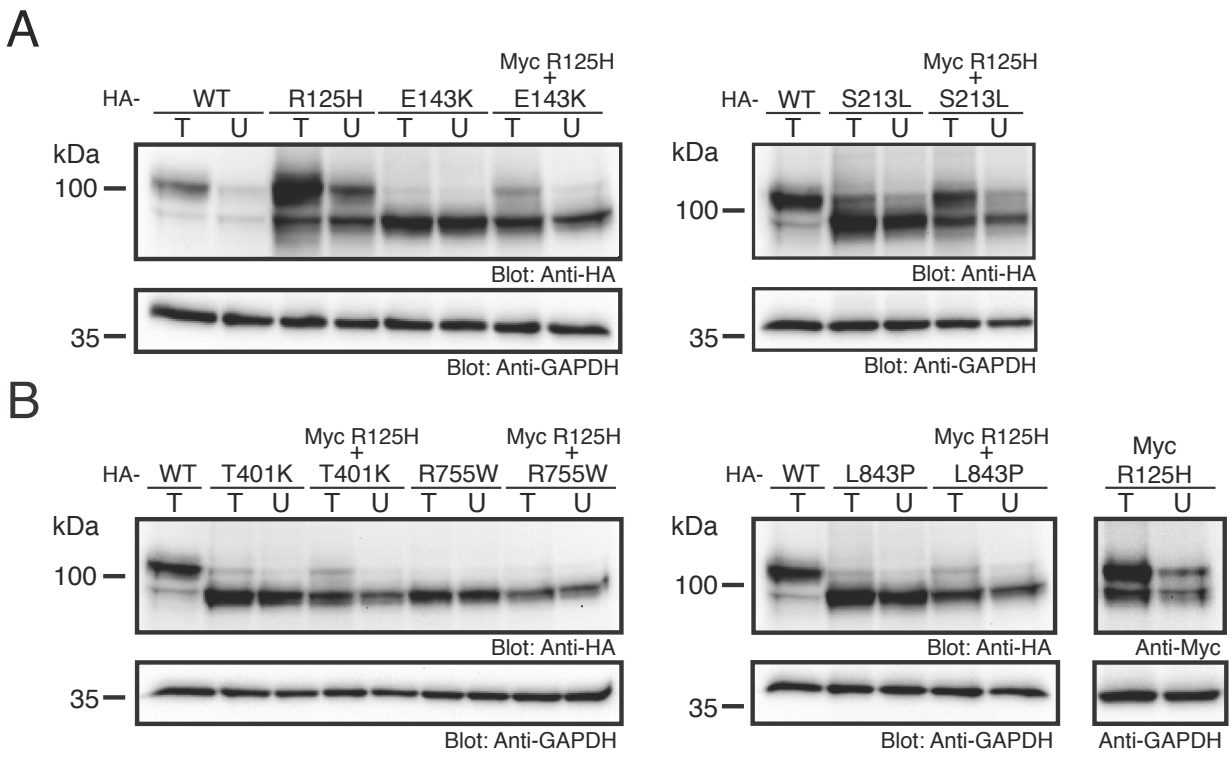

Figure 3.8 Cell surface processing efficiency of CHED2 mutants of SLC4A11 with or without R125H-SLC4A11. HEK293 cells were transfected with cDNA encoding indicated HA-tagged versions of SLC4A11 or co-transfected with Myc-tagged R125H SLC4A11 and HA-tagged versions of CHED2 mutants as shown. Cells were labeled with membrane-impermeant Sulfo-NHS-SS-biotin (SNSB). Cell lysates were divided into two equal fractions and one was incubated with streptavidin Sepharose resin to remove biotinylated proteins. The unbound fraction (U) and the total cell lysate (T) were processed for immunoblots and SLC4A11 was detected, using anti-HA or anti-Myc antibodies as shown. GAPDH, an internal control, was detected using anti-GAPDH antibody.

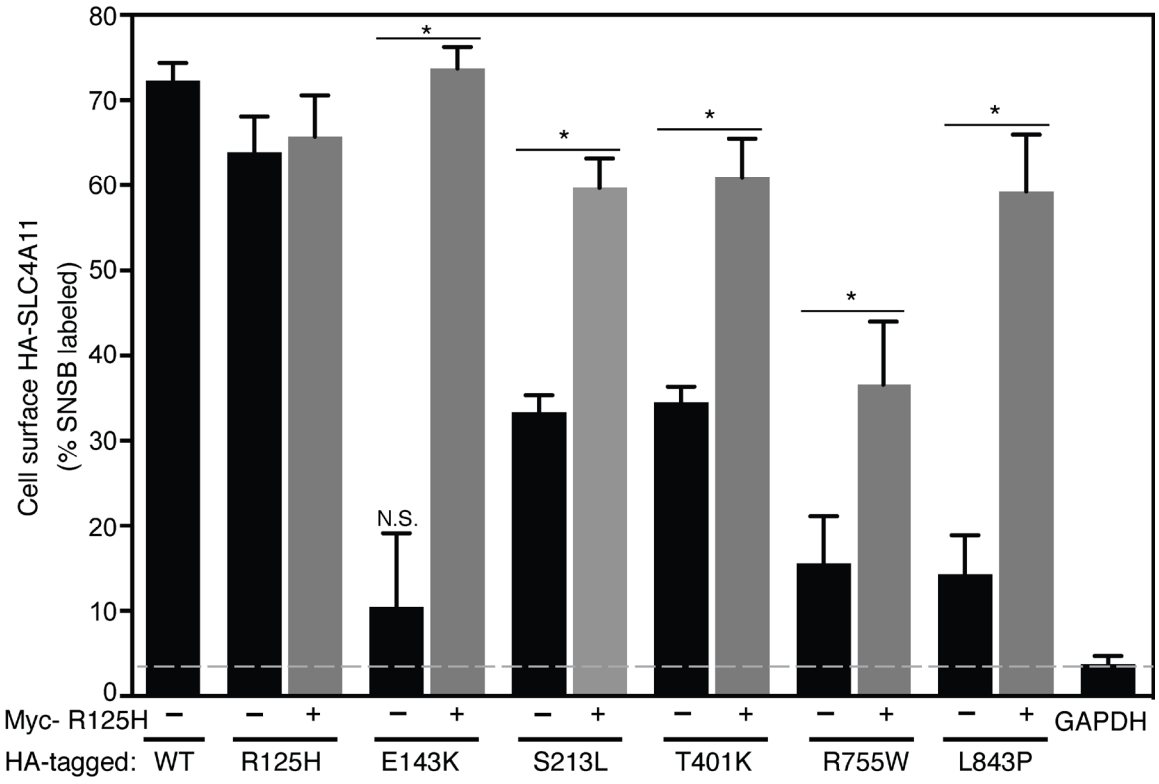

Figure 3.9 Effect of R125H-SLC4A11 on cell surface processing efficiency of CHED2-SLC4A11. HEK293 cells were transfected with cDNA encoding indicated HA-tagged versions of SLC4A11 or co-transfected with Myc-tagged R125H SLC4A11 and HA-tagged versions of CHED2 mutants as shown. Cells were labeled with membrane-impermeant Sulfo-NHS-SS-biotin (SNSB). The fraction of SLC4A11 and GAPDH labeled by SNSB was calculated. Error bars represent SEM (n=3-5). Dashed line indicates the background for this assay, as indicated by labeling of GAPDH. *: Significant difference ($P<0.05$) between the cell surface processing in the presence and absence of Myc-tagged R125H. N.S.: Not statistically significant ($P>0.05$) when compared to background (GAPDH).

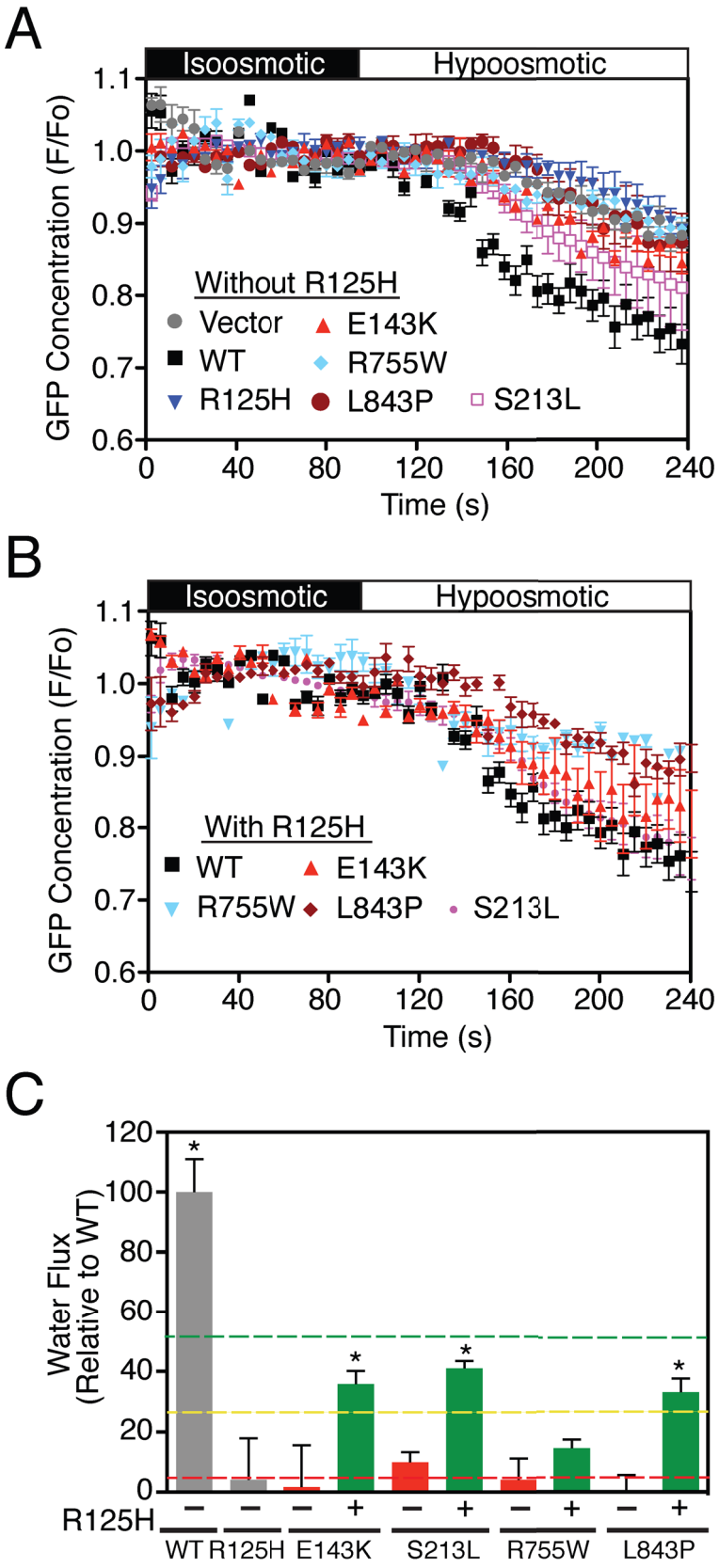
A
Isoosmotic
Hypoosmotic
GFP Concentration (F/Fo)
Time (s)
Without R125H
Vector
WT
R125H
E143K
R755W
L843P
S213L
B
Isoosmotic
Hypoosmotic
GFP Concentration (F/Fo)
Time (s)
With R125H
WT
E143K
R755W
L843P
S213L
C
Water Flux
(Relative to WT)
R125H
WT R125H E143K S213L R755W L843P

Figure 3.10 Osmotically driven water flux in cells expressing ER-retained CHED2 mutants, with or without R125H-SLC4A11. **(A)** HEK293 cells, grown on coverslips, were transiently co-transfected with cDNA encoding eGFP along with empty vector or HA-WT SLC4A11 alone or the indicated HA-tagged CHED2 mutants with or without Myc-tagged R125H SLC4A11. Cells were perfused alternately with isosmotic (black bar) and hypoosmotic (white bar) media. **(B)** Water flux assay in HEK293 cells expressing HA-tagged WT SLC4A11, or HA-tagged CHED2 mutants and Myc-tagged R125H, as indicated. **(C)** Water flux values were corrected for activity of vector-transfected cells and normalized to the rate found for cell expressing WT-SLC4A11. Data represent the mean ± SEM of water flux in cells from three independent experiments with 8-10 cells measured per coverslip. *: Significant difference ($P<0.05$) when compared to vector transfected cells. Dashed lines indicate the level of activity found in cells mimicking CHED2 patients (red), FECD patients (yellow) and CHED2 carriers (green), as determined in Fig. 1.

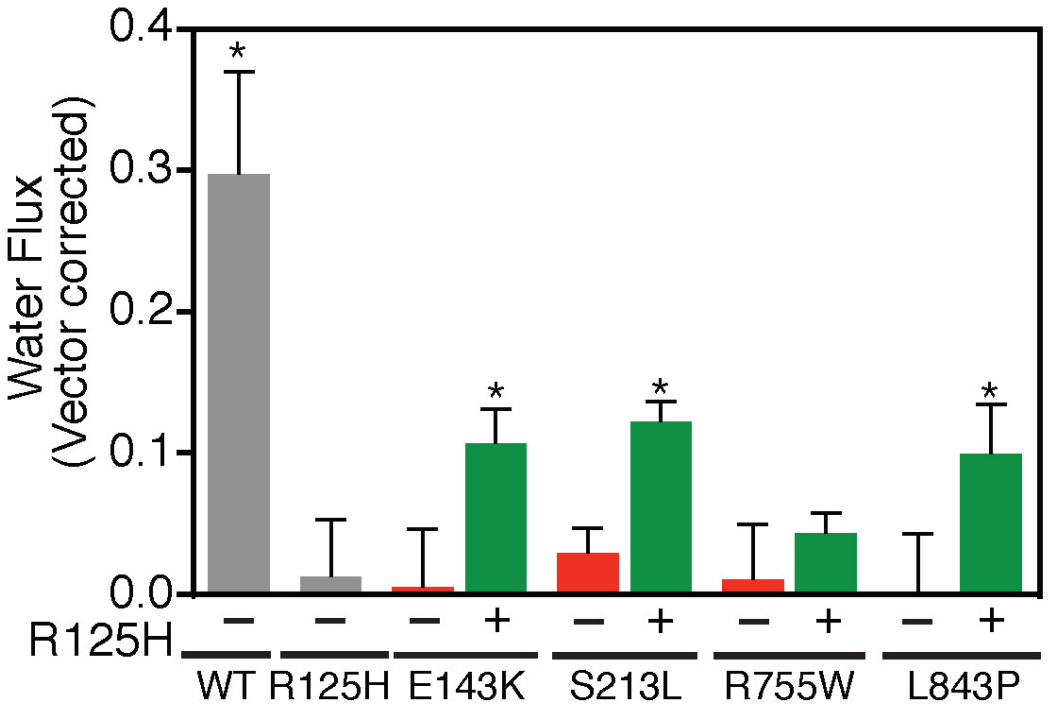

Figure 3.11 Osmotically driven water flux in cells expressing ER-retained CHED2 mutants, with or without R125H-SLC4A11. HEK293 cells were transiently co-transfected with cDNA encoding eGFP along with empty vector or HA-WT SLC4A11 alone or the indicated HA-tagged CHED2 mutants with or without Myc-tagged R125H SLC4A11. Cells were perfused alternately with isosmotic and hypoosmotic media. Rate of fluorescence change was calculated and corrected for activity arising from vector-transfected cells ($0.18 \pm 0.03\ s^{-1}$). Data represent the mean ± SEM of water flux in cells from 3 independent experiments with 8-10 cells measured per coverslip. *: Significant difference ($P<0.05$) when compared to vector transfected cells.

3.2.5 Increased cell surface processing and functional activity of CHED2-SLC4A11 grown at 30 °C

An established strategy to rescue the ER-retained mutant membrane proteins is lowering the cell culture temperature. For example, the cystic fibrosis gene product, ΔF508-CFTR, has increased targeting to the plasma membrane when grown at 30 °C [22]. Similarly, some CHED2 mutants when grown at 30 °C had increased plasma membrane targeting [3]. We chose two of those mutants (A269V and C386R-SLC4A11) and performed biotinylation assay to measure their cell surface processing ability when grown at 30 °C, compared to 37 °C (Fig. 3.12A and B). A269V and C386R SLC4A11 grown at 30 °C had significantly increased cell surface expression, which was similar to WT levels at 37 °C (Fig. 3.12C). Cell surface expression of WT-SLC4A11 was indistinguishable at 37 °C or 30 °C (Fig. 3.12C).

We next measured SLC4A11 functional activity arising in cells grown at 30 °C. WT-SLC4A11 expressed in HEK293 cells had the same water flux activity, whether grown at 37 °C or 30 °C (Figs. 3.13 and 3.14). Remarkably, cells expressing CHED2 SLC4A11 mutants, A269V and C386R, had significant increases in water flux grown at 30 °C, when compared to 37 °C. These CHED2-SLC4A11 expressing cells had more than 25% (but less than 60%) of WT-SLC4A11 functional activity (Fig. 3.13C). Taken together, these data suggest, that it is possible to rescue some CHED2 SLC4A11 mutants to the cell surface. This rescue can induce a significant SLC4A11 mediated water flux, with the potential to ameliorate the disease symptoms of CHED2 patients.

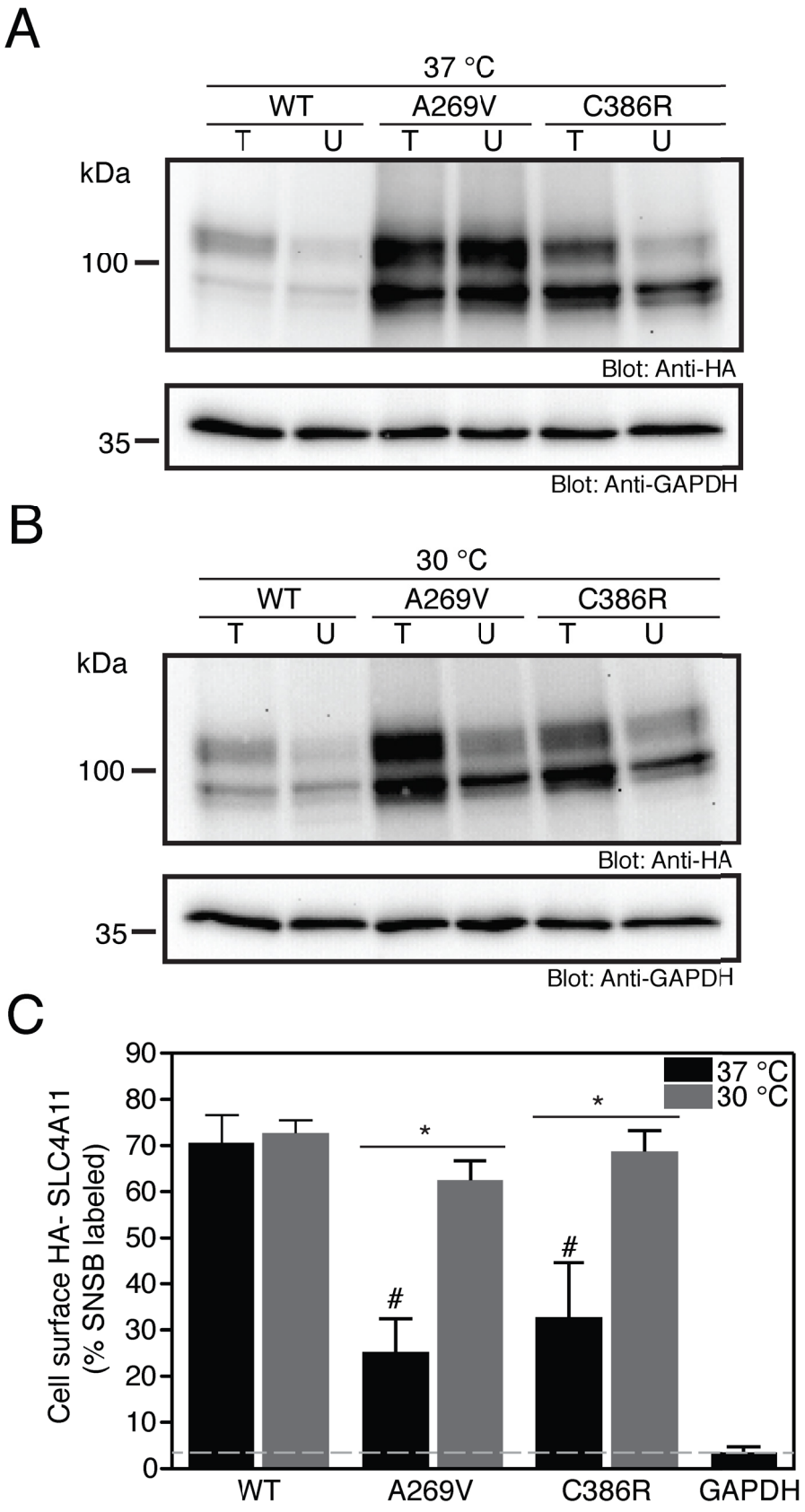
A
37 °C
WT
A269V
C386R
T
U
T
U
T
U
kDa
100
Blot: Anti-HA
35
Blot: Anti-GAPDH
B
30 °C
WT
A269V
C386R
T
U
T
U
T
U
kDa
100
Blot: Anti-HA
35
Blot: Anti-GAPDH
C
Cell surface HA- SLC4A11
(% SNSB labeled)
90
80
70
60
50
40
30
20
10
0
37 °C
30 °C
*
*
#
#
WT
A269V
C386R
GAPDH

Figure 3.12 Cell surface processing of SLC4A11 mutants grown at 30 °C. **(A)** HEK293 cells were transfected with cDNA encoding HA-tagged WT, A269V or C386R-SLC4A11 and grown at 37 °C for 48 h. Cells were then labeled with membrane-impermeant Sulfo-NHS-SS-biotin (SNSB) and lysed. Cell lysates were divided into two equal fractions. In one fraction, the biotinylated proteins were removed by incubation with streptavidin Sepharose resin. The unbound fraction (U) and the total cell lysate (T) were processed on immunoblots and probed with anti-HA and anti-GAPDH antibodies. **(B)** The same assay was carried out except that the cells were grown at 30 °C for 72 h. **(C)** The fraction of SLC4A11 and GAPDH labeled by SNSB was calculated for each experiment. Dashed line indicates the background for this assay, representing the level of labeling for cytosolic GAPDH. Error bars represent SEM (n=3-5). *: Significant difference ($P<0.05$) between the cell surface processing ability of the mutant SLC4A11 grown at 37 °C compared to 30 °C. #: Significant difference ($P<0.001$) when compared to all other conditions.

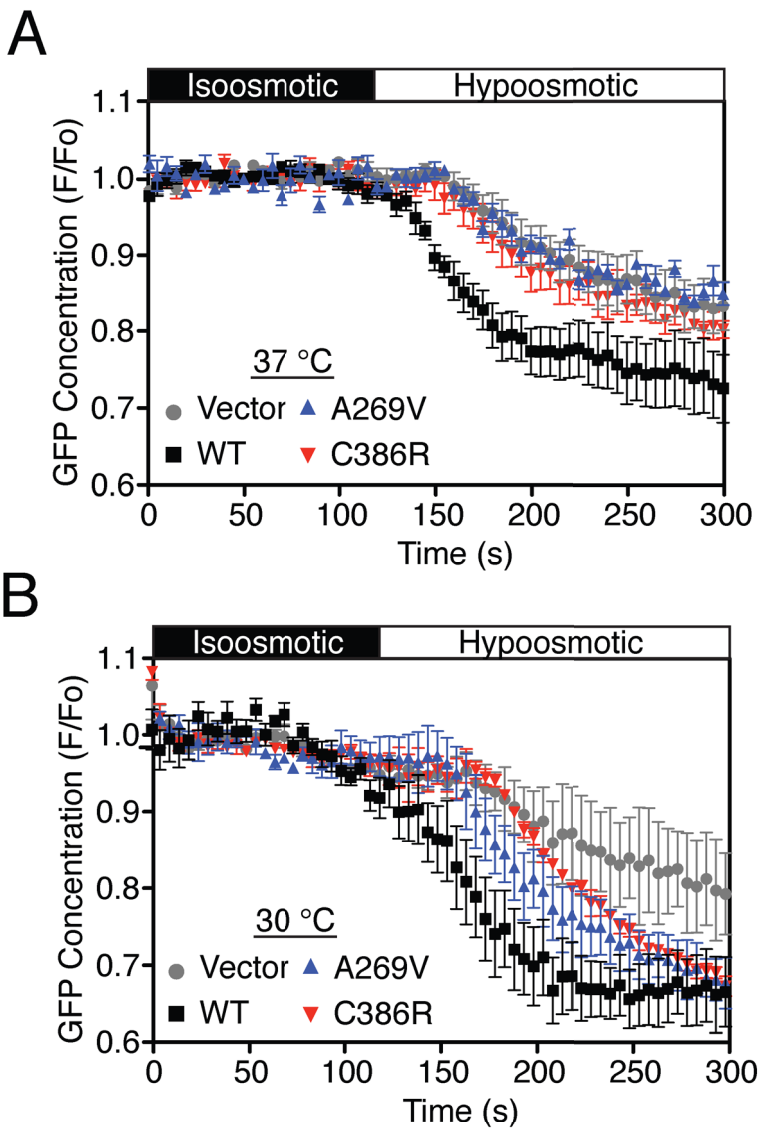
A
Isoosmotic
Hypoosmotic
GFP Concentration (F/Fo)
1.1
1.0
0.9
0.8
0.7
0.6
37 °C
Vector
A269V
WT
C386R
0
50
100
150
200
250
300
Time (s)
B
Isoosmotic
Hypoosmotic
GFP Concentration (F/Fo)
30 °C
Vector
A269V
WT
C386R
Time (s)
C
Water Flux
(Relative to WT)
140
120
100
80
60
40
20
0
37 °C
30 °C
*
*
WT
A269V
C386R

Figure 3.13 Osmotically driven water flux in cells expressing CHED2 SLC4A11 mutants grown at 37 °C and 30 °C. **(A)** HEK293 cells were co-transfected with cDNA encoding eGFP and empty vector, HA-tagged WT, A269V or C386R. Transfected cells, grown on coverslips at 37 °C for 48 h,, were perfused alternately with isosmotic (black bar) and hypoosmotic (white bar) medium. **(B)** The same assay was repeated for cells grown at 30 °C for 72 h post-transfection. **(C)** Rate of fluorescence change was calculated, corrected for vector transfected cells and normalized to the rate found for WT-SLC4A11 at 37 °C and 30 °C respectively. Data represent the mean ± SEM of water flux in cells from three independent experiments with 8-10 cells measured per coverslip Dashed lines indicate the level of activity found in cells mimicking CHED2 patients (red), FECD patients (yellow) and CHED2 carriers (green), as determined in Fig. 1. *: Significant difference ($P<0.05$) when compared to cells grown at 37 °C.

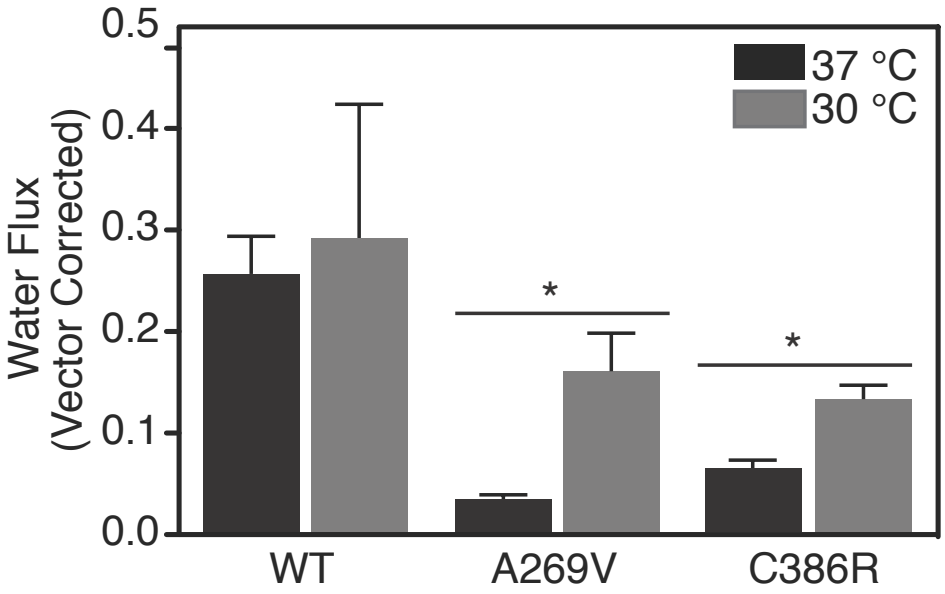

Figure 3.14 Water flux in cells expressing CHED2 SLC4A11 mutants grown at 37 °C and 30 °C. HEK293 cells were co-transfected with cDNA encoding eGFP and empty vector, HA-tagged WT, A269V or C386R. The transfected cells were grown on coverslips at 37 °C for 48 h or 30 °C for 72 h. Then the cells were perfused alternately with isosmotic and hypoosmotic medium. Rate of fluorescence change was calculated and corrected for vector transfected cells grown at 37 °C (0.16 ± 0.02) and 30 °C (0.17 ± 0.03). Data represent the mean ± SEM of water flux in cells from three independent experiments with 8-10 cells measured per coverslip. *: Significant difference ($P<0.05$) when compared to cells grown at 37 °C.

3.2.6 Expression of SLC4A11 mutants does not induce apoptosis or cell death

In CHED2 and FECD patients, there is a gradual reduction in endothelial cell number in addition to loss of function [1, 23]. Accumulation of ER-retained proteins, in some cases, leads to apoptotic cell death [24]. We thus determined whether expression of mutant SLC4A11 is associated with apoptotic cell death. Expression of caspase-3 and cleaved caspase-3 (a marker of apoptotic activation) were assessed in HEK293 cells stably expressing HA-tagged WT, E143K or G709E SLC4A11 or empty vector (Fig. 3.15). As a control, cells were treated with the protein kinase inhibitor, staurosporine, an established apoptotic activator [25]. While staurosporine treatment induced significant caspase-3 cleavage, expression of SLC4A11 variants did not affect the level of caspase-3 cleavage (Fig. 3.17A).

We next examined whether expression of disease-causing mutants of SLC4A11 induces cell death by any mechanism. Cell viability was measured in HEK293 cells stably expressing SLC4A11 variants, using a fluorescence-activated cell sorting approach (Fig. 3.16). The percentage of live cells was not significantly different between those stably expressing SLC4A11 variants and untransfected cells or empty-vector transfected cells. Similarly, the percentage of dead and injured HEK293 cells stably expressing the SLC4A11 variants was not significantly different from either untransfected cells or empty vector transfected cells (Fig. 3.17B). Importantly, HEK293 cells treated with hydrogen peroxide (which induces cell death [26]) had significant levels of dead and injured cells (Fig. 3.17B). Taken together, these experiments suggest that the expression of SLC4A11 mutants did not induce cell death, at least in this *in vitro* model.

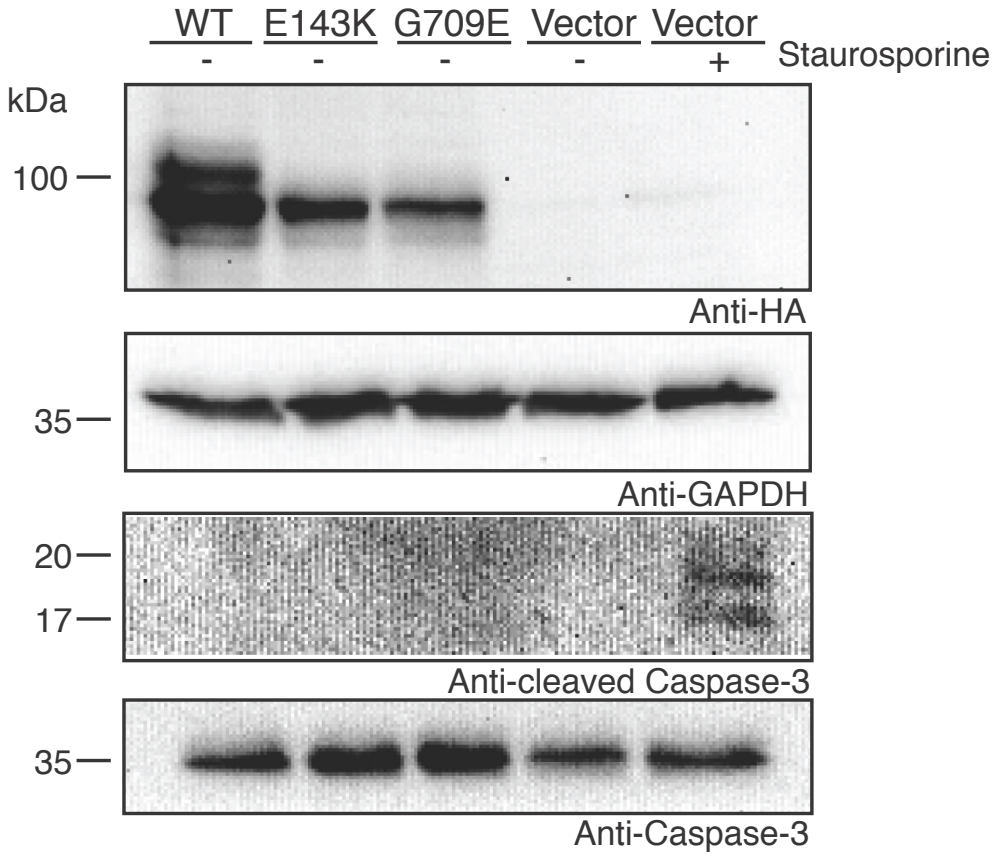

Figure 3.15 Expression of full length Caspase-3 and cleaved Caspase-3. HEK293 cells were stably transfected with cDNAs encoding vector, HA-tagged WT, E143K and G709E SLC4A11 variants. Cells were cultured for 10 days and one flask of vector-transfected cells were treated with Staurosporine (3 hrs, 1 μM). Cells were lysed and probed on immunoblots, using appropriate antibodies.

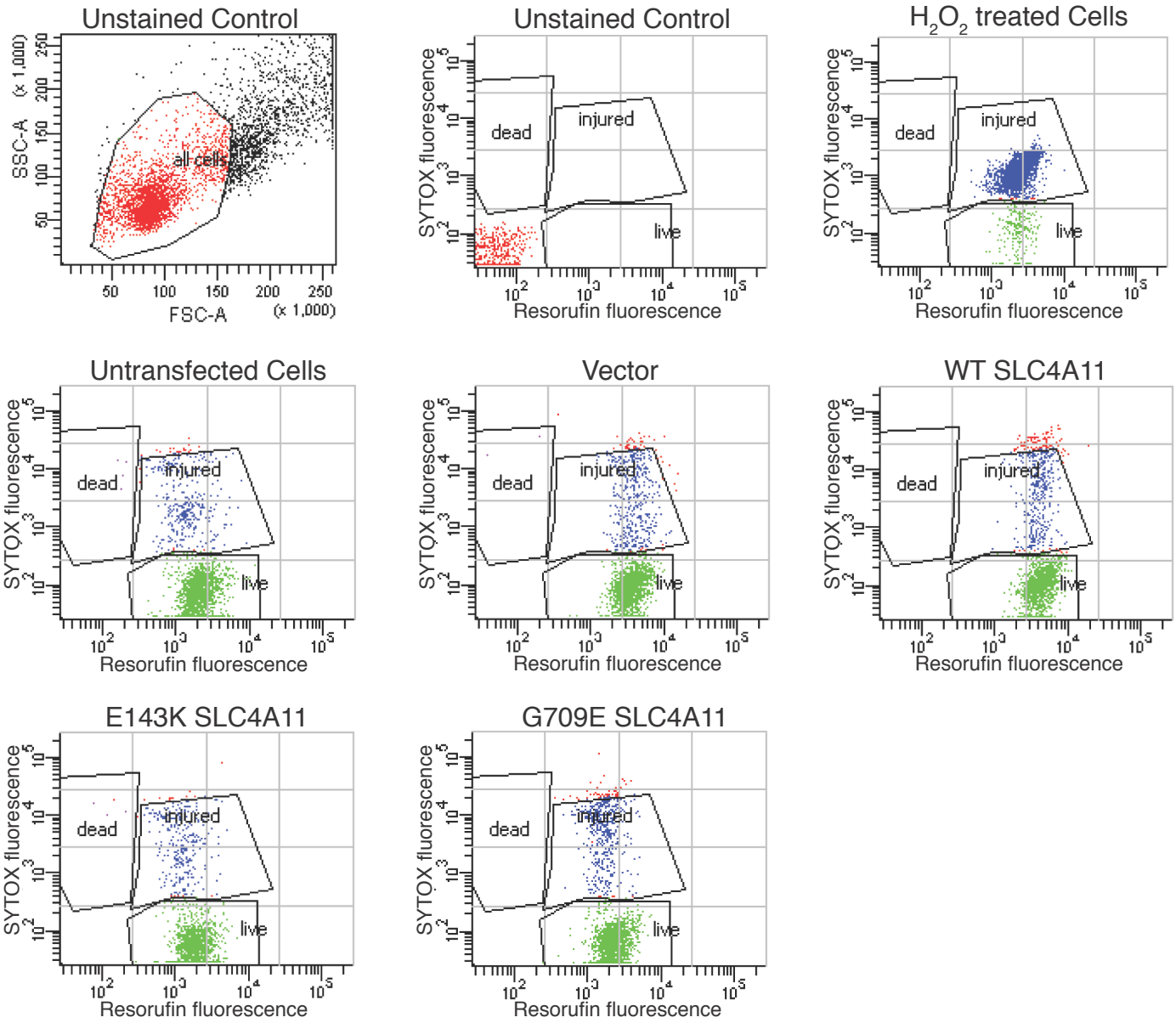

Figure 3.16 Quantification of live and dead HEK293 cells, stably expressing SLC4A11 variants, using Flow cytometry. HEK293 cells were stably transfected with cDNAs encoding vector, HA-tagged WT, E143K and G709E SLC4A11 variants. Cells were cultured for 10 days and one flask of vector-transfected cells were treated with 2 μM H_2O_2 for 4 hrs before staining. Using C_{12} –resazurin and SYTOX, live and dead cells

were stained. Unstained HEK293 cells were used as a control to sort the individual cells in Flow cytometry and then the cells expressing SLC4A11 variants were sorted for the amount of live and dead + injured cells. The dot plot of SYTOX Green fluorescence versus C_{12}–resorufin shows the resolution of live, injured and dead cells.

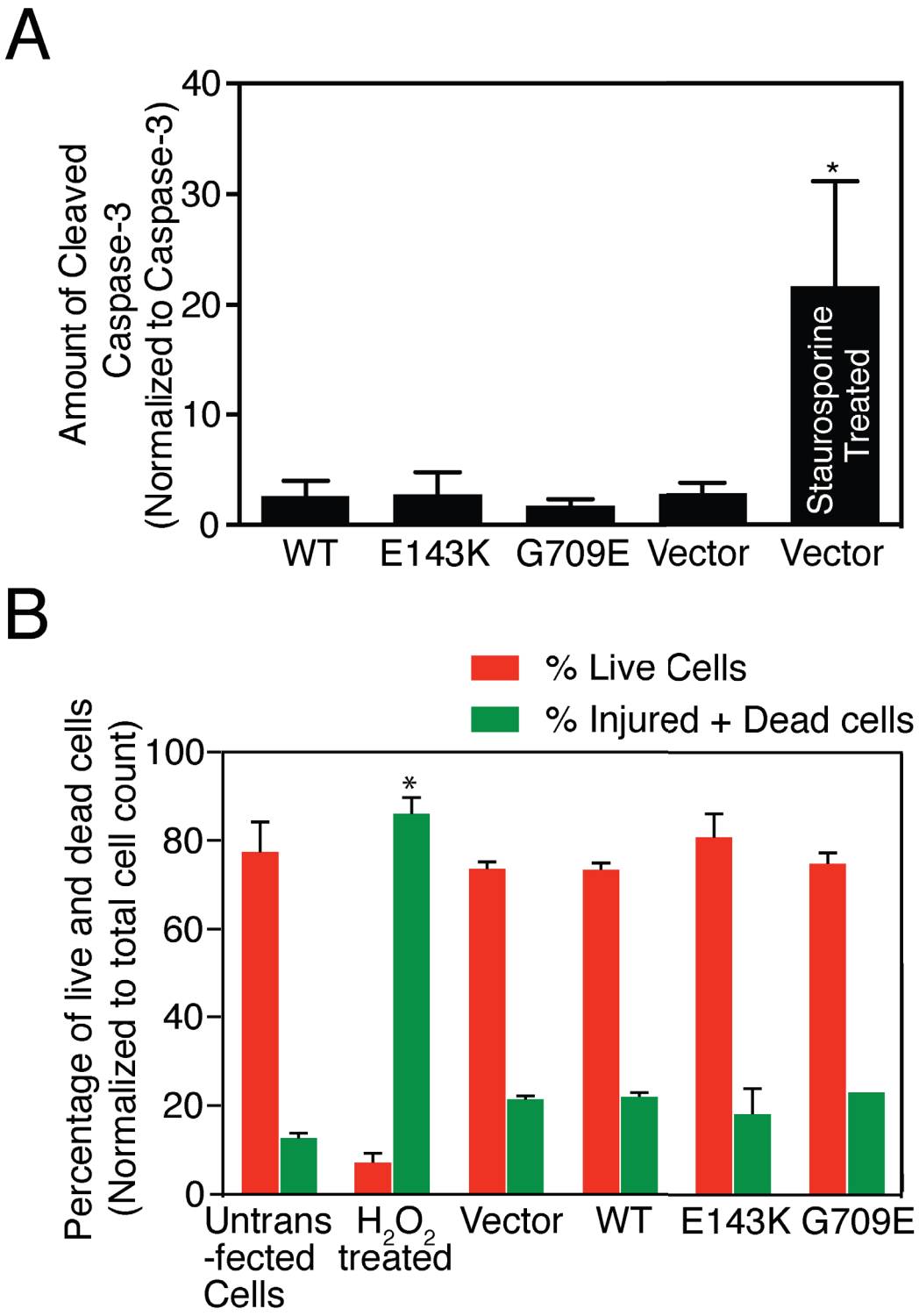

Figure 3.17 Cleaved Caspase-3 activity and vitality of HEK293 cells stably expressing SLC4A11 variants. **(A)** HEK293 cells, stably transfected with vector or cDNA encoding

the indicated HA-tagged SLC4A11 variant, were treated with 1 μM staurosporine for 3 h. Cells were lysed and processed for immunoblots. Densitometric analysis of cleaved Caspase-3 and total Caspase-3 was performed. Error bars represent SEM (n=3-5). *: Significant difference ($P<0.05$) when compared with staurosporine treated vector cells. **(B)** HEK293 cells, stably transfected with vector or cDNA encoding the indicated HA-tagged SLC4A11 variant, were treated (or not) with 2 μM H_2O_2 for 4 h. Live and dead cells were stained with C_{12}-resazurin and SYTOX, respectively, and cells were analyzed by Flow cytometry. Error bars represent SEM (n=3-4). *: Significant difference ($P<0.05$) among % injured + dead cells when compared with H_2O_2-treated.

3.3 Discussion

The goal of this study was to determine whether rescue of diseased SLC4A11 to the cell surface could be a viable approach to treat CHED2 and FECD. Most SLC4A11 mutants that have been characterized are retained in the ER [3, 16]. SLC4A11 functional activity, under conditions mimicking CHED2 patients, CHED2 carriers and individuals with FECD, suggested that restoration of about 25% of WT function will delay disease onset, and about 60% would prevent disease symptoms all together. This finding is significant because it provides benchmark values for the relative level of functional activity of SLC4A11 likely present in the corneal endothelial cells of CHED2 or FECD patients. Further it establishes a goal for any therapeutic treatments designed to move ER-retained SLC4A11 to the cell surface. CHED2 mutant SLC4A11 was rescued to the cell surface by heterodimerization with R125H-SLC4A11, or by reducing cell culture temperature to 30 °C. Cell surface rescued mutant SLC4A11 conferred significant water flux activity on cells. Finally, we assessed whether expression of mutant SLC4A11 causes cell death, since cell surface rescue might not be therapeutic, if cells die when they express the mutant. SLC4A11 variants do not lead to cell death, when expressed in HEK293 cells. Together we conclude that rescue of SLC4A11 to the cell surface is a feasible approach to treat CHED and FECD caused by SLC4A11 mutations.

Cystic fibrosis, a recessive genetic disorder, affecting lungs, pancreas and liver is caused by mutations in the large integral membrane protein, CFTR [18, 20]. One CFTR disease allele, ΔF508, which occurs in more than 80% of patients, causes CFTR to be retained in the ER [27]. CFTR, a plasma-membrane anion channel, cannot perform its essential function when retained intracellularly [20]. A thorough understanding of the cell

biology of ΔF508-CFTR led to the conclusion that it is possible to rescue ER-retained ΔF508 CFTR to the cell surface. Rescue of ΔF508-CFTR to the plasma membrane surface has been attempted, using chemical compounds, molecular chaperones and low temperature incubation or combination of all these methods [28-31]. The similarity of the molecular defects of ΔF508-CFTR and SLC4A11 mutants (ER retention) led us consider whether rescue to the cell surface could be a viable therapeutic strategy for CHED2 and FECD SLC4A11 mutants.

Here we established benchmark values for the level of SLC4A11 function in health and disease. These values were obtained in a transfected cell culture model, so they are limited in many ways including, expression under an exogenous (strong) promoter and expression in model cells instead of the corneal endothelium. Limitations to experimentation on humans and absence of animal models mean that although the data collected here have caveats; they represent the only available approach.

The transfected cell model revealed benchmark values for SLC4A11 activity that can be used to guide development of therapeutics. CHED2 patients have less than 5% of WT levels of water flux activity. Since CHED2 carriers are asymptomatic, their activity level, about 50% of WT, suffices to prevent disease. FECD mutant SLC4A11, expressed heterozygously as occurs in patients, had about 27% of WT activity. Thus, therapeutic strategies aimed at treating corneal dystrophies caused by SLC4A11 function have as their goal achieving 50% of WT function as a complete treatment for the disease. For a CHED2 patient, if 27% of WT activity were achieved then symptoms could be delayed for decades as FECD arises in the 30-50 age range [1, 2].

The observation that CHED2 carriers have about 50% of WT SLC4A11 function carries additional significance. This result suggests that in cornea there is two-fold excess functional activity over what is required to prevent disease. While it appears that this level of activity is enough in the cornea, it may be insufficient in other tissues, expressing the SLC4A11. In particular, the renal descending loop of Henle expresses the gene and urinary concentrating defects are found in *slc4a11*-null mice [32]. CHED2 carriers might therefore manifest similar dysfunction.

To assess the rescued protein's functional activity, CHED2 mutants of SLC4A11 were rescued to the cell surface in two ways. Co-expression with functionally inactive, but normally trafficked, R125H-SLC4A11 approximately doubled the fraction of CHED2 mutant SLC4A11 at the cell surface. Co-immunoprecipitation revealed that this arose from heterodimerization with R125H-SLC4A11. Similarly, reducing cell culture temperature from 37 to 30 °C was also associated with about a doubling of the fraction of CHED2-SLC4A11 at the cell surface. The ability to increase the cell surface processing of CHED2-SLC4A11 in two different ways underscores the feasibility of cell surface rescue as a therapeutic approach.

The major goal of this work was to determine whether cell surface rescue of ER-retained SLC4A11 mutants is potentially therapeutic. The answer to this question comes from measurements of water fluxes associated R125H-, or 30 °C-rescued SLC4A11. Cells expressing CHED2-SLC4A11 homozygously had water flux activity far below the benchmark level required to delay the onset of symptoms (i.e. below yellow line Figs 4 and 6). Cell surface rescue of CHED2-SLC4A11, by either approach, raised the water flux above the late-onset symptom threshold (Figs 4 and 6). Cell surface rescue thus can

confer functional activity exceeding the level found in the FECD state. That said, R755W-SLC4A11 subjected to rescue therapy did not exceed the late-onset threshold. It may be that R755W represents a severe allele, with profound misfolding, resistant to targeting correction. Individual CHED2 alleles will need to be assessed to determine whether they are likely candidates for rescue. We conclude that cell surface rescue is a viable therapeutic approach for corneal dystrophies caused by SLC4A11 mutation.

Low temperature incubation is established to increase plasma membrane targeting of some CHED2 mutants [3]. This is exciting because, at least for some CHED2 patients whose SLC4A11 mutants are not grossly misfolded, reducing the temperature of their cornea might provide symptomatic relief. Interestingly, the temperature of human cornea is 34 °C [33], significantly lower than body temperature. Data here suggest that reduction of corneal temperature to 30 °C would be useful in treating some CHED2 patients. In future, low temperature treatment might be combined with small molecule therapies to rescue ER-retained SLC4A11 to the cell surface.

CHED2 and FECD patients experience gradual loss of endothelial cell count along with loss of function [1, 23]. If accumulation of mutant SLC4A11 in endothelium alone is responsible for causing cell death, then cell surface rescue might not be therapeutic. Caspase activation assays revealed that expression of WT or mutant SLC4A11 did not induce apoptosis. More broadly, cell vitality assays indicated that expression of SLC4A11 variants did not give rise to a loss of cell viability. These results suggest that expression of mutant SLC4A11 is insufficient to explain the cell loss in corneal dystrophy patients. Rather, it suggests that endothelial cell loss arises from loss of some essential SLC4A11 function. The caveat to this conclusion is that data were

obtained only in HEK293 cells and the possibility remains that SLC4A11 mutants might have different effects in the context of the corneal endothelium.

Three independent *slc4a11*-null mouse lines have been reported, all of which recapitulate the corneal edema found in corneal endothelial patients [32, 34, 35]. Two of the reports do not mention decreased corneal endothelial cell density [32, 34], suggesting that loss of SLC4A11 function is insufficient to explain increased cell death. Increased loss of endothelial cell density, however, was observed in aged *slc4a11*-null mice (12 month) [35]. This is consistent with our conclusion that loss of SLC4A11 function is sufficient to explain the cell death found in SLC4A11-caused corneal dystrophies.

Our data lead to three conclusions regarding corneal dystrophies associated with SLC4A11 mutations. First, we defined the relative levels of SLC4A11 function required to prevent, or delay onset of corneal dystrophy symptoms. Second, we found that some ER-retained SLC4A11 mutants had significant functional activity upon rescue to the plasma membrane. Third, although not conclusive, our data suggest that expression of SLC4A11 mutants is not responsible for the cell loss observed in CHED2 and FECD patients. Together this sets the stage for therapeutic strategies centered on moving ER-retained SLC4A11 mutants to the cell surface to treat corneal dystrophies.

3.4 References

1. Klintworth, G. K. (2009) Corneal dystrophies. Orphanet. J. Rare Dis. **4**, 7
2. Schmedt, T., Silva, M. M., Ziaei, A. and Jurkunas, U. (2012) Molecular bases of corneal endothelial dystrophies. Experimental Eye Research. **95**, 24-34
3. Vilas, G. L., Morgan, P. E., Loganathan, S., Quon, A. and Casey, J. R. (2011) Biochemical Framework for SLC4A11, the Plasma Membrane Protein Defective in Corneal Dystrophies. Biochemistry. **50**, 2157-2169
4. Hemadevi, B., Veitia, R. A., Srinivasan, M., Arunkumar, J., Prajna, N. V., Lesaffre, C. and Sundaresan, P. (2008) Identification of mutations in the SLC4A11 gene in patients with recessive congenital hereditary endothelial dystrophy. Arch Ophthalmol. **126**, 700-708
5. Jiao, X., Sultana, A., Garg, P., Ramamurthy, B., Vemuganti, G. K., Gangopadhyay, N., Hejtmancik, J. F. and Kannabiran, C. (2007) Autosomal recessive corneal endothelial dystrophy (CHED2) is associated with mutations in SLC4A11. J Med Genet. **44**, 64-68.
6. Ramprasad, V. L., Ebenezer, N. D., Aung, T., Rajagopal, R., Yong, V. H., Tuft, S. J., Viswanathan, D., El-Ashry, M. F., Liskova, P., Tan, D. T., Bhattacharya, S. S., Kumaramanickavel, G. and Vithana, E. N. (2007) Novel SLC4A11 mutations in patients with recessive congenital hereditary endothelial dystrophy (CHED2). Mutation in brief #958. Online. Hum. Mutat. **28**, 522-523
7. Sultana, A., Garg, P., Ramamurthy, B., Vemuganti, G. K. and Kannabiran, C. (2007) Mutational spectrum of the SLC4A11 gene in autosomal recessive congenital hereditary endothelial dystrophy. Mol Vis. **13**, 1327-1332
8. Vithana, E. N., Morgan, P., Sundaresan, P., Ebenezer, N. D., Tan, D. T., Mohamed, M. D., Anand, S., Khine, K. O., Venkataraman, D., Yong, V. H., Salto-Tellez, M., Venkatraman, A., Guo, K., Hemadevi, B., Srinivasan, M., Prajna, V., Khine, M., Casey, J. R., Inglehearn, C. F. and Aung, T. (2006) Mutations in sodium-borate cotransporter SLC4A11 cause recessive congenital hereditary endothelial dystrophy (CHED2). Nature Genetics. **38**, 755-757

9. Desir, J. and Abramowicz, M. (2008) Congenital hereditary endothelial dystrophy with progressive sensorineural deafness (Harboyan syndrome). Orphanet J Rare Dis. **3**, 28-36

10. Vithana, E. N., Morgan, P. E., Ramprasad, V., Tan, D. T., Yong, V. H., Venkataraman, D., Venkatraman, A., Yam, G. H., Nagasamy, S., Law, R. W., Rajagopal, R., Pang, C. P., Kumaramanickevel, G., Casey, J. R. and Aung, T. (2008) SLC4A11 Mutations in Fuchs Endothelial Corneal Dystrophy (FECD). Hum. Mol. Genet. **17**, 656-666

11. Stehouwer, M., Bijlsma, W. R. and Van der Lelij, A. (2011) Hearing disability in patients with Fuchs' endothelial corneal dystrophy: unrecognized co-pathology? Clin. Ophthalmol. **5**, 1297-1301

12. Cordat, E. and Casey, J. R. (2009) Bicarbonate transport in cell physiology and disease. Biochem. J. **417**, 423-439

13. Jalimarada, S. S., Ogando, D. G., Vithana, E. N. and Bonanno, J. A. (2013) Ion Transport Function of SLC4A11 in Corneal Endothelium. Investigative Ophthalmology & Visual Science. **54**, 4330-4340

14. Park, M., Li, Q., Shcheynikov, N., Zeng, W. and Muallem, S. (2004) NaBC1 is a ubiquitous electrogenic Na^+ -coupled borate transporter essential for cellular boron homeostasis and cell growth and proliferation. Mol. Cell. **16**, 331-341

15. Vilas, G. L., Loganathan, S. K., Liu, J., Riau, A. K., Young, J. D., Mehta, J. S., Vithana, E. N. and Casey, J. R. (2013) Transmembrane water-flux through SLC4A11: a route defective in genetic corneal diseases. Human Molecular Genetics. **22**, 4579-4590

16. Vilas, G. L., Loganathan, S., Quon, A., Sundaresan, P., Vithana, E. N. and Casey, J. R. (2012) Oligomerization of SLC4A11 protein and the severity of FECD and CHED2 corneal dystrophies caused by SLC4A11 mutations. Human Mutation. **33**, 419-428

17. Desir, J., Moya, G., Reish, O., Van Regemorter, N., Deconinck, H., David, K. L., Meire, F. M. and Abramowicz, M. (2007) Borate transporter SLC4A11 mutations cause both Harboyan syndrome and non-syndromic corneal endothelial dystrophy. J. Med. Genet. **44**, 322-326

18. Riordan, J. R., Rommens, J. M., Kerem, B., Alon, N., Rozmahel, R., Grzelczak, Z., Zielenski, J., Lok, S., Plavsic, N., Chou, J. L., Drumm, M. L., Iannuzzi, M. C., Collins, F. S. and Tsui, L. C. (1989) Identification of the cystic fibrosis gene: cloning and characterization of complementary DNA. Science. **245**, 1066-1073

19. Cheng, S. H., Gregory, R. J., Marshall, J., Paul, S., Souza, D. W., White, G. A., O'Riordan, C. R. and Smith, A. E. (1990) Defective intracellular transport and processing of CFTR is the molecular basis of most cystic fibrosis. Cell. **63**, 827-834.

20. Lukacs, G. L. and Verkman, A. S. (2012) CFTR: folding, misfolding and correcting the ΔF508 conformational defect. Trends in Molecular Medicine. **18**, 81-91

21. Zhang, W., Fujii, N. and Naren, A. P. (2012) Recent advances and new perspectives in targeting CFTR for therapy of cystic fibrosis and enterotoxin-induced secretory diarrheas. Future Medicinal Chemistry. **4**, 329-345

22. Denning, G. M., Anderson, M. P., Amara, J. F., Marshall, J., Smith, A. E. and Welsh, M. J. (1992) Processing of mutant cystic fibrosis transmembrane conductance regulator is temperature-sensitive. Nature. **358**, 761-764.

23. Liu, J., Seet, L.-F., Koh, L. W., Venkatraman, A., Venkataraman, D., Mohan, R. R., Praetorius, J., Bonanno, J. A., Aung, T. and Vithana, E. N. (2012) Depletion of SLC4A11 Causes Cell Death by Apoptosis in an Immortalized Human Corneal Endothelial Cell Line. Investigative Ophthalmology & Visual Science. **53**, 3270-3279

24. Xu, C., Bailly-Maitre, B. and Reed, J. C. (2005) Endoplasmic reticulum stress: cell life and death decisions. The Journal of Clinical Investigation. **115**, 2656-2664

25. Chae, H.-J., Kang, J.-S., Byun, J.-O., Han, K.-S., Kim, D.-U., Oh, S.-M., Kim, H.-M., Chae, S.-W. and Kim, H.-R. (2000) Molecular mechanism of staurosporine-induced apoptosis in osteoblasts. Pharmacological Research. **42**, 373-381

26. Whittemore, E. R., Loo, D. T., Watt, J. A. and Cotmans, C. W. (1995) A detailed analysis of hydrogen peroxide-induced cell death in primary neuronal culture. Neuroscience. **67**, 921-932

27. Kulczycki, L. L., Kostuch, M. and Bellanti, J. A. (2003) A clinical perspective of cystic fibrosis and new genetic findings: relationship of CFTR mutations to genotype-phenotype manifestations. Am J Med Genet. **116A**, 262-267

28. Wang, Y., Bartlett, M. C., Loo, T. W. and Clarke, D. M. (2006) Specific rescue of cystic fibrosis transmembrane conductance regulator processing mutants using pharmacological chaperones. Mol Pharmacol. **70**, 297-302.

29. Robert, R., Carlile, G. W., Liao, J., Balghi, H., Lesimple, P., Liu, N., Kus, B., Rotin, D., Wilke, M., de Jonge, H. R., Scholte, B. J., Thomas, D. Y. and Hanrahan, J. W. (2010) Correction of the Delta phe508 cystic fibrosis transmembrane conductance regulator trafficking defect by the bioavailable compound glafenine. Mol Pharmacol. **77**, 922-930

30. Riordan, J. R. (2008) CFTR function and prospects for therapy. Annu Rev Biochem. **77**, 701-726

31. Pedemonte, N., Lukacs, G. L., Du, K., Caci, E., Zegarra-Moran, O., Galietta, L. J. and Verkman, A. S. (2005) Small-molecule correctors of defective DeltaF508-CFTR cellular processing identified by high-throughput screening. J Clin Invest. **115**, 2564-2571.

32. Groeger, N., Froehlich, H., Maier, H., Olbrich, A., Kostin, S., Braun, T. and Boettger, T. (2010) Slc4a11 prevents osmotic imbalance leading to corneal endothelial dystrophy, deafness, and polyuria. J. Biol. Chem. **285**, 14467-14474

33. Tan, L., Cai, Z. Q. and Lai, N. S. (2009) Accuracy and sensitivity of the dynamic ocular thermography and inter-subjects ocular surface temperature (OST) in Chinese young adults. Cont Lens Anterior Eye. **32**, 78-83

34. Lopez, I. A., Rosenblatt, M. I., Kim, C., Galbraith, G. G., Jones, S. M., Kao, L., Newman, D., Liu, W., Yeh, S., Pushkin, A., Abuladze, N. and Kurtz, I. (2009) Slc4a11 gene disruption in mice: Cellular targets of sensorineuronal abnormalities. J. Biol. Chem. **28**, 26882-26896

35. Han, S. B., Ang, H.-P., Poh, R., Chaurasia, S. S., Peh, G., Liu, J., Tan, D. T. H., Vithana, E. N. and Mehta, J. S. (2013) Mice With a Targeted Disruption of Slc4a11 Model the Progressive Corneal Changes of Congenital Hereditary

Endothelial Dystrophy. Investigative Ophthalmology & Visual Science. **54**, 6179-6189

Chapter 4: Role of Cytoplasmic Domain in Stabilization and Dimerization of SLC4A11, a Protein Mutated in Corneal Dystrophies

A version of this chapter is prepared for submission as Loganathan, S. K., Lukowski, C.M. and Casey, J. R. (2015). Role of Cytoplasmic Domain in Stabilization and Dimerization of SLC4A11, a Protein Mutated in Corneal Dystrophies**.** Biochemical Journal.

(All experiments were carried out by Sampath Loganathan except Figure 4.8, bacterial expression of SLC4A11 cytoplasmic domain, which was carried out by Chris Lukowski).

4.1 Introduction

SLC4A11 protein is widely expressed but most significantly in kidney and cornea [1, 2]. Mutations in *SLC4A11* gene cause three posterior corneal dystrophies: 1) recessive congenital hereditary endothelial dystrophy type 2 (CHED2) (MIM# 217700) [3-7], 2) recessive Harboyan syndrome (HS) (MIM# 217400) [8] (a combination of corneal dystrophy and perceptive deafness) and 3) dominant late-onset Fuchs endothelial corneal dystrophy (FECD) (MIM# 136800) [7-9]. Heterodimerization between WT and diseased monomers of SLC4A11 provides a molecular explanation for the recessive and dominant inheritance of CHED2 and FECD respectively [10]. A urinary concentrating defect has been identified in mice lacking SLC4A11 [11] but renal deficits have not been reported in people with SLC4A11 mutations.

SLC4A11 is located in the water transporting thin descending portion of the loop of Henle [11, 12] and in the corneal endothelial layer, where it faces the corneal stroma [1]. The *SLC4A11* gene (MIM# 610206) encodes an 891 amino acid long membrane protein, featuring an N-terminal 370 amino acid cytoplasmic domain, a 500 amino acid integral membrane domain with 14 transmembrane segments, and a very short cytoplasmic C-terminal tail [13]. SLC4A11 is a member of SLC4 family of bicarbonate transporters [14]. Similar to Anion Exchanger 1 (AE1/SLC4A1), a well-studied protein in the SLC4 family, SLC4A11 exists as dimers [10]. Although it belongs to SLC4 family of bicarbonate transporters, it has no reported bicarbonate transport activity [15, 16]. Human SLC4A11 was reported to be a Na^+ coupled borate transporter [17], which was not subsequently confirmed [15, 16]. Some reports show that SLC4A11 is a Na^+ coupled OH^- transporter [15, 16] and SLC4A11-C (a variant of SLC4A11) to be a Na^+ independent

$H^+(OH^-)$ transporter [18]. We reported that human SLC4A11 facilitates trans-membrane water movement when there is an established osmotic gradient [1, 19]. This is the first protein, shown to move water osmotically, that does not belong to major intrinsic protein (MIP) family [1].

About 60 SLC4A11 point mutations have been identified so far [3-7, 9, 20-26]. Of those, 19 are located on the cytoplasmic domain and the rest are in membrane domain. The mutations are distributed throughout the protein without any distinguishable pattern (Fig. 4.1B). CHED2 and FECD mutations cause SLC4A11 protein to be retained intracellularly in the endoplasmic reticulum, while a few of them may be functionally inactive, including SLC4A11 R125H [19]. Endoplasmic reticulum-retained SLC4A11 mutants can be rescued to the plasma membrane surface where they display functional activity [19].

Many SLC4A11 mutants are found in the cytoplasmic domain, indicating an important role in function, yet the role of the cytoplasmic domain is unknown. Interestingly, the R125H functional mutation resides in the cytoplasmic domain, indicating a role of this domain in SLC4A11 membrane transport activity. In this study, we set out to investigate 1) the presence of a substrate translocation pathway in the membrane domain that extends through the cytoplasmic domain of SLC4A11, 2) a role for the cytoplasmic domain in functional activity of the protein 3) the nature of association between cytoplasmic and membrane domains and 4) the role of membrane and cytoplasmic domains in SLC4A11 dimerization.

4.2 Results

4.2.1 Role of SLC4A11 cytoplasmic domain

Most disease–causing point mutations of SLC4A11 protein lead to misfolding and retention in the endoplasmic reticulum (ER), thereby impairing its water flux activity at the plasma membrane [19]. By contrast, the disease mutation R125H, which is localized in the SLC4A11 cytoplasmic domain (Fig. 4.1A), is catalytically inactive. The mutation does not cause the protein to be ER-retained, rather, the protein processes to the plasma membrane just like wild type SLC4A11 (WT-SLC4A11), albeit with no water flux activity [1]. This led us to consider how mutations in the cytoplasmic domain might affect the SLC4A11 transport function. Studies of the Na^+/HCO_3^- co-transporter, NBCe1 (SLC4A4), suggested that this SLC4 family member has cytoplasmic domain pore through which substrate translocates [27]. SLC4A11, being an SLC4 family member might function similarly to NBCe1. A substrate translocation pathway or pore might pass through the cytoplasmic domain, leading substrate through the membrane domain of SLC4A11 (Fig. 4.1A). Mutation of R125 could impair this cytoplasmic pathway.

To test whether the membrane domain of SLC4A11 alone has functional activity, the four membrane domain variants of SLC4A11 were expressed in HEK293 cells (Fig. 4.2A). We prepared four truncation mutants of the cytoplasmic domain of SLC4A11: HA-353-MD, HA-347-MD, HA-329-MD and HA-307-MD-SLC4A11, where an N-terminal Hemagglutinin (HA) epitope tag was added to membrane domain (MD) sequences starting at the indicated residue (Fig. 4.1B). Densitometric analysis and normalization to GAPDH revealed that HA-353-MD, HA-347-MD and HA-329-MD-SLC4A11 had only 5%, 10% and 15% expression relative to WT-SLC4A11, respectively

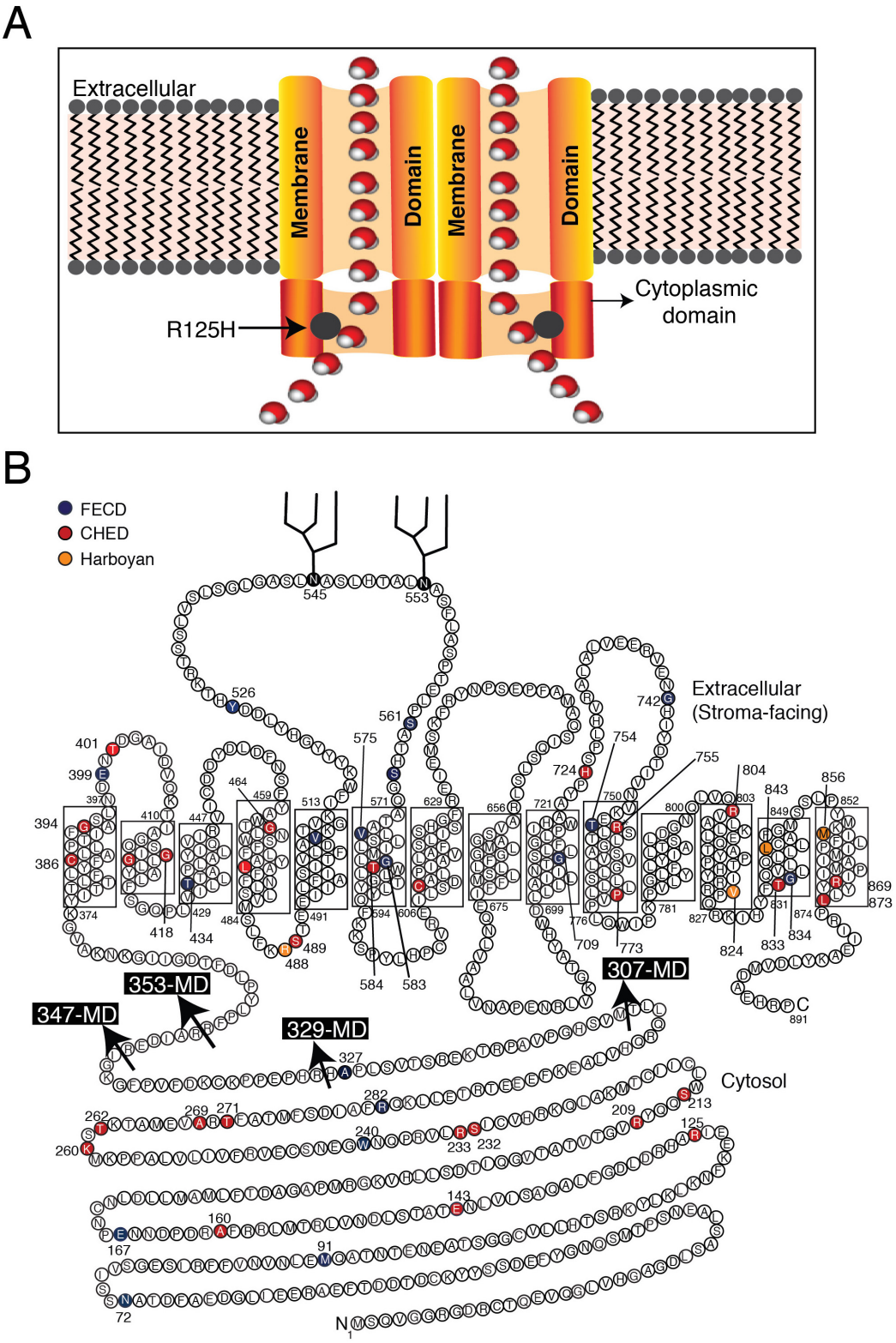

Figure 4.1 Substrate translocation pore along the cytoplasmic and membrane domains of dimeric SLC4A11. (**A**) SLC4A11 has a 374 amino acid N-terminal cytoplasmic domain

(CD) that may form an extension of the substrate translocation pore of the membrane domain (MD). Catalytically inactive mutants like R125H may occlude the cytosolic pathway interfering with the transport function but not folding of the protein. (**B**) Topology model of SLC4A11 indicating (black arrows) positions of the various membrane domain (MD) constructs (HA-353-MD, HA-347-MD, HA-329-MD and HA-307-MD). Inset legend indicates colors associated with disease mutations of Fuchs endothelial corneal dystrophy (FECD), congenital hereditary endothelial dystrophy (CHED2) and Harboyan syndrome (Harboyan) [3-7,9,20-26].

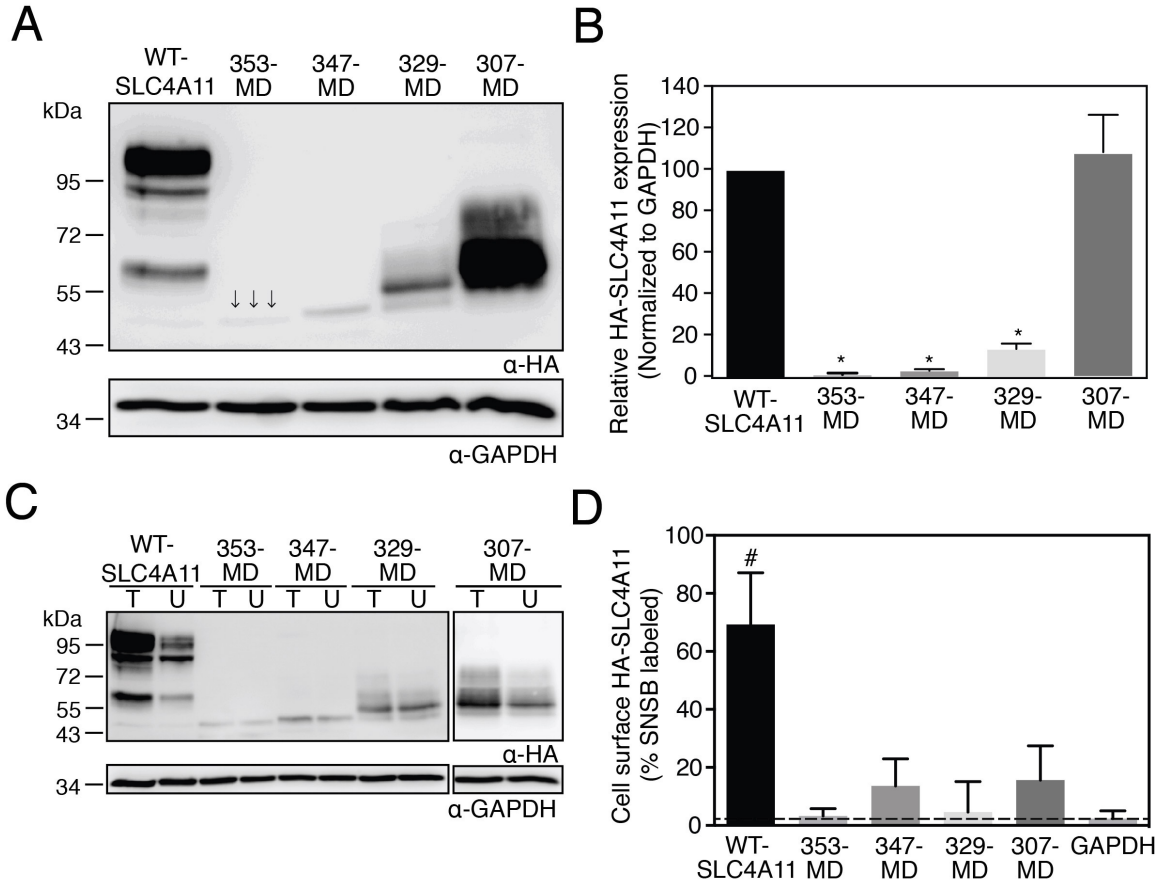

Figure 4.2 Expression and plasma membrane localization of SLC4A11 membrane domain constructs. (**A**) HEK293 cells were transfected with cDNA containing HA-epitope tagged WT-SLC4A11 and the indicated variants of MD-SLC4A11. Cell lysates (50 μg protein) were loaded on the SDS-PAGE gel and processed for immunoblotting with anti-HA (α-HA) and anti-GAPDH (α-GAPDH) antibodies. Black arrows indicate the location of HA-353-MD-SLC4A11. (**B**) Densitometric analysis of the expression of SLC4A11 variants were normalized to GAPDH and plotted relative to WT-SLC4A11. (**C**) HEK293 cells were transfected with cDNA encoding indicated HA-tagged versions of SLC4A11 as shown. Cells were labeled with membrane-impermeant Sulfo-NHS-SS-

biotin (SNSB). Cell lysates were divided into two equal fractions and one was incubated with streptavidin Sepharose resin to remove biotinylated proteins. The unbound fraction (U) and the total cell lysate (T) were processed for immunoblots, using anti-HA antibody as shown. (**D**) The fraction of SLC4A11 and GAPDH labeled by SNSB was calculated. Error bars represent SEM (n=3). Dashed line indicates the level of biotinylated GAPDH, which is a background for this assay. Significant difference ($P<0.05$) when compared to *: WT-SLC4A11 and HA-307-MD and #: GAPDH background.

(Fig. 4.2B). Only HA-307-MD-SLC4A11 had significant expression (~95%) comparable to WT-SLC4A11. These data show that the membrane domain of SLC4A11 requires the cytoplasmic domain to enable protein accumulation.

One technique to assess the state of protein maturation of these variants was the use of glycosidase enzymes. The migration position of fully deglycosylated protein was established upon treatment with N glycosidase F (PNG-F) (Fig. 4.3). Core glycosylated protein, carrying immature glycosylation associated with ER location, is sensitive to cleavage by Endo glycosidase H (Endo-H) whereas mature glycosylated chains are insensitive to this cleavage. Consistent with mature glycosylation of WT-SLC4A11, the protein was resistant to Endo-H, but its carbohydrate was cleaved by PNG-F. In contrast, the cytoplasmic domain mutants were sensitive to Endo-H to varying degrees. This suggests that the mutants predominantly fail to mature. HA-329-MD-SLC4A11 however, shows some resistance to Endo-H, consistent with partial maturation (Fig. 4.3) [9].

To test further the localization of all the membrane domain variants, cell surface biotinylation assay [13] was carried out (Fig. 4.2C). The fraction of biotin labeled (plasma membrane localized) protein was calculated relative to WT-SLC4A11 (Fig. 4.2D). None of the SLC4A11 membrane domain variants localized to the cell surface significantly. As a result, the functional activity of the membrane domain by itself cannot be assessed, as functional assays require cell surface localization.

4.2.2 GFP and mNectarine fusion proteins to cover hydrophobic surface

A possible explanation for the instability of the isolated SLC4A11 membrane domain is that the membrane domain must be associated with the cytoplasmic domain, perhaps to satisfy hydrophobic bonding requirements. To test this, we created two fusion

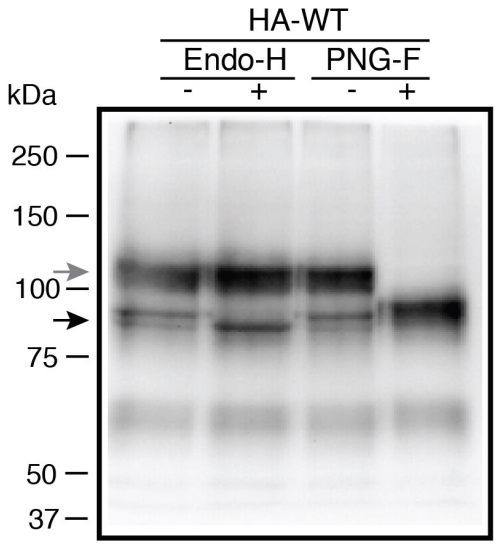
HA-WT
Endo-H
PNG-F
- + - +
kDa
250
150
100
75
50
37

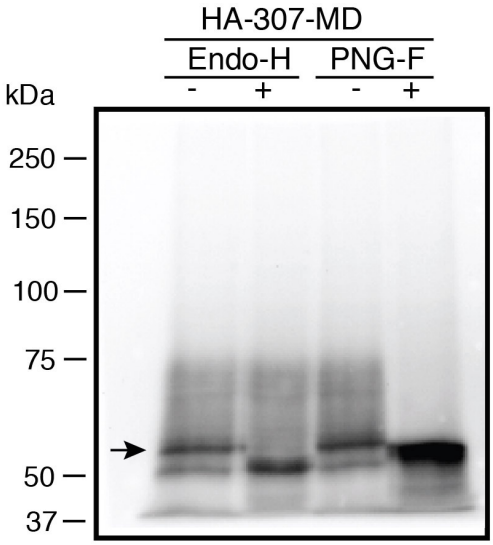
HA-307-MD
Endo-H
PNG-F
- + - +
kDa
250
150
100
75
50
37

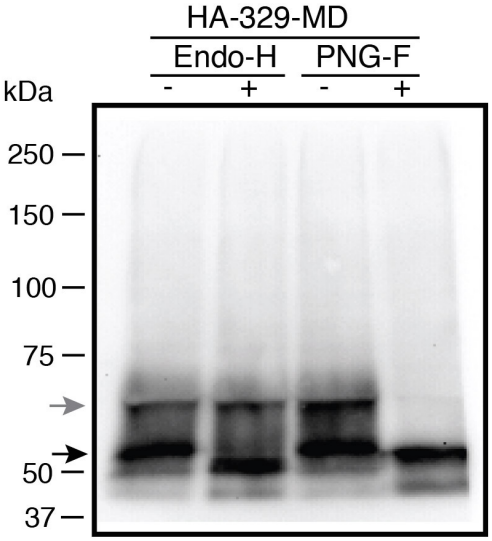
HA-329-MD
Endo-H
PNG-F
- + - +
kDa
250
150
100
75
50
37

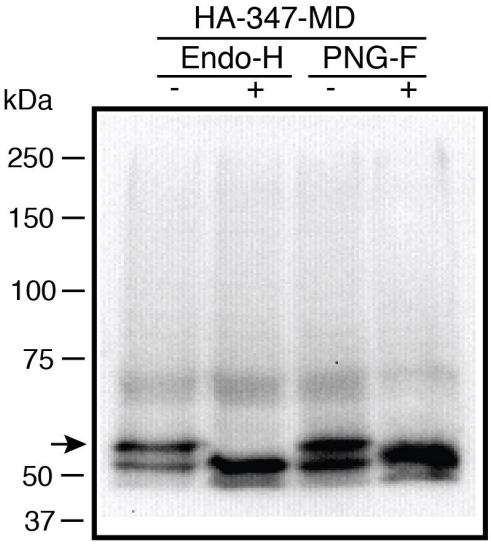
HA-347-MD
Endo-H
PNG-F
- + - +
kDa
250
150
100
75
50
37

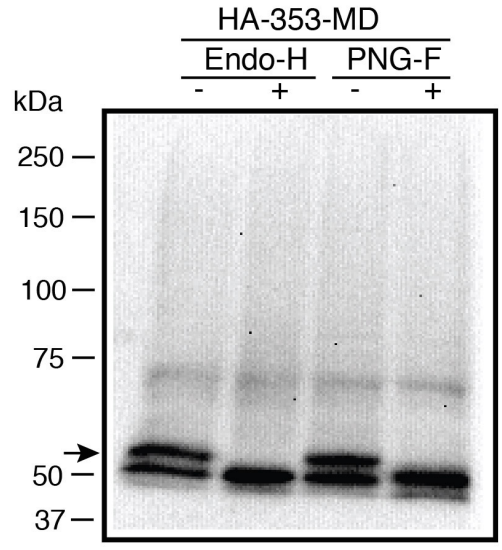
HA-353-MD
Endo-H
PNG-F
- + - +
kDa
250
150
100
75
50
37

Figure 4.3 Glycosylation state of the various membrane domain constructs of SLC4A11. HEK293 cells were transfected with cDNA containing HA- epitope tagged WT-SLC4A11 and the indicated variants of MD-SLC4A11. Cell lysates containing 25 μg of total protein were denatured at 65 °C and then treated with Endo H or PNGase F (PNG F) for 1 h at 37 °C. All the enzyme treated or untreated cell lysates were loaded on the SDS-PAGE gel and processed for immunoblotting with anti-HA antibody as shown. Grey and black arrows indicate the Endo H resistant and sensitive form of the protein respectively.

proteins: 1) Green fluorescent protein (GFP) and 2) mNectarine (a variant of Red fluorescent protein) [28] fused to varying lengths of SLC4A11 membrane domain (Fig. 4.4A). GFP and mNectarine differ in their oligomeric state. GFP is dimeric when fused to integral membrane proteins while mNectarine is monomeric [28-30]. We considered the possibility that the required role of the cytoplasmic domain might be to cause SLC4A11 to dimerize, a function that would be complemented by GFP, but not mNectarine. GFP-368-MD, mNect-368-MD, GFP-307-MD and mNect-307-MD-SLC4A11 were expressed in HEK293 cells and their expression assessed on immunoblots (Fig. 4.4B). Expression of fusion protein variants was quantified densitometrically and normalized to GAPDH expression and plotted relative to WT-SLC4A11 expression assessed on the same blot (Fig. 4.4C). GFP-368-MD and mNect-368-MD accumulated to less than 5% of the level of WT-SLC4A11, while GFP-307-MD and mNect-307-MD had close to 15% expression levels. Cell surface processing assays revealed that plasma membrane surface expression was insignificant for the four fusion variants (Figs. 4.4D & E). Fusion of GFP or mNectarine failed to rescue the processing defect of SLC4A11 membrane domain. Neither providing a surface covering on the SLC4A11 membrane domain nor forced dimerization of the cytoplasmic domain is sufficient to induce rescue of the membrane domain to the cell surface.

4.2.3 AE1 cytoplasmic domain and SLC4A11 membrane domain chimera

Since the fusion of GFP and mNectarine did not stabilize the SLC4A11 membrane domain, we hypothesized that the membrane domain requires a protein with a similar structural fold as SLC4A11 cytoplasmic domain. To identify a protein with a

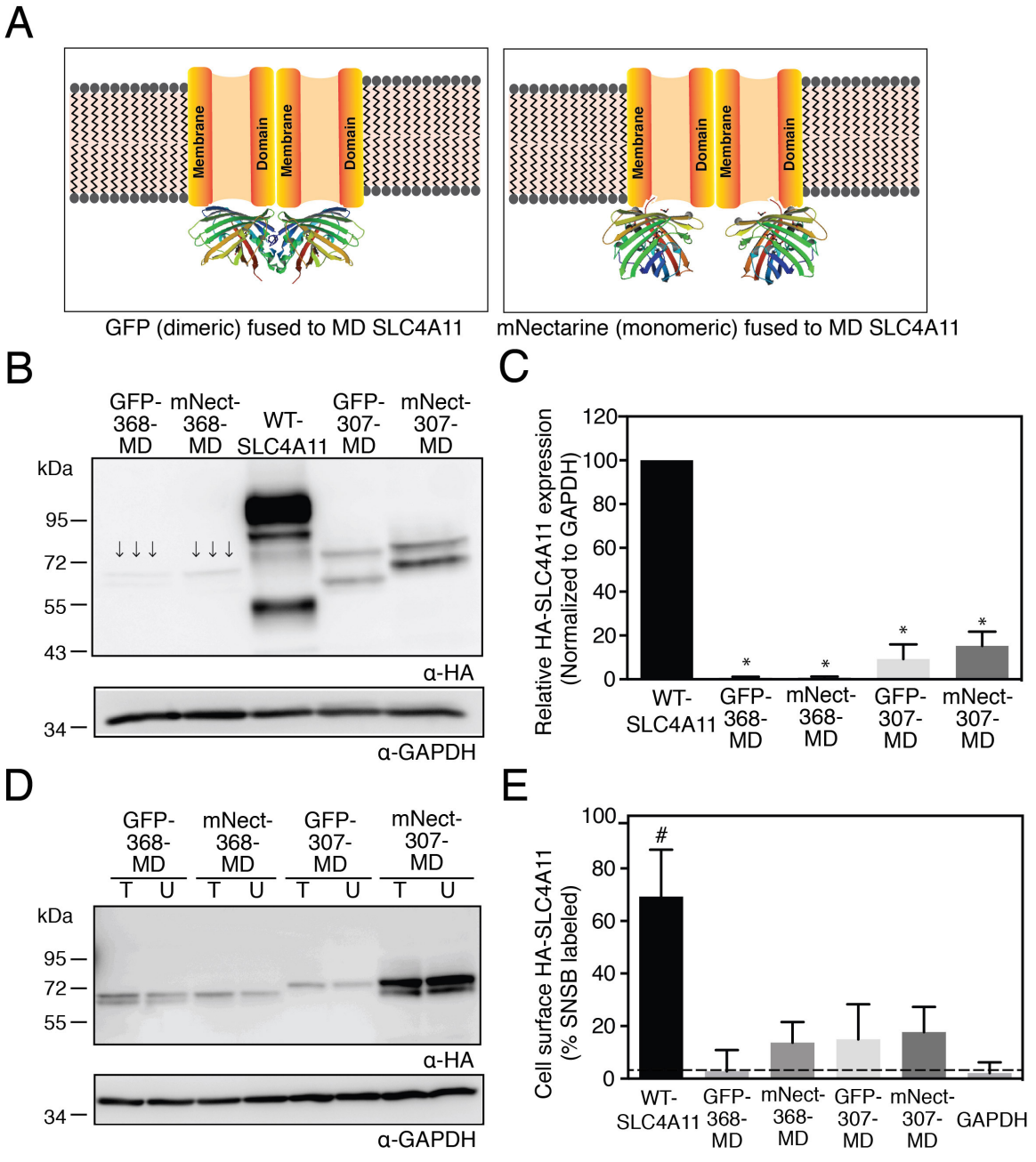

Figure 4.4 Expression and plasma membrane localization of enhanced Green fluorescent protein (GFP) and mNectarine protein (mNect) fused variants of MD SLC4A11. (**A**) Enhanced Green fluorescent protein and mNectarine (a modified form of Red fluorescent protein), which exist as dimer and monomer respectively were fused to the N-terminus of

MD-SLC4A11 either at 368 (GFP-368-MD and mNect-368-MD) or 307 (GFP-307-MD and mNect-307-MD) amino acid residue. (**B**) HEK293 cells were transfected with cDNA encoding HA-epitope tagged WT-SLC4A11 and the indicated variants of GFP or mNectarine fused MD-SLC4A11. Equal amount of total protein from cell lysates were loaded on the SDS-PAGE gel and processed for immunoblotting with anti-HA and anti-GAPDH antibodies. (**C**) Densitometric analysis of the expression of SLC4A11 variants were normalized to GAPDH and plotted relative to WT-SLC4A11. (**D**) HEK293 cells were transfected with cDNA encoding indicated HA-tagged versions of SLC4A11 and subjected to cell surface biotinylation assays. The unbound fraction (U) and the total cell lysate (T) were immunobloted using anti-HA and anti-GAPDH antibodies, as shown. (**E**) The fraction of SLC4A11 and GAPDH labeled by SNSB was calculated. Error bars represent SEM (n=3). Dashed line indicates the level of biotinylated GAPDH, which is a background for this assay. Significant difference ($P<0.05$) when compared to *: WT-SLC4A11 and #: GAPDH background.

similar structural fold as SLC4A11 cytoplasmic domain, we submitted the domain's sequence (amino acids 1-370) to Protein Homology/AnalogY Recognition Engine (PHYRE2), a protein structure prediction server [31]. The highest probability structure was based on AE1 (SLC4A1), a Cl^-/HCO_3^- exchanger also in the SLC4 family with SLC4A11. The predicted structure of SLC4A11 cytoplasmic domain based on AE1 crystal structure [32] had four beta sheets and several alpha helices (Fig. 4.5A). Only the amino acids R125-P341 of SLC4A11 had a structural alignment with 100% confidence to AE1 template (Fig. 4.5B), while remainder of SLC4A11 had less than 20% confidence (Fig. 4.5C, highlighted in grey color). Considering the sequence identity of just 18% between human AE1 and SLC4A11 cytoplasmic domains, the structural alignment confidence of 100% from R125-P341 is remarkable. Amino acids Q301-P331 of SLC4A11 (Figs. 4.5B,C, red color) correspond to the dimeric interface of amino acids F314-R344 in AE1 cytoplasmic domain crystal structure [32]. The catalytically inactive mutant R125H, highlighted in yellow maps to the middle of the predicted structure and there is a possibility that it could line a substrate translocation pathway. Unfortunately, we cannot be confident of this assumption since there is low confidence in the structural alignment with AE1 in the SLC4A11 amino acids 1-124 and 341-371.

On the basis of the structural alignment (Fig. 4.5 and Fig. 4.6), amino acids 1-354 of AE1 cytoplasmic domain and amino acids 341-891 of SLC4A11 membrane domain were fused to create a chimeric protein (CD-AE1-MD-SLC4A11). Expression and its localization in HEK293 cells were assessed (Figs. 4.7A,C). CD-AE1-MD-SLC4A11 has a similar expression levels as WT-SLC4A11 (Fig. 4.7B) and a significant presence at the cell surface when compared to background levels (Fig. 4.7D).

A

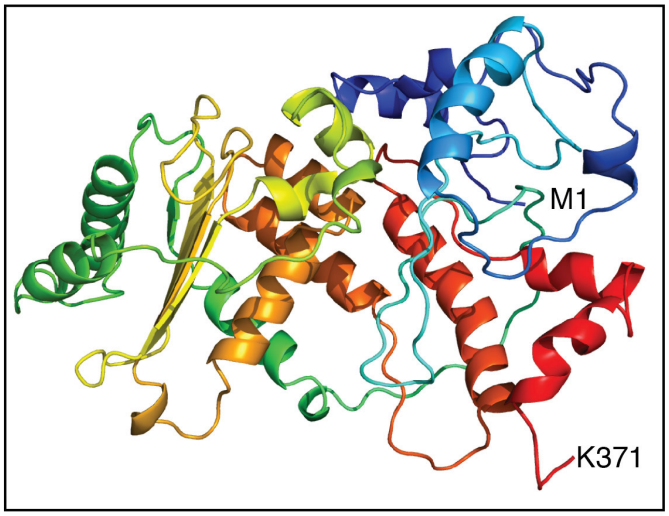

B

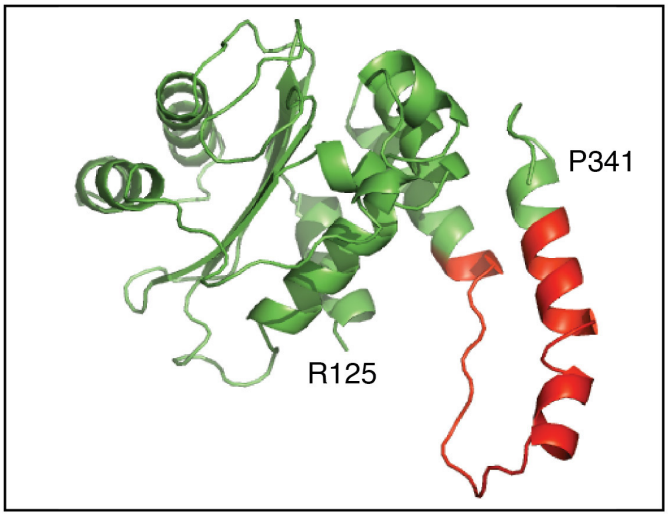

C

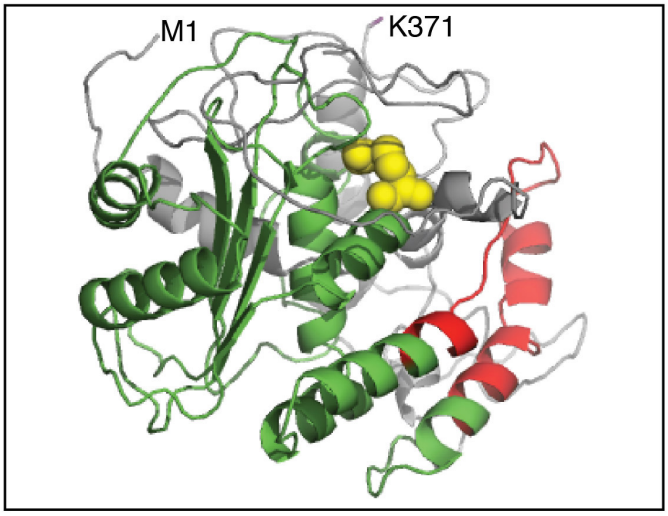

Figure 4.5 Homology modeling of SLC4A11 cytoplasmic domain. (**A**) Homology model of cytoplasmic domain (CD) of SLC4A11 (amino acids M1-K371) was predicted using Protein Homology/AnalogY Recognition Engine 2 (Phyre2) software and Cytoplasmic domain of AE1 (SLC4A1) as a template. (**B**) Homology model (amino acids R125-P341) of CD-SLC4A11 based on structural alignment with 100% confidence on CD-AE1. Red color indicates the SLC4A11 region corresponding to the AE1 dimerization motif (amino acids Q301-P331). (**C**) Homology model of CD-SLC4A11 with R125 highlighted as space-filling model in yellow and dimeric interface in red. Residues with high probability of correct structural prediction (100%) in Phyre2 are in green and red, while low confidence structural fitting (~18%) in Phyre2 are colored in grey.

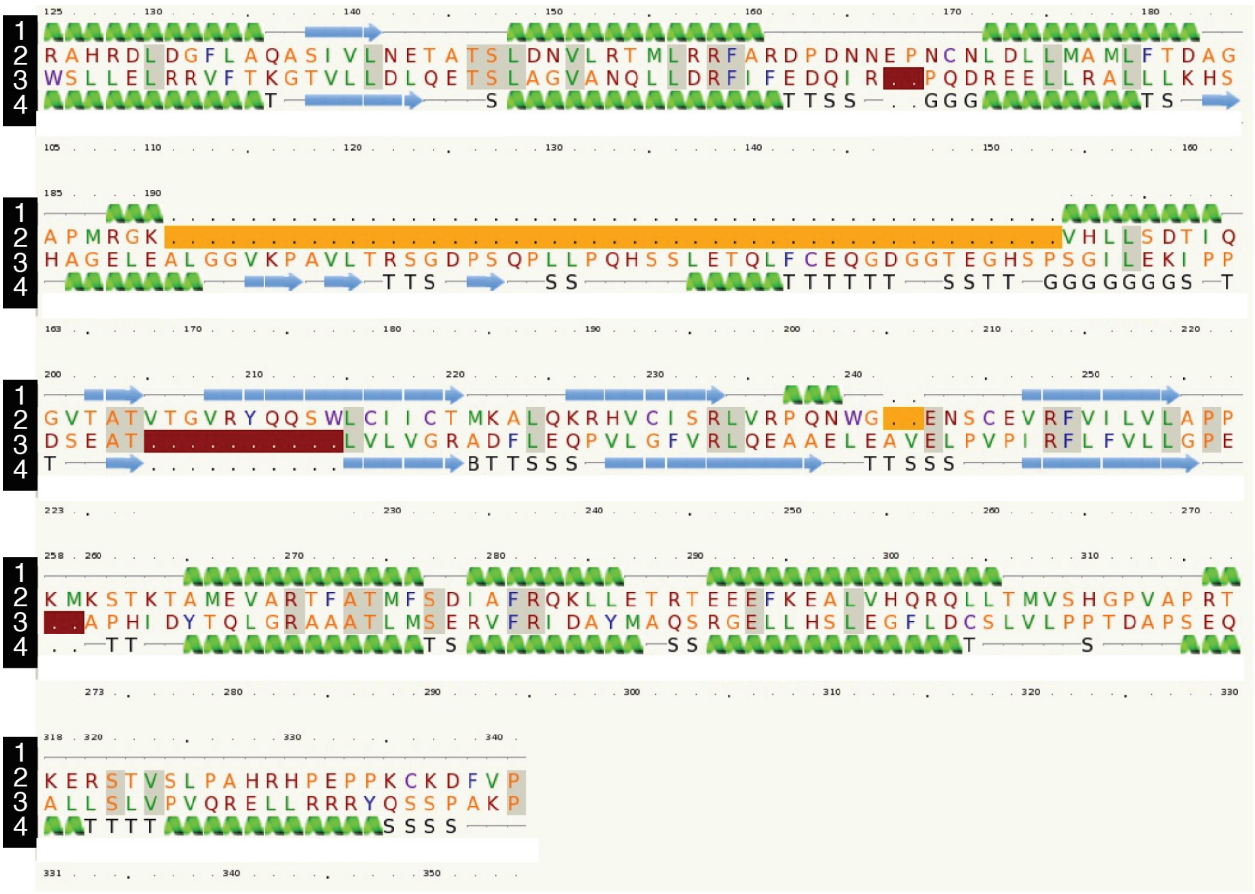

1 - Predicted SLC4A11 cytoplasmic domain structure
2 - SLC4A11 sequence
3 - AE1 sequence
4 - Crystal structure of AE1 cytoplasmic domain

Figure 4.6 Phyre2 alignment of SLC4A11 and AE1 cytoplasmic domains. To generate a homology model for SLC4A11 cytoplasmic domain, the amino acid sequence of SLC4A11 (1-370 residues) was submitted in the Protein Homology/AnalogY Recognition Engine 2 (Phyre2) software. Amino acid residues of SLC4A11 that have similar structural fold with AE1 were aligned as shown. The top and bottom row numbers indicate the amino acids of SLC4A11 and AE1. Row 1 and Row 4 indicate the

predicted SLC4A11 cytoplasmic domain structure and crystal structure of AE1 cytoplasmic domain from PDB respectively.

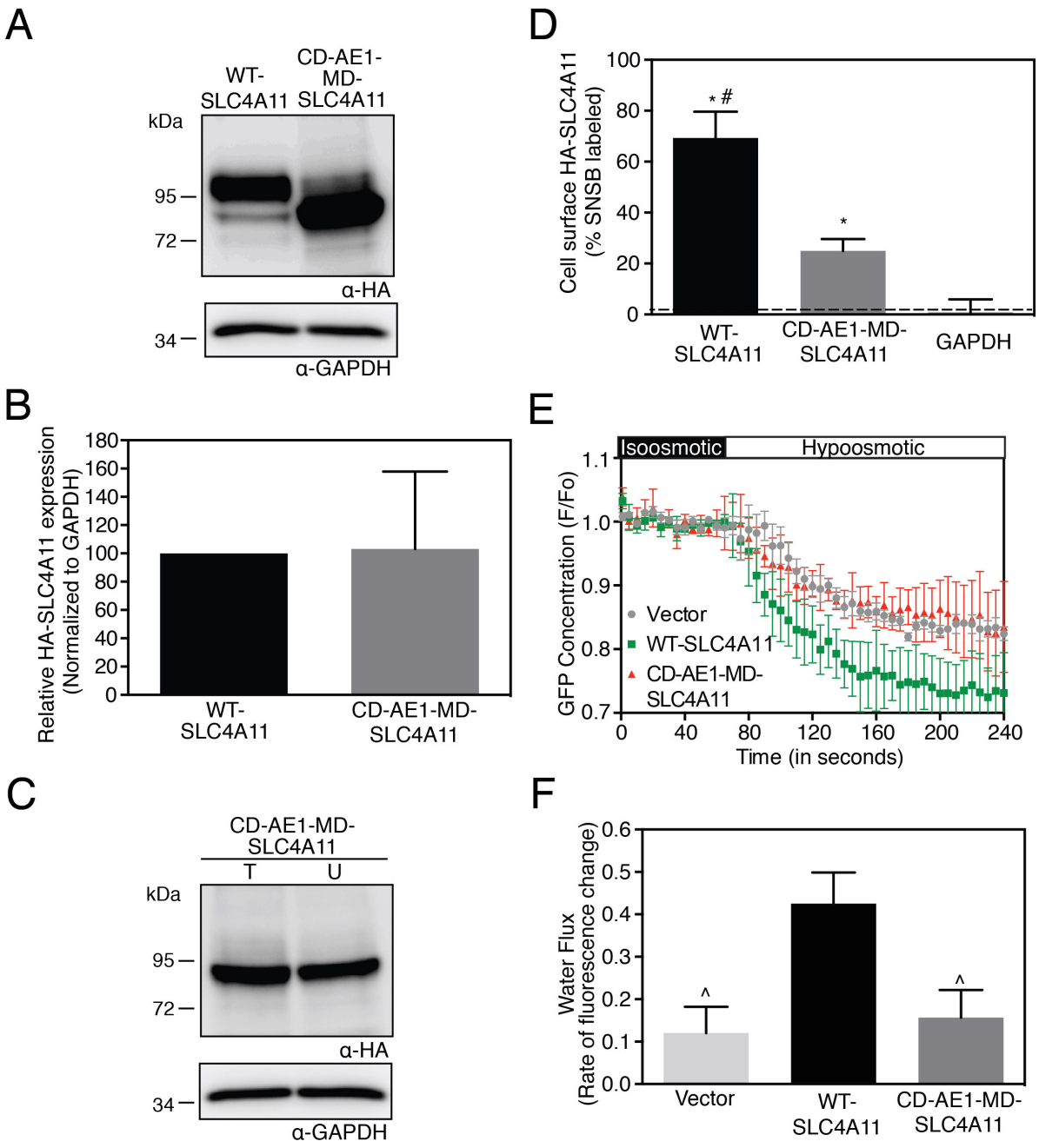

Figure 4.7 Expression, plasma membrane localization and functional activity of AE1 cytoplasmic domain (CD-AE1) fused to MD-SLC4A11. (**A**) HEK293 cells were transfected with cDNA containing HA- epitope tagged WT-SLC4A11 and CD-AE1-MD-

SLC4A11. Cell lysates were immunoblotted with Anti-HA and Anti-GAPDH antibodies. (**B**) Expression level of CD-AE1-MD-SLC4A11 was normalized to GAPDH and plotted relative to WT-SLC4A11. (**C**) HEK293 cells transfected with cDNA encoding HA-epitope tagged WT-SLC4A11 and CD-AE1-MD-SLC4A11 were labeled with membrane-impermeant Sulfo-NHS-SS-biotin (SNSB) to perform cell surface biotinylation assay. Samples were processed on immunoblots with anti-HA and anti-GAPDH antibodies. (**D**) The fraction of WT-SLC4A11, CD-AE1-MD-SLC4A11 and GAPDH labeled by SNSB was calculated. Error bars represent SEM (n=3). Dashed line indicates the level of biotinylated GAPDH, which is a background for this assay. (**E**) HEK293 cells, grown on coverslips, were transiently co-transfected with cDNA encoding eGFP along with empty vector or HA-WT-SLC4A11 or CD-AE1-MD-SLC4A11. Cells were perfused with isosmotic (black bar) and hypoosmotic (white bar) media. (**F**) Rate of fluorescence change was calculated, which represents the water flux. Data represent the mean ± SEM of water flux in cells from three independent experiments with 8-10 cells measured per coverslip. Significant difference ($P<0.05$) when compared to *: GAPDH background, #: CD-AE1-MD-SLC4A11 and ^: WT-SLC4A11.

Since CD-AE1-MD-SLC4A11 was expressed at the cell surface at ~40% of WT-SLC4A11 levels, we were able to assess its functional activity as described earlier [1]. Cell swelling assays were performed in HEK293 cells co-expressing GFP and either WT-SLC4A11 or CD-AE1-MD-SLC4A11. Cytoplasmic GFP concentration was monitored while switching from isotonic to hypotonic solution (Fig. 4.7E). The rate of fluorescence change, representing dilution of GFP in the cytoplasm, is a surrogate for water flux activity. CD-AE1-MD-SLC4A11 expressing cells had water flux similar to vector transfected cells (Fig. 4.7F), while WT-SLC4A11 conferred significant water flux as reported earlier [1]. Overall, CD-AE1-MD-SLC4A11 shows that a protein with similar structural fold is required to stabilize the SLC4A11 membrane domain allowing it to process to the cell surface. The absence of SLC4A11 cytoplasmic domain, however, impairs water flux activity.

4.2.4 Bacterial over-expression of SLC4A11 cytoplasmic domain

Understanding the structure of SLC4A11 cytoplasmic domain might rationalize the cytoplasmic domain mutants that cause corneal dystrophies. We thus expressed the cytoplasmic domain (amino acids 1-368) in *E. coli* in hopes of performing structural studies on recombinant protein. When expressed in *E. coli,* the native sequence of CD-SLC4A11 was expressed to low levels (Fig. 4.8A). We thus optimized codon usage for *E. coli*, replacing rare *E. coli* codons in the SLC4A11 cDNA. *E. coli* extracts from codon-optimized CD-SLC4A11 revealed a band of the expected size (~40 kDa) on immunoblots (Fig. 4.8A). As expression level was low, we fused glutathione-S-transferase (GST) to the N-terminus of SLC4A11 cytoplasmic domain (GST-CD-SLC4A11-His_{10}) and

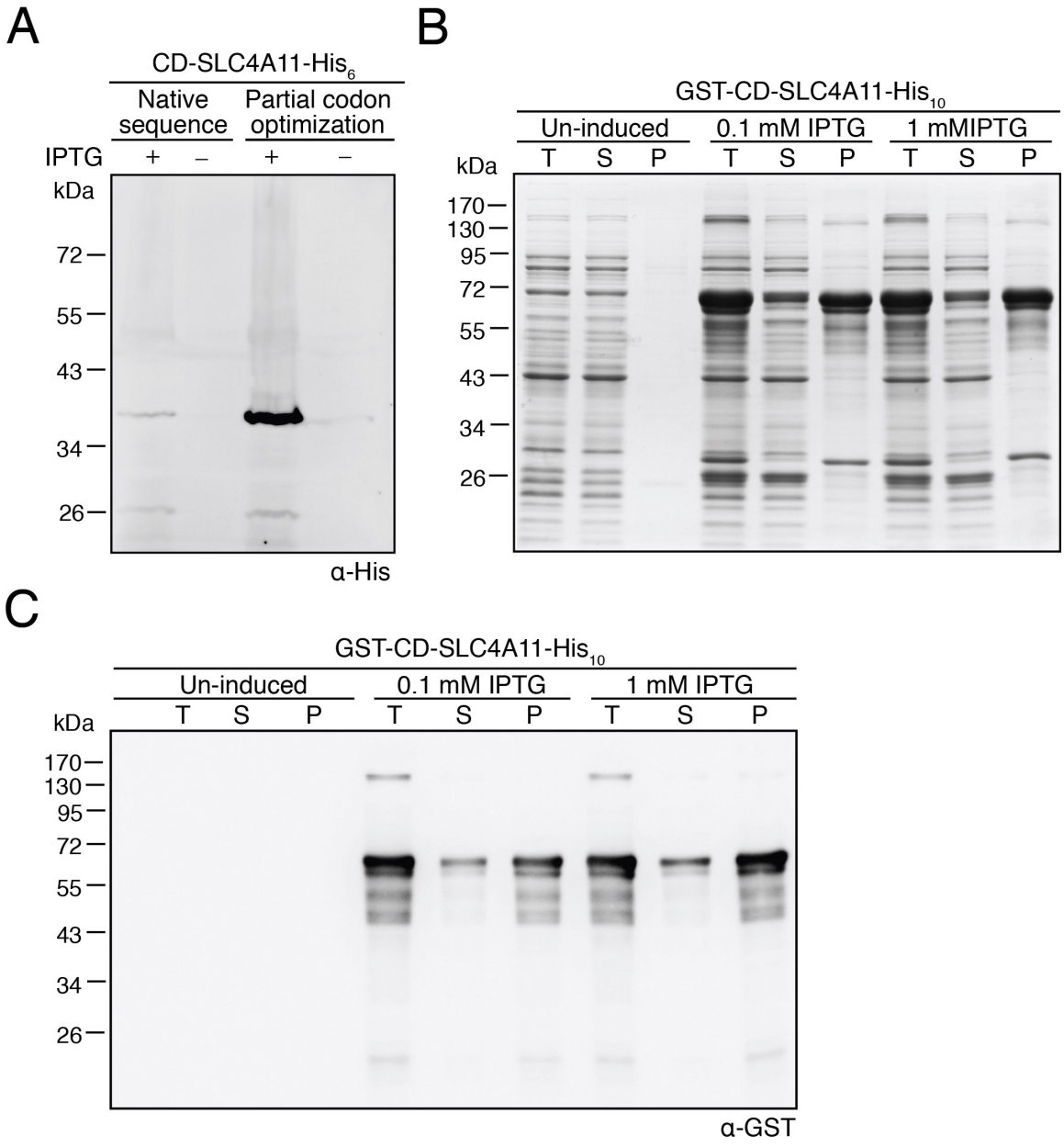

Figure 4.8 Bacterial expression of SLC4A11 cytoplasmic domain. (**A**) Native human or partial codon optimized (for *E. coli*) sequence of SLC4A11 cytoplasmic domain (1-368 amino acids) cDNA, tagged with 6x Histidine, was transformed into *E. coli* and grown in LB medium (CD-SLC4A11-His_6). IPTG was used to induce protein expression. After 2-4

h, the cells were centrifuged, sonicated and processed for immunoblotting using Anti-His antibody. (**B & C**) cDNA of SLC4A11 cytoplasmic domain with GST at N-terminus and His tag at C-terminus was transformed into *E. coli* (GST-CD-SLC4A11-His_{10}). After induction with IPTG, the cells were collected and sonicated. The total cell lysate (T) was centrifuged and the supernatant (S) and pellet (P) fractions were collected. Samples were processed for SDS-PAGE and stained with Coomassie blue dye (B) or immunoblotted using anti-GST antibody (C).

expressed in *E. coli*. A 72-kDa band on Coomassie stained SDS-PAGE gels was evident in induced cell extracts (Fig. 4.8B). Supernatants and pellets of *E. coli* cell lysates were assessed on Coomassie blue stained gels and immunoblots. Majority of CD-SLC4A11 was found in the pellet (Fig. 4.8C), whether expressed alone or fused to GST. This suggests that CD-SLC4A11 is insoluble, even when fused to soluble GST.

4.2.5 Cytoplasmic domain and membrane domain of SLC4A11 strongly associate

Experiments here show that the removal of the cytoplasmic domain destabilizes the membrane domain of SLC4A11. Similarly, CD-SLC4A11 does not express as a soluble protein without MD-SLC4A11. We hypothesized that the cytoplasmic and membrane domains might strongly associate in the SLC4A11 native structure, such that neither domain was stable unless folded against the other. We assessed a possible interaction between Myc-epitope tagged cytoplasmic domain of SLC4A11 (Myc-CD-SLC4A11) and HA-epitope tagged membrane domain of SLC4A11 (HA-307-MD-SLC4A11). When co-expressed in HEK293 cells, HA-307-MD-SLC4A11 and Myc-CD-SLC4A11 co-immunoprecipitated (Fig. 4.9A & 4.10A), indicating that the domains associate. When the epitope tags were reveresed, we found that HA-CD-SLC4A11 co-immunoprecipitated with Myc-307-MD-SLC4A11 (Fig. 4.9B & 4.10B).

Interaction between the domains was specific, as the Myc-CD-SLC4A11 does not associate with the membrane domain of AE1 (340-MD-AE1) (Fig. 4.9C & 4.10C). No signal was found in any of the samples while using non-immune serum (N.I.) for immunoprecipitation, indicating the specificity of the antibody. These immunoprecipitation data confirm that the cytoplasmic domain and membrane domain of SLC4A11 strongly and specifically associate.

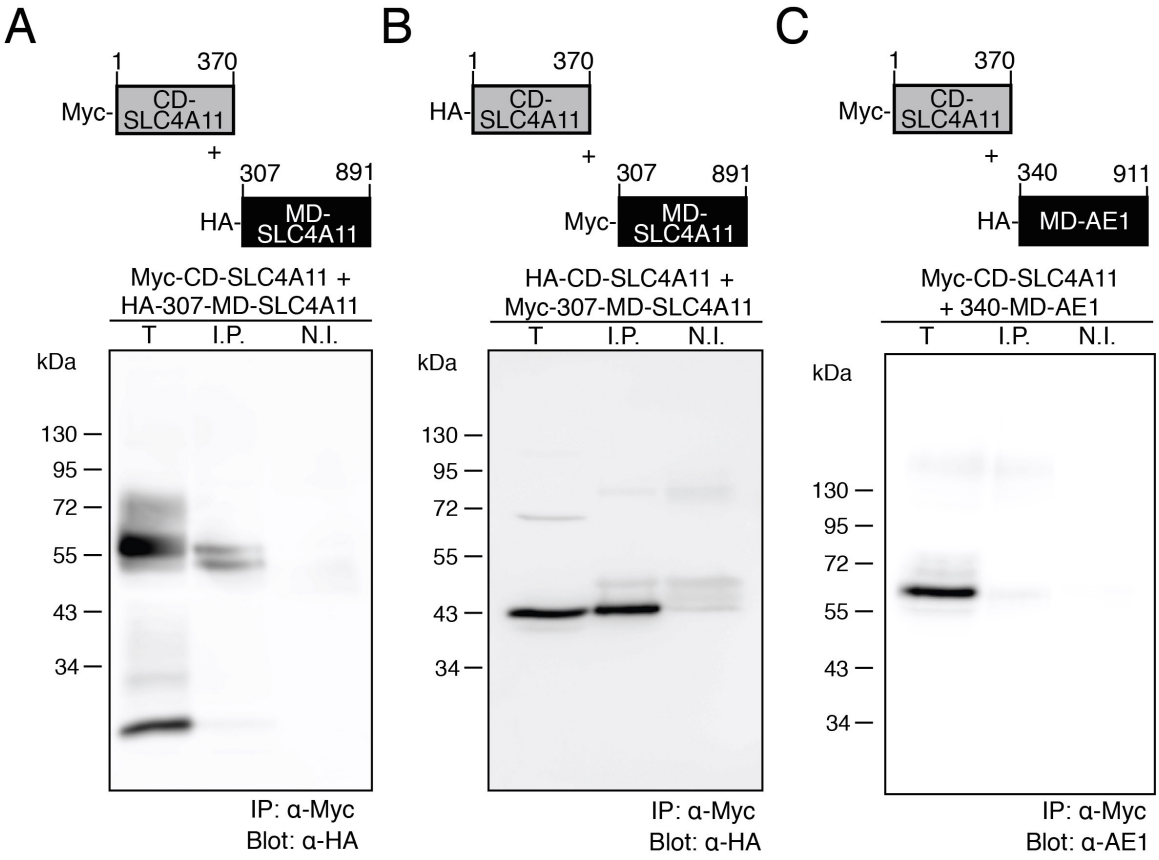

Figure 4.9 Association between SLC4A11 cytoplasmic and membrane domains. HEK293 cells were co-transfected with (**A**) Myc-tagged CD-SLC4A11 and HA-tagged 307-MD-SLC4A11 or (**B**) Myc-tagged 307-MD-SLC4A11 and HA-tagged CD-SLC4A11 or (**C**) Myc-tagged CD-SLC4A11 and HA-tagged 340-MD-AE1. Cell lysates (100 μg of total protein) were incubated either with rabbit polyclonal anti-Myc antibody (IP) or rabbit non-immune serum (NI). Immunoprecipitates (both IP and NI) and 50 μg of total protein cell lysate (T) were probed on immunoblots with anti-HA and anti-AE1 antibody as indicated.

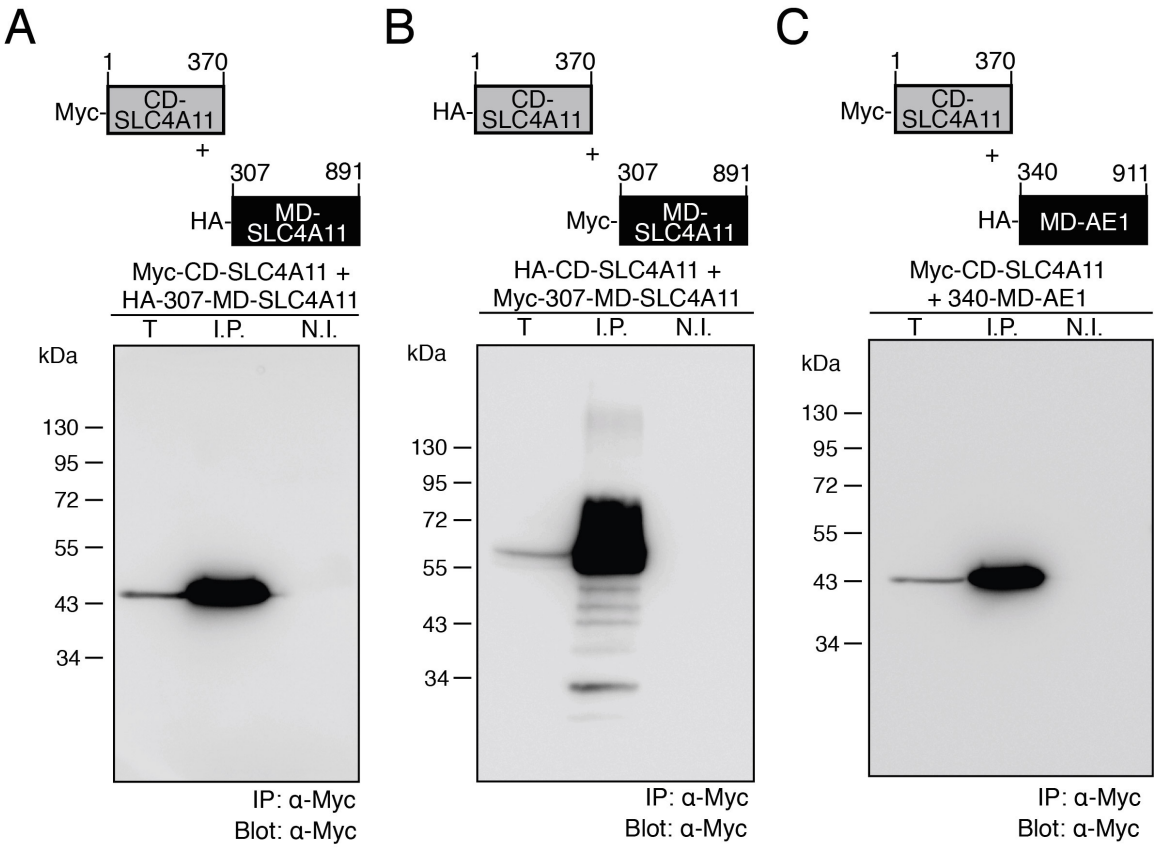

Figure 4.10 Association of SLC4A11 cytoplasmic and membrane domains. HEK293 cells were co-transfected with (**A**) Myc-CD-SLC4A11 and HA-307-MD-SLC4A11 or (**B**) Myc-307-MD-SLC4A11 and HA-CD-SLC4A11 or (**C**) Myc-CD-SLC4A11 and HA-340-MD-AE1 (AE1 was used as a control). Cell lysates (100 μg of total protein) were incubated either with rabbit polyclonal anti-Myc antibody (IP) or rabbit non-immune serum (NI). Immunoprecipitates (both IP and NI) were washed, recovered and along with 50 μg of total protein cell lysate (T) were probed on immunoblots with mouse monoclonal anti-MYC antibody.

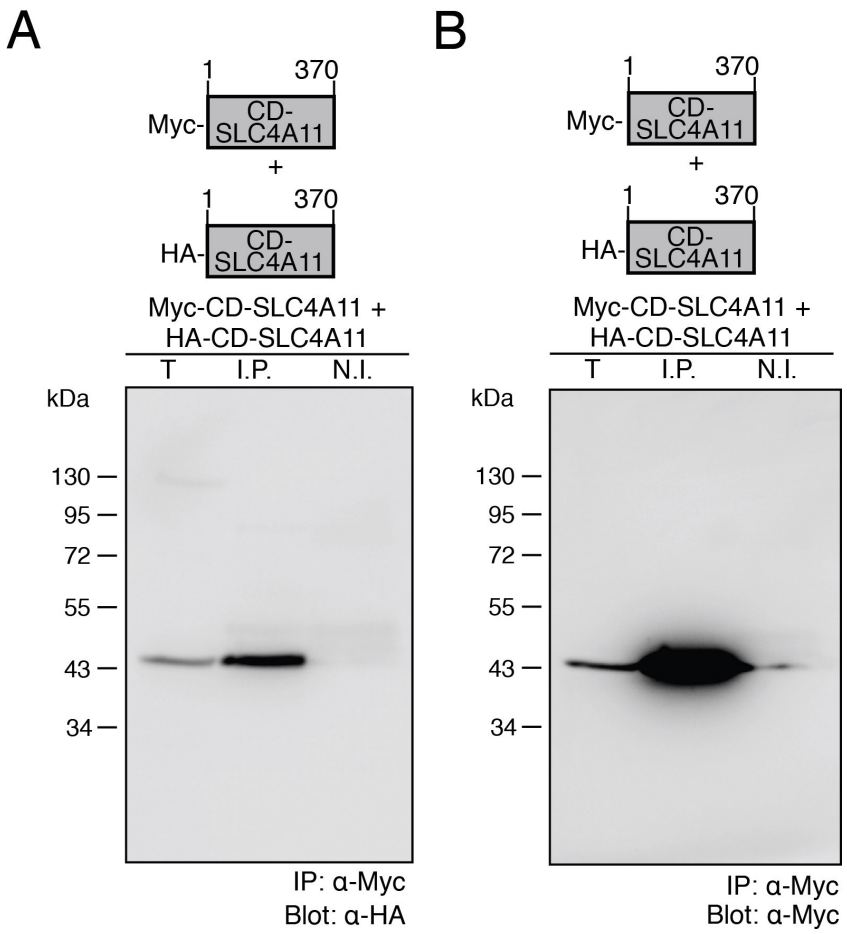

Figure 4.11 SLC4A11 cytoplasmic domains are dimeric. HEK 293 cells were cotransfected with cDNAs encoding N-terminally HA-tagged CD-SLC4A11 and Myc-tagged CD-SLC4A11. Cells were solubilized 48 h post-transfection and a 50-µg total protein aliquot (T) was set aside. Two aliquots (100 µg protein each) were incubated for 16 h at 4°C with either rabbit polyclonal anti-Myc (IP) or rabbit non-immune serum (NI). Immunocomplexes were recovered, washed, and all the samples (T, IP and NI) were processed for immunoblotting. Immunoblots were successively probed with anti-HA and anti-Myc monoclonal antibodies to detect HA-CD-SLC4A11 (**A**) and Myc-CD-SLC4A11 (**B**), respectively.

4.2.6 SLC4A11 cytoplasmic domain dimerizes independently of the membrane domain

WT-SLC4A11 is dimeric [10], raising the important question whether the monomers of SLC4A11 cytoplasmic domain dimerize independently of the membrane domain? The cytoplasmic domain of SLC4A11 was tagged with HA-epitope and Myc-epitope and co-transfected in HEK293 cells in equal amounts. Immunoprecipitation studies suggest that when the Myc-CD-SLC4A11 was pulled down (Fig. 4.11B), the HA-CD-SLC4A11 associates with Myc-CD-SLC4A11 (Fig. 4.11A). No signal was found when non-immune serum (N.I.) was used to pull down the protein. Taken together, these experiments show that the cytoplasmic domain of SLC4A11 dimerizes independently of the membrane domain.

4.3 Discussion

In this study, we explored the role of SLC4A11 cytoplasmic and membrane domains in protein's function. Our results indicate that the SLC4A11 cytoplasmic domain is essential for the stability of the membrane domain. Further, the SLC4A11 cytoplasmic domain is required for membrane transport function of SLC4A11. Modeling studies suggest similarities in the structures of AE1 and SLC4A11 cytoplasmic domains. Finally, the cytoplasmic and membrane domains of SLC4A11 associate strongly with each other and the cytoplasmic domain can dimerize on its own. These findings are significant because about one third of corneal dystrophy causing mutations are located in the SLC4A11 cytoplasmic domain and for the first time, this work provides insights into the role of the cytoplasmic domain in the function of SLC4A11.

4.3.1 Role of the cytoplasmic domain in SLC4A11 membrane domain stabilization

The cytoplasmic domain has a key role in stabilizing the full length protein. About one third of all identified SLC4A11 point mutations map to the cytoplasmic domain and many of these result in a molecular phenotype marked by retention of the protein in the ER [10, 19, 23]. This itself suggests a key role of the domain permitting maturation of SLC4A11 to the cell surface. Point mutations could, however, cause SLC4A11 cytoplasmic domain to misfold, resulting in surveillance by the ER quality control apparatus.

Experiments presented here indicate that the role of the cytoplasmic domain is more than permissive. Deletion of the cytoplasmic domain led to progressive dysfunction, such that the greater the truncation of the cytoplasmic domain, the less the membrane domain was able to accumulate. This is consistent with endoplasmic reticulum-associated degradation of proteins recognized as misfolded, leading to reduced levels of steady-state accumulation. All of the SLC4A11 cytoplasmic domain truncation mutants failed to process to the cell surface. Point mutants with a misfolded cytoplasmic domain inhibit SLC4A11 membrane domain maturation, as does removal of the domain. Thus a properly folded cytoplasmic domain is required for SLC4A11 maturation.

What is the role of SLC4A11 cytoplasmic domain in membrane domain stabilization? As discussed above, SLC4A11 membrane domain is unstable when expressed alone, but we also found that bacterially over-expressed cytoplasmic domain was insoluble. These observations could be unified if the two domains strongly associate in the mature full length protein. Expression of the two domains independently would thus expose surfaces that are normally buried, likely hydrophobic and prone to

aggregation. Supporting this model, co-expressed cytoplasmic and membrane domains co-associated in immunoprecipitates.

Our data support a specific role of the SLC4A11 cytoplasmic domain in stabilizing the membrane domain. The idea that the membrane domain has a surface that must be covered, suggests that the function could be complemented by any properly-folded domain. In contrast, we found that fusion of two different, properly folded fluorescent proteins failed to rescue the processing defect of SLC4A11 membrane domain. This indicates that for SLC4A11 to mature, close association with a specific domain is required.

Structural modeling revealed for the first time evidence that SLC4A11 and AE1 cytoplasmic domains have regions with significant structural similarity. Lending support to this idea, the AE1 cytoplasmic domain rescued SLC4A11 membrane domain trafficking to the cell surface. This suggests that AE1 has structural features sufficiently similar to SLC4A11's domain that it passes surveillance by the cell's quality control apparatus and permits appropriate folding of the membrane domain.

Another possible obligatory role of the cytoplasmic domain is to assist with SLC4A11 dimerization, since the full length protein is dimeric [10]. Against this idea, we found that fusion of GFP, a dimeric protein, to SLC4A11 failed to rescue SLC4A11 membrane domain trafficking to the same degree as mNectarine, a monomeric fluorescent protein. While the AE1 cytoplasmic domain is dimeric [33-35], the failure of GFP to rescue the membrane domain indicates that the SLC4A11 cytoplasmic domain contributes more than dimerization to the protein's stability. Further arguing against a requisite role of the cytoplasmic domain in protein dimerization is AE1, another member

of the SLC4 family. The AE1 cytoplasmic and membrane domains are both independently dimeric [33-35].

AE1 does, however, provide interesting contrasts with the data we have revealed for SLC4A11. AE1 (SLC4A1) and SLC4A11 belong to the same protein family and likely thus share a common fold of their membrane domains. The AE1 membrane domain can, however, be stably expressed without the cytoplasmic domain [36] and the AE1 cytoplasmic domain is sufficiently stable by itself that it has been over-expressed and crystallized [32]. The two domains can be readily proteolytically cleaved and separated under mild conditions, indicating weak interactions between the domains [37]. Data here thus indicate that while the two proteins may be similar, there are major differences between them.

4.3.2. Role of SLC4A11 in membrane transport activity

As discussed above, the cytoplasmic domain has an important and specific role in membrane domain folding, stability and trafficking. There is additional evidence that the domain has a role in the membrane transport functions of SLC4A11. The SLC4A11 R125H mutation causes CHED2 and resides in the cytoplasmic domain [1]. R125H-SLC4A11 targets normally to the cell surface, but does not support the water flux activity observed in cells expressing WT-SLC4A11 [1]. We assume that if the mutation affected the folding of SLC4A11, the ER quality control apparatus would retain the protein in the ER. How can a cytoplasmic domain mutation affect membrane transport function?

One possibility is that the SLC4A11 cytoplasmic domain contains a pathway through which transported substrates traverse. Such pathways are well established in some ion channels, for example the voltage gated K^+-channel [38, 39]. Similarly, the

CFTR Cl^- channel was recently proposed to have "fenestrations" in its cytoplasmic domain, guiding substrate Cl^- to the transmembrane pore [40]. Closer to SLC4A11, the electrogenic Na^+/HCO_3^- co-transporter, NBCe1 (SLC4A4) has been proposed to have a channel through its cytoplasmic domain, guiding HCO_3^- to the membrane domain, on the basis of structural modeling studies and a cytoplasmic domain mutant (R298S), which affects the transport function, but not cell surface trafficking of NBCe1 [27].

Amino acid sequence alignment with ClustalW2 indicates that the corresponding residue to R298 of NBCe1 is R270 in SLC4A11 and interestingly this site is flanked by two CHED2 mutations, A269V and T271M. Further, Chang *et al*. showed that NBCe1 R298 is located in a largely solvent inaccessible polar subsurface pocket [27]. In contrast, in the SLC4A11 homology model, we did not find any such pocket for R125 (Fig. 4.12). The predicted salt bridges using VMD software [41] were not close to R125, but this could be due to the low confidence in the homology structure between 1-125 amino acids of SLC4A11. Moreover, removal of SLC4A11 cytoplasmic domain destabilized the membrane domain and hence we were not able to investigate whether there is a substrate translocation pathway that transverse via cytoplasmic domain.

Our data are consistent with a role of the cytoplasmic domain in membrane transport function. Co-immunoprecipitations revealed close association of the cytoplasmic and membrane domains, as one would expect if the cytoplasmic domain had a pathway guiding substrate to the membrane domain. More importantly, we found that it was possible to traffic the membrane domain to the cell surface by fusion of the AE1 cytoplasmic domain. The AE1-SLC4A11 fusion, however, did not support water flux activity. This strongly suggests that the cytoplasmic domain has a role in contributing to

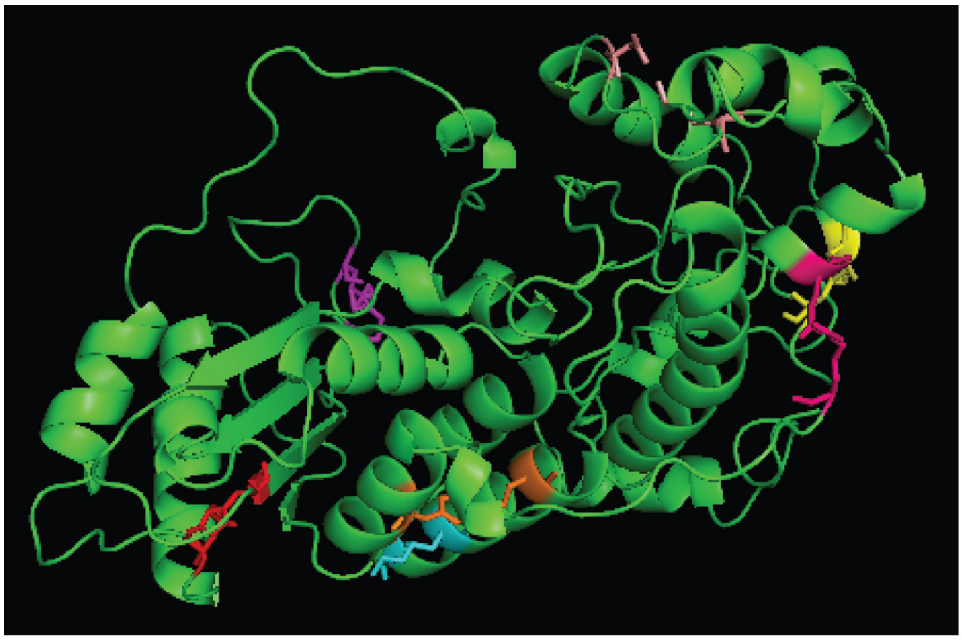

Salt Bridge	Highlighted color
ASP164-HIS228	Red
ASP54-LYS49	Light orange
GLU246-ARG248	Magenta
GLU291-LYS295	Blue
ASP131-ARG302	Orange
GLU348-ARG112	Hot pink
ASP349-HIS109	Yellow

Figure 4.12 Possible salt bridges on the SLC4A11 cytoplasmic domain homology model. PHYRE2 SLC4A11 cytoplasmic domain homology model in PDB format was submitted to VMD 1.9.2. The possible salt bridges calculated by VMD software were mapped on the homology model. Each salt bridge is highlighted in different color as indicated in the table.

the membrane transport activity of the protein. The loss of functional activity in chimeric protein could be due to 1) the absence of the transport pore in AE1 cytoplasmic domain even though it might have similar structural fold as SLC4A11 based on PHYRE2 prediction. A recent report shows that the substrate access tunnel in the cytoplasmic domain is not an important feature of AE1 [42] or 2) the absence of specific residues of SLC4A11 that might be involved in water translocation or 3) the cytoplasmic domain of SLC4A11 could have some unique interactions/features that is absent in any other SLC4 family member. Our data alone do not allow us to conclude what the cytoplasmic domain contributes to membrane domain function, but providing a pathway for substrate funneling to the membrane domain, as proposed for NBCe1, is a possibility. Nevertheless, all these experiments show that the cytoplasmic domain is very important for the stabilization and function of SLC4A11.

4.3.3 Dimerization of SLC4A11 cytoplasmic domain

We found that the cytoplasmic domain of SLC4A11 can dimerize independent of the membrane domain. However, there is a caveat to this finding and the data has to be interpreted with great degree of caution. SLC4A11 cytoplasmic domain variants might aggregate in HEK293 cells (as bacterial expression of SLC4A11 cytoplasmic domain was insoluble) and when immunoprecipitated, they associate possibly due to either dimerization or aggregation. In AE1, both the membrane domain and cytoplasmic domain dimerize independent of each other [32, 43, 44]. SLC4A11 might also have both cytoplasmic and membrane domains dimerize independently of each other. Unfortunately we could not test the oligomerization of membrane domain of SLC4A11, as it was not stable and does not reach the cell surface.

Interestingly, the dimeric interface of cytoplasmic domain mapped to amino acids 301-331 of SLC4A11, based on AE1 dimeric interface (amino acids 314-344), seems to be critical in stabilizing the membrane domain expression. The variants HA-353-MD, HA-347-MD and HA-329-MD do not contain the amino acids responsible for dimeric interface and their expression is very weak whereas HA-307-MD-SLC4A11 contains the majority of dimeric interface residues and its expression is equivalent to WT-SLC4A11 (Fig. 4.2B). So it is evident that the amino acids 301-331 of SLC4A11 is very important in the stabilization or folding or dimerization of the protein and it will be interesting to test these particular residues in future studies. Also a point mutation, A327V (Fig. 4.1B), maps to this location and causes FECD.

4.4 Conclusions

Taken together, we conclude that 1) the cytoplasmic domain of SLC4A11 is required for the stability of the membrane domain, 2) the cytoplasmic domain is required for SLC4A11 functional activity (possibly forming an extension of the substrate translocation pathway from the membrane domain of SLC4A11), 3) the cytoplasmic domain and membrane domain of SLC4A11 strongly associate and 4) SLC4A11 cytoplasmic domain is dimeric, independent of the membrane domain.

4.5 References

1. Vilas, G. L., Loganathan, S. K., Liu, J., Riau, A. K., Young, J. D., Mehta, J. S., Vithana, E. N. and Casey, J. R. (2013) Transmembrane water-flux through SLC4A11: a route defective in genetic corneal diseases. Human Molecular Genetics. **22**, 4579-4590
2. Parker, M. D., Ourmozdi, E. P. and Tanner, M. J. (2001) Human BTR1, a New Bicarbonate Transporter Superfamily Member and Human AE4 from Kidney. Biochem. Biophys. Res. Commun. **282**, 1103-1109
3. Hemadevi, B., Veitia, R. A., Srinivasan, M., Arunkumar, J., Prajna, N. V., Lesaffre, C. and Sundaresan, P. (2008) Identification of mutations in the SLC4A11 gene in patients with recessive congenital hereditary endothelial dystrophy. Arch Ophthalmol. **126**, 700-708
4. Jiao, X., Sultana, A., Garg, P., Ramamurthy, B., Vemuganti, G. K., Gangopadhyay, N., Hejtmancik, J. F. and Kannabiran, C. (2007) Autosomal recessive corneal endothelial dystrophy (CHED2) is associated with mutations in SLC4A11. J Med Genet. **44**, 64-68.
5. Ramprasad, V. L., Ebenezer, N. D., Aung, T., Rajagopal, R., Yong, V. H., Tuft, S. J., Viswanathan, D., El-Ashry, M. F., Liskova, P., Tan, D. T., Bhattacharya, S. S., Kumaramanickavel, G. and Vithana, E. N. (2007) Novel SLC4A11 mutations in patients with recessive congenital hereditary endothelial dystrophy (CHED2). Mutation in brief #958. Online. Hum. Mutat. **28**, 522-523
6. Sultana, A., Garg, P., Ramamurthy, B., Vemuganti, G. K. and Kannabiran, C. (2007) Mutational spectrum of the SLC4A11 gene in autosomal recessive congenital hereditary endothelial dystrophy. Mol Vis. **13**, 1327-1332
7. Vithana, E. N., Morgan, P., Sundaresan, P., Ebenezer, N. D., Tan, D. T., Mohamed, M. D., Anand, S., Khine, K. O., Venkataraman, D., Yong, V. H., Salto-Tellez, M., Venkatraman, A., Guo, K., Hemadevi, B., Srinivasan, M., Prajna, V., Khine, M., Casey, J. R., Inglehearn, C. F. and Aung, T. (2006) Mutations in sodium-borate cotransporter SLC4A11 cause recessive congenital hereditary endothelial dystrophy (CHED2). Nature Genetics. **38**, 755-757

8. Desir, J. and Abramowicz, M. (2008) Congenital hereditary endothelial dystrophy with progressive sensorineural deafness (Harboyan syndrome). Orphanet J Rare Dis. **3**, 28-36
9. Vithana, E. N., Morgan, P. E., Ramprasad, V., Tan, D. T., Yong, V. H., Venkataraman, D., Venkatraman, A., Yam, G. H., Nagasamy, S., Law, R. W., Rajagopal, R., Pang, C. P., Kumaramanickevel, G., Casey, J. R. and Aung, T. (2008) SLC4A11 Mutations in Fuchs Endothelial Corneal Dystrophy (FECD). Hum. Mol. Genet. **17**, 656-666
10. Vilas, G. L., Loganathan, S., Quon, A., Sundaresan, P., Vithana, E. N. and Casey, J. R. (2012) Oligomerization of SLC4A11 protein and the severity of FECD and CHED2 corneal dystrophies caused by SLC4A11 mutations. Human Mutation. **33**, 419-428
11. Groeger, N., Froehlich, H., Maier, H., Olbrich, A., Kostin, S., Braun, T. and Boettger, T. (2010) Slc4a11 prevents osmotic imbalance leading to corneal endothelial dystrophy, deafness, and polyuria. J. Biol. Chem. **285**, 14467-14474
12. Praetorius, J., Kim, Y. H., Bouzinova, E. V., Frische, S., Rojek, A., Aalkjaer, C. and Nielsen, S. (2004) NBCn1 is a basolateral Na^+-HCO_3^- cotransporter in rat kidney inner medullary collecting ducts. Am J Physiol Renal Physiol. **286**, F903-912
13. Vilas, G. L., Morgan, P. E., Loganathan, S., Quon, A. and Casey, J. R. (2011) Biochemical Framework for SLC4A11, the Plasma Membrane Protein Defective in Corneal Dystrophies. Biochemistry. **50**, 2157-2169
14. Alka, K. and Casey, J. R. (2014) Bicarbonate transport in health and disease. IUBMB Life. **66**, 596-615
15. Jalimarada, S. S., Ogando, D. G., Vithana, E. N. and Bonanno, J. A. (2013) Ion Transport Function of SLC4A11 in Corneal Endothelium. Investigative Ophthalmology & Visual Science. **54**, 4330-4340
16. Ogando, D. G., Jalimarada, S. S., Zhang, W., Vithana, E. N. and Bonanno, J. A. (2013) SLC4A11 is an EIPA-sensitive Na^+ permeable pHi regulator. American Journal of Physiology - Cell Physiology. **305**, C716-C727

17. Park, M., Li, Q., Shcheynikov, N., Zeng, W. and Muallem, S. (2004) NaBC1 is a ubiquitous electrogenic Na^+ -coupled borate transporter essential for cellular boron homeostasis and cell growth and proliferation. Mol. Cell. **16**, 331-341
18. Kao, L., Azimov, R., Abuladze, N., Newman, D. and Kurtz, I. (2015) Human SLC4A11-C functions as a DIDS-stimulatable $H^+(OH^-)$ permeation pathway: partial correction of R109H mutant transport. American Journal of Physiology - Cell Physiology. **308**, C176-C188
19. Loganathan, S. K. and Casey, J. R. (2014) Corneal Dystrophy-Causing SLC4A11 Mutants: Suitability for Folding-Correction Therapy. Human Mutation. **35**, 1082-1091
20. Desir, J., Moya, G., Reish, O., Van Regemorter, N., Deconinck, H., David, K. L., Meire, F. M. and Abramowicz, M. (2007) Borate transporter SLC4A11 mutations cause both Harboyan syndrome and non-syndromic corneal endothelial dystrophy. J. Med. Genet. **44**, 322-326
21. Puangsricharern, V., Yeetong, P., Charumalai, C., Suphapeetiporn, K. and Shotelersuk, V. (2014) Two novel mutations including a large deletion of the SLC4A11 gene causing autosomal recessive hereditary endothelial dystrophy. British Journal of Ophthalmology. **98**, 1460-1462
22. Kodaganur, S. G., Kapoor, S., Veerappa, A. M., Tontanahal, S. J., Sarda, A., Yathish, S., Prakash, D. R. and Kumar, A. (2013) Mutation analysis of the SLC4A11 gene in Indian families with congenital hereditary endothelial dystrophy 2 and a review of the literature. Molecular Vision. **19**, 1694-1706
23. Soumittra, N., Loganathan, S. K., Madhavan, D., Ramprasad, V. L., Arokiasamy, T., Sumathi, S., Karthiyayini, T., Rachapalli, S. R., Kumaramanickavel, G., Casey, J. R. and Rajagopal, R. (2014) Biosynthetic and functional defects in newly identified SLC4A11 mutants and absence of COL8A2 mutations in Fuchs endothelial corneal dystrophy. J Hum Genet. **59**, 444-453
24. Aldahmesh, M. A., Khan, A. O., Meyer, B. F. and Alkuraya, F. S. (2009) Mutational Spectrum of SLC4A11 in Autosomal Recessive CHED in Saudi Arabia. Investigative Ophthalmology & Visual Science. **50**, 4142-4145

25. Aldave, A. J., Yellore, V. S., Bourla, N., Momi, R. S., Khan, M. A., Salem, A. K., Rayner, S. A., Glasgow, B. J. and Kurtz, I. (2007) Autosomal Recessive CHED Associated With Novel Compound Heterozygous Mutations in SLC4A11. Cornea. **26**, 896-900

26. Kumar, A., Bhattacharjee, S., Prakash, D. R. and Sadanand, C. S. (2007) Genetic analysis of two Indian families affected with congenital hereditary endothelial dystrophy: two novel mutations in SLC4A11. Mol Vis. **13**, 39-46.

27. Chang, M. H., Dipiero, J., Sonnichsen, F. D. and Romero, M. F. (2008) Entry to "HCO_3^- tunnel" revealed by SLC4A4 human mutation and structural model. J Biol Chem. **283**, 18402-18410

28. Johnson, D. E., Ai, H.-W., P., W., Young, J. D., Campbell, R. E. and Casey, J. R. (2009) Red fluorescent protein pH biosensor to detect concentrative nucleoside transport. J. Biol. Chem. **284**, 20499-20511

29. Ilagan, R. P., Rhoades, E., Gruber, D. F., Kao, H.-T., Pieribone, V. A. and Regan, L. (2010) A new bright green-emitting fluorescent protein – engineered monomeric and dimeric forms. FEBS Journal. **277**, 1967-1978

30. Tsien, R. Y. (1998) The Green Fluorescent Protein. Annual Review of Biochemistry. **67**, 509-544

31. Kelley, L. A. and Sternberg, M. J. E. (2009) Protein structure prediction on the Web: a case study using the Phyre server. Nat. Protocols. **4**, 363-371

32. Zhang, D., Kiyatkin, A., Bolin, J. T. and Low, P. S. (2000) Crystallographic structure and functional interpretation of the cytoplasmic domain of erythrocyte membrane band 3. Blood. **96**, 2925-2933

33. Cuppoletti, J., Goldinger, J., Kang, B., Jo, I., Berenski, C. and Jung, C. Y. (1985) Anion carrier in the human erythrocyte exists as a dimer. J. Biol. Chem. **260**, 15714-15717

34. Wang, D. N. (1994) Band 3 protein: structure, flexibility and function. FEBS Lett. **346**, 26-31.

35. Nigg, E. and Cherry, R. J. (1979) Dimeric association of Band 3 in the erythrocyte membrane demonstrated by protein diffusion measurements. Nature. **277**, 493-494

36. Bonar, P. T. and Casey, J. R. (2010) Over-expression and Purification of Functional Human AE1, Expressed in *Saccharomyces cerevisiae* Suitable for Protein Crystallography. Protein Exp. Purif. **74**, 106-115

37. Grinstein, S., Ship, S. and Rothstein, A. (1978) Anion transport in relation to proteolytic dissection of Band 3 protein. Biochim. Biophys. Acta. **507**, 294-304

38. Long, S. B., Campbell, E. B. and Mackinnon, R. (2005) Crystal Structure of a Mammalian Voltage-Dependent Shaker Family K^+ Channel. Science. **309**, 897-903

39. Long, S. B., Campbell, E. B. and Mackinnon, R. (2005) Voltage sensor of Kv1.2: structural basis of electromechanical coupling. Science. **309**, 903-908

40. El Hiani, Y. and Linsdell, P. (2015) Functional Architecture of the Cytoplasmic Entrance to the Cystic Fibrosis Transmembrane Conductance Regulator Chloride Channel Pore. Journal of Biological Chemistry, *in press*

41. Humphrey, W., Dalke, A. and Schulten, K. (1996) VMD: Visual molecular dynamics. Journal of Molecular Graphics. **14**, 33-38

42. Shnitsar, V., Li, J., Li, X., Calmettes, C., Basu, A., Casey, J. R., Moraes, T. F. and Reithmeier, R. A. F. (2013) A Substrate Access Tunnel in the Cytosolic Domain Is Not an Essential Feature of the Solute Carrier 4 (SLC4) Family of Bicarbonate Transporters. Journal of Biological Chemistry. **288**, 33848-33860

43. Casey, J. R. and Reithmeier, R. A. F. (1991) Analysis of the oligomeric state of Band 3, the anion transport protein of the human erythrocyte membrane, by size exclusion high performance liquid chromatography: oligomeric stability and origin of heterogeneity. J. Biol. Chem. **266**, 15726-15737

44. Basu, A., Mazor, S. and Casey, J. R. (2010) Measurement of Distances Within a Concatamer of the Plasma Membrane Cl^-/HCO_3^- Exchanger, AE1. Biochemistry. **49**, 9226-9240

Chapter 5: Summary and Future Directions

5.1 Summary

The objectives of the thesis were to 1) Test the feasibility of rescuing ER-retained SLC4A11 disease causing mutants to the cell surface and whether the rescued protein is functional at the plasma membrane. This is critical to develop therapeutic strategies to treat the corneal dystrophies caused by *SLC4A11* mutations, thereby reducing the wait times for corneal transplantation. 2) Understand the role of cytoplasmic domain in the structure and function of SLC4A11. The cytoplasmic domain of SLC4A11 has low sequence identity (less than ~18%) among SLC4 family of bicarbonate transporters and deciphering the role it plays in transport function of the protein is important to treat catalytic mutants like R125H.

5.1.1 Rescuing ER-retained SLC4A11 mutants to plasma membrane

SLC4A11 mutations cause some cases of CHED2, HS and FECD [1-18]. The majority of the disease-causing mutations induce SLC4A11 protein misfolding and retention in ER. We tested the feasibility of rescuing misfolded SLC4A11 protein to the plasma membrane as a therapeutic approach to treat the patients suffering from these corneal dystrophies. First, to establish benchmark level of SLC4A11 activity to avoid disease symptoms, we measured functional activity present under genotypes mimicking unaffected individuals, CHED2 carriers and affected CHED2 and FECD individuals using a transfected HEK293 cell model. In this model, CHED2 carriers, CHED2 patients and FECD patients manifest respectively about 60%, 5% and 25% of WT function. To rescue the ER-retained SLC4A11 mutants, we employed two strategies. 1) Co-expression with a catalytically inactive mutant R125H (which processes to the cell surface similarly to WT levels but without functional activity) and 2) Reduced temperature growth

conditions (30 °C), which gives more time for the protein folding machinery to process some of the mildly misfolded SLC4A11 mutant proteins. The strategy of co-expression with catalytically inactive mutant R125H rescued ER-retained CHED2 mutant SLC4A11 proteins to the plasma membrane where they retained 25-30% of WT water flux levels. Further, the second strategy of culturing HEK293 cells expressing some ER-retained CHED2 mutants at 30 °C helped the protein to mature and to have increased water flux compared to 37 °C culture. We also examined whether expression of mutant SLC4A11 is associated with apoptotic cell death as accumulation of ER-retained proteins, in some cases, leads to apoptotic cell death [19]. Caspase activation and cell vitality assays revealed that expression of mutant SLC4A11 by itself did not induce cell death in transiently or stably transfected HEK293 cell culture models. Overall, the results from Chapter 3 show therapeutic strategies that will be able to increase cell surface localization of ER-retained SLC4A11 mutants holds promise to treat patients suffering from CHED2 and FECD corneal eye diseases.

5.1.2 Role of cytoplasmic domain in SLC4A11 structure and function

About one third of all reported *SLC4A11* disease-causing mutations are located on the 370 amino acid cytoplasmic domain of SLC4A11 protein [20]. However, very little is known about the role of SLC4A11 cytoplasmic domain in protein function. The presence of a catalytically inactive CHED2 mutant, R125H [21], on the cytoplasmic domain indicates a functional role of this domain in the SLC4A11 protein. Several membrane proteins, including voltage gated potassium channel, NBCe1 and CFTR, have a transport pore in their membrane domain that extends into the cytoplasmic domain [22-25]. We tested whether SLC4A11 has a similar transport pore by removing the cytoplasmic

domain of the protein and expressing the truncated protein in HEK293 cell culture model. Interestingly, we found that removal of the cytoplasmic domain destabilizes the membrane domain of SLC4A11 and resulted in the protein accumulating in the ER. Fusing the soluble proteins GFP or mNectarine to cover any exposed hydrophobic surface in membrane domain of SLC4A11 did not help the protein to reach the plasma membrane surface. Homology modeling studies suggested that SLC4A11 cytoplasmic domain has similar structural fold to AE1 cytoplasmic domain. A chimeric fusion of AE1 cytoplasmic domain with SLC4A11 membrane domain helped the protein to reach the cell surface to a significant level, but no functional activity was observed. This suggests that in addition to stabilizing the protein, SLC4A11 cytoplasmic domain also has an important role in the transport function of the protein. Co-immunoprecipitation studies showed that a strong and specific association between the SLC4A11 cytoplasmic domain and membrane domain when co-expressed independently in HEK293 cells. Similar to AE1, the monomers of cytoplasmic domain of SLC4A11 dimerize independently of the membrane domain. Taken together, data from Chapter 4 shows for the first time that SLC4A11 cytoplasmic domain is essential for the transport function and stabilization of the protein. The SLC4A11 cytoplasmic domain can also dimerize and has a similar structural fold to AE1 cytoplasmic domain.

5.2 Future directions

As discussed in Chapter 3, the feasibility of rescuing the ER-retained disease causing SLC4A11 mutants to the cell surface opens up the possibility of screening chemical compounds that could act as molecular chaperones or scaffold to enable proper

folding of the mutant protein. A high-throughput assay has been developed to screen a large library of chemical compounds to identify small molecule correctors for the misfolded mutant protein ΔF508 in CFTR [26]. Similar assay can be adapted to screen a large library of chemical compounds in order to rescue the ER-retained SLC4A11 mutant protein to the plasma membrane. Briefly, an epitope tag can be introduced on the extracellular loop of the protein that faces the outside environment. Using an antibody against the epitope tag combined with fluorescence molecules, the amount of SLC4A11 on the plasma membrane can be quantified.

After identifying the potential small molecule correctors that can rescue SLC4A11 mutant protein to the cell surface by high-throughput assay, the amount of rescued protein can be quantified using cell surface biotinylation labeling experiments (section 2.9). Using assays described in section 2.4, the functional activity of the rescued protein can be tested. Only the small molecule correctors that rescue the SLC4A11 mutant protein to the cell surface and restores functional activity can be further considered for therapeutic purposes. Any small molecular corrector drugs identified through this screening would be significant since it can be administered easily as eye drops in animal and clinical studies. This would help the CHED2 patients immensely as the disease is caused exclusively by *SLC4A11* mutations and the onset of disease symptoms can be prolonged to later stages of life.

Depletion of SLC4A11 causes cell death in cultured corneal endothelial cells implying that SLC4A11 could be essential for endothelial cell survival [27]. Any drug administered as eye drops that corrects the misfolding of FECD mutant SLC4A11 protein and rescues it to the cell surface could potentially reduce the depletion of SLC4A11 in

the corneal endothelium of FECD patients. This might increase the endothelial cell survival thereby slowing down the endothelial cell loss and corneal edema. In FECD patients, the identified drug could prolong the onset of disease symptoms from 4-5th decade of life to later decades of life, thereby reducing the wait times for corneal transplantation. This could lead to better quality of life for FECD patients who could avoid the invasive surgeries to restore their vision.

Interestingly, in some cases of FECD patients, hearing abnormalities were associated with disease progression [28]. The involvement of SLC4A11 is possible as it is expressed in both cornea and inner ear [29]. More specifically, if clinical techniques can be developed to deliver drugs (that corrects the SLC4A11 misfolding) to the inner ear, the hearing loss in FECD patients could be treated.

As mentioned in section 1.5.3, in addition to *SLC4A11* mutations, FECD is also caused by *TCF4* mutations [30]. TCF4 is a transcription factor and hence it would be interesting to test whether the expression levels of SLC4A11 protein are affected in the FECD patients carrying *TCF4* mutations. FECD corneas removed from patients who underwent corneal transplantation can be lysed with protease inhibitors and the amount of SLC4A11 protein can be quantified using both western blot techniques with a specific antibody against N-terminus of SLC4A11 and mass spectrometry. The peptides identified by mass spectrometry can be used to study the effect of TCF4 mutation on the biogenesis of SLC4A11 in the FECD patients carrying *TCF4* mutations. This would shed light on developing possible therapeutic strategies for FECD patients carrying *TCF4* mutations.

The work carried out in Chapter 4 of this thesis shows that the cytoplasmic domain is very important for the stabilization and function of the SLC4A11 protein.

Further, the cytoplasmic domain of SLC4A11 is 370 amino acids long, typical of SLC4 family of bicarbonate transporters as AE1 also has a 400 amino acid long cytoplasmic domain. This raises the question whether SLC4A11 cytoplasmic domain is involved in some interactions with other proteins in the corneal endothelium? For example, the cytoplasmic domain of AE1 is essential for the interaction with cytoskeleton proteins ankyrin G (in kidney) and ankyrin R (red blood cells), [31, 32]. There is a possibility that SLC4A11 cytoplasmic domain might be involved with other cytoskeletal proteins of corneal endothelium. To identify any such cytoskeletal proteins interacting with SLC4A11, recombinant human SLC4A11 or SLC4A11 protein from bovine corneas can be immobilized on protein G resin using appropriate antibodies. The resin with immobilized SLC4A11 can be incubated with bovine corneal lysate and washed to remove non-specific protein interactions. SLC4A11 and the proteins associated with it can be eluted from the protein G resin and using SDS-PAGE and mass spectrometry, the interacting proteins can be identified. The association between SLC4A11 and its interactors can be further confirmed by co-immunoprecipitation (section 2.6) in HEK293 cells culture model and proximity ligation assay studies in human or bovine corneal sections [33]. Future studies involving the identification of these interacting proteins might shed more light on the trafficking and regulation of SLC4A11 to the baso-lateral side of the corneal endothelial cells.

Apart from that, solving the high-resolution structure of SLC4A11 using X-ray crystallography could help us to understand the transport function and other structural details. Recombinant expression of membrane proteins poses a great challenge and obstacles. For example, in Chapter 4, when we tried to express the SLC4A11 cytoplasmic

domain in bacteria with the aim of structural studies, the recombinant protein was present mainly in the insoluble fraction. In fact, SLC4A11 cytoplasmic and membrane domains are dependent on each other for the stability of the protein. Hence to solve the high-resolution structure of SLC4A11, possibly the full-length protein has to be expressed recombinantly. The full length SLC4A11 with their putative glycosylation residues on the extracellular loop mutated to alanine can be cloned into yeast expression vector. Yeast transformed with the SLC4A11 vector can be grown under various test conditions to identify the appropriate growth environment where the expression of recombinant SLC4A11 protein is significant. Large-scale cultures can then be prepared to purify enough quantities of SLC4A11 protein for structural studies. Solving the structure of SLC4A11 would significantly advance our understanding of the protein and the disease causing mutants.

Clinically, it would be interesting to test the CHED2 and HS patients for other abnormalities as the knockout mouse model of SLC4A11 has diluted urine, poly uria and hearing abnormalities apart from corneal abnormalities [21, 29, 34]. There is only one study so far where a Harboyan syndrome patient with a homozygous mutation that causes the SLC4A11 protein to prematurely stop at Arginine 730 was examined thoroughly [35]. The particular patient had vision loss (corrected by corneal transplantation) and hearing abnormalities but no renal abnormalities. This is in contrast to the phenotype observed in SLC4A11 knockout mouse models. However, more studies are required to confirm the prognosis of other complications that might arise from the mutation of *SLC4A11* in CHED2 patients as SLC4A11 is expressed in various tissues.

5.3 References

1. Vithana, E. N., Morgan, P. E., Ramprasad, V., Tan, D. T., Yong, V. H., Venkataraman, D., Venkatraman, A., Yam, G. H., Nagasamy, S., Law, R. W., Rajagopal, R., Pang, C. P., Kumaramanickevel, G., Casey, J. R. and Aung, T. (2008) SLC4A11 Mutations in Fuchs Endothelial Corneal Dystrophy (FECD). Hum. Mol. Genet. **17**, 656-666
2. Riazuddin, S. A., Vithana, E. N., Seet, L. F., Liu, Y., Al-Saif, A., Koh, L. W., Heng, Y. M., Aung, T., Meadows, D. N., Eghrari, A. O., Gottsch, J. D. and Katsanis, N. (2010) Missense mutations in the sodium borate co-transporter SLC4A11 cause late onset Fuchs corneal dystrophy. Hum. Mutat. **31**, 1261-1268
3. Soumittra, N., Loganathan, S. K., Madhavan, D., Ramprasad, V. L., Arokiasamy, T., Sumathi, S., Karthiyayini, T., Rachapalli, S. R., Kumaramanickavel, G., Casey, J. R. and Rajagopal, R. (2014) Biosynthetic and functional defects in newly identified SLC4A11 mutants and absence of COL8A2 mutations in Fuchs endothelial corneal dystrophy. J Hum Genet. **59**, 444-453
4. Minear, M. A., Li, Y.-J., Rimmler, J., Balajonda, E., Watson, S., Allingham, R. R., Hauser, M. A., Klintworth, G. K., Afshari, N. A. and Gregory, S. G. (2013) Genetic screen of African Americans with Fuchs endothelial corneal dystrophy. Molecular Vision. **19**, 2508-2516
5. Desir, J., Moya, G., Reish, O., Van Regemorter, N., Deconinck, H., David, K. L., Meire, F. M. and Abramowicz, M. (2007) Borate transporter SLC4A11 mutations cause both Harboyan syndrome and non-syndromic corneal endothelial dystrophy. J. Med. Genet. **44**, 322-326
6. Puangsricharern, V., Yeetong, P., Charumalai, C., Suphapeetiporn, K. and Shotelersuk, V. (2014) Two novel mutations including a large deletion of the SLC4A11 gene causing autosomal recessive hereditary endothelial dystrophy. British Journal of Ophthalmology. **98**, 1460-1462
7. Hemadevi, B., Veitia, R. A., Srinivasan, M., Arunkumar, J., Prajna, N. V., Lesaffre, C. and Sundaresan, P. (2008) Identification of mutations in the SLC4A11 gene in patients with recessive congenital hereditary endothelial dystrophy. Arch Ophthalmol. **126**, 700-708

8. Jiao, X., Sultana, A., Garg, P., Ramamurthy, B., Vemuganti, G. K., Gangopadhyay, N., Hejtmancik, J. F. and Kannabiran, C. (2007) Autosomal recessive corneal endothelial dystrophy (CHED2) is associated with mutations in SLC4A11. J Med Genet. **44**, 64-68.
9. Ramprasad, V. L., Ebenezer, N. D., Aung, T., Rajagopal, R., Yong, V. H., Tuft, S. J., Viswanathan, D., El-Ashry, M. F., Liskova, P., Tan, D. T., Bhattacharya, S. S., Kumaramanickavel, G. and Vithana, E. N. (2007) Novel SLC4A11 mutations in patients with recessive congenital hereditary endothelial dystrophy (CHED2). Mutation in brief #958. Online. Hum. Mutat. **28**, 522-523
10. Sultana, A., Garg, P., Ramamurthy, B., Vemuganti, G. K. and Kannabiran, C. (2007) Mutational spectrum of the SLC4A11 gene in autosomal recessive congenital hereditary endothelial dystrophy. Mol Vis. **13**, 1327-1332
11. Vithana, E. N., Morgan, P., Sundaresan, P., Ebenezer, N. D., Tan, D. T., Mohamed, M. D., Anand, S., Khine, K. O., Venkataraman, D., Yong, V. H., Salto-Tellez, M., Venkatraman, A., Guo, K., Hemadevi, B., Srinivasan, M., Prajna, V., Khine, M., Casey, J. R., Inglehearn, C. F. and Aung, T. (2006) Mutations in sodium-borate cotransporter SLC4A11 cause recessive congenital hereditary endothelial dystrophy (CHED2). Nature Genetics. **38**, 755-757
12. Park, S. H., Jeong, H. J., Kim, M. and Kim, M. S. (2013) A Novel Nonsense Mutation of the SLC4A11 Gene in a Korean Patient With Autosomal Recessive Congenital Hereditary Endothelial Dystrophy. Cornea. **32**, e181-e182
13. Paliwal, P., Sharma, A., Tandon, R., Sharma, N., Titiyal, J. S., Sen, S., Nag, T. C. and Vajpayee, R. B. (2010) Congenital hereditary endothelial dystrophy - mutation analysis of SLC4A11 and genotype-phenotype correlation in a North Indian patient cohort. Mol Vis. **16**, 2955-2963
14. Aldahmesh, M. A., Khan, A. O., Meyer, B. F. and Alkuraya, F. S. (2009) Mutational Spectrum of SLC4A11 in Autosomal Recessive CHED in Saudi Arabia. Investigative Ophthalmology & Visual Science. **50**, 4142-4145
15. Shah, S. S., Al-Rajhi, A., Brandt, J. D., Mannis, M. J., Roos, B., Sheffield, V. C., Syed, N. A., Stone, E. M. and Fingert, J. H. (2008) Mutation in the SLC4A11

gene associated with autosomal recessive congenital hereditary endothelial dystrophy in a large Saudi family. Ophthalmic Genet. **29**, 41-45

16. Aldave, A. J., Yellore, V. S., Bourla, N., Momi, R. S., Khan, M. A., Salem, A. K., Rayner, S. A., Glasgow, B. J. and Kurtz, I. (2007) Autosomal Recessive CHED Associated With Novel Compound Heterozygous Mutations in SLC4A11. Cornea. **26**, 896-900
17. Kumar, A., Bhattacharjee, S., Prakash, D. R. and Sadanand, C. S. (2007) Genetic analysis of two Indian families affected with congenital hereditary endothelial dystrophy: two novel mutations in SLC4A11. Mol Vis. **13**, 39-46.
18. Desir, J. and Abramowicz, M. (2008) Congenital hereditary endothelial dystrophy with progressive sensorineural deafness (Harboyan syndrome). Orphanet J Rare Dis. **3**, 28-36
19. Xu, C., Bailly-Maitre, B. and Reed, J. C. (2005) Endoplasmic reticulum stress: cell life and death decisions. The Journal of Clinical Investigation. **115**, 2656-2664
20. Loganathan, S. K. and Casey, J. R. (2014) Corneal Dystrophy-Causing SLC4A11 Mutants: Suitability for Folding-Correction Therapy. Human Mutation. **35**, 1082-1091
21. Vilas, G. L., Loganathan, S. K., Liu, J., Riau, A. K., Young, J. D., Mehta, J. S., Vithana, E. N. and Casey, J. R. (2013) Transmembrane water-flux through SLC4A11: a route defective in genetic corneal diseases. Human Molecular Genetics. **22**, 4579-4590
22. Chang, M. H., Dipiero, J., Sonnichsen, F. D. and Romero, M. F. (2008) Entry to "HCO_3^- tunnel" revealed by SLC4A4 human mutation and structural model. J Biol Chem. **283**, 18402-18410
23. El Hiani, Y. and Linsdell, P. (2015) Functional Architecture of the Cytoplasmic Entrance to the Cystic Fibrosis Transmembrane Conductance Regulator Chloride Channel Pore. Journal of Biological Chemistry, *in press*
24. Long, S. B., Campbell, E. B. and Mackinnon, R. (2005) Crystal Structure of a Mammalian Voltage-Dependent Shaker Family K^+ Channel. Science. **309**, 897-903

25. Long, S. B., Campbell, E. B. and Mackinnon, R. (2005) Voltage sensor of Kv1.2: structural basis of electromechanical coupling. Science. **309**, 903-908

26. Pedemonte, N., Lukacs, G. L., Du, K., Caci, E., Zegarra-Moran, O., Galietta, L. J. and Verkman, A. S. (2005) Small-molecule correctors of defective DeltaF508-CFTR cellular processing identified by high-throughput screening. J Clin Invest. **115**, 2564-2571.

27. Liu, J., Seet, L.-F., Koh, L. W., Venkatraman, A., Venkataraman, D., Mohan, R. R., Praetorius, J., Bonanno, J. A., Aung, T. and Vithana, E. N. (2012) Depletion of SLC4A11 Causes Cell Death by Apoptosis in an Immortalized Human Corneal Endothelial Cell Line. Investigative Ophthalmology & Visual Science. **53**, 3270-3279

28. Stehouwer, M., Bijlsma, W. R. and Van der Lelij, A. (2011) Hearing disability in patients with Fuchs' endothelial corneal dystrophy: unrecognized co-pathology? Clin. Ophthalmol. **5**, 1297-1301

29. Groeger, N., Froehlich, H., Maier, H., Olbrich, A., Kostin, S., Braun, T. and Boettger, T. (2010) Slc4a11 prevents osmotic imbalance leading to corneal endothelial dystrophy, deafness, and polyuria. J. Biol. Chem. **285**, 14467-14474

30. Igo, R. P., Jr., Kopplin, L. J., Joseph, P., Truitt, B., Fondran, J., Bardenstein, D., Aldave, A. J., Croasdale, C. R., Price, M. O., Rosenwasser, M., Lass, J. H., Iyengar, S. K. and for the, F. G. M.-c. S. G. (2012) Differing Roles for *TCF4* and *COL8A2* in Central Corneal Thickness and Fuchs Endothelial Corneal Dystrophy. PLoS ONE. **7**, e46742

31. Genetet, S., Ripoche, P., Le Van Kim, C., Colin, Y. and Lopez, C. (2015) Evidence of a Structural and Functional Ammonium Transporter RhBG·Anion Exchanger 1·Ankyrin-G Complex in Kidney Epithelial Cells. Journal of Biological Chemistry. **290**, 6925-6936

32. Cordat, E. and Reithmeier, R. A. F. (2014) Chapter One - Structure, Function, and Trafficking of SLC4 and SLC26 Anion Transporters. In Current Topics in Membranes (Mark, O. B., ed.). pp. 1-67, Academic Press

33. Vilas, G., Krishnan, D., Loganathan, S. K., Malhotra, D., Liu, L., Beggs, M. R., Gena, P., Calamita, G., Jung, M., Zimmermann, R., Tamma, G., Casey, J. R. and

Alexander, R. T. (2015) Increased water flux induced by an aquaporin-1/carbonic anhydrase II interaction. Molecular Biology of the Cell. **26**, 1106-1118

34. Han, S. B., Ang, H.-P., Poh, R., Chaurasia, S. S., Peh, G., Liu, J., Tan, D. T. H., Vithana, E. N. and Mehta, J. S. (2013) Mice With a Targeted Disruption of Slc4a11 Model the Progressive Corneal Changes of Congenital Hereditary Endothelial Dystrophy. Investigative Ophthalmology & Visual Science. **54**, 6179-6189

35. Liskova, P., Dudakova, L., Tesar, V., Bednarova, V., Kidorova, J., Jirsova, K., Davidson, A. E. and Hardcastle, A. J. (2015) Detailed Assessment of Renal Function in a Proband with Harboyan Syndrome Caused by a Novel Homozygous SLC4A11 Nonsense Mutation. Ophthalmic Research. **53**, 30-35

BIBLIOGRAPHY

Abuladze, N., Lee, I., Newman, D., Hwang, J., Boorer, K., Pushkin, A. and Kurtz, I. (1998) Molecular cloning, chromosomal localization, tissue distribution, and functional expression of the human pancreatic sodium bicarbonate cotransporter. J. Biol. Chem. **273**, 17689-17695

Aldahmesh, M., Khan, A., Meyer, B. and Alkuraya, F. (2009) Mutational Spectrum of SLC4A11 in Autosomal Recessive CHED in Saudi Arabia. Invest Ophthalmol Vis Sci. **50**, 4142-4145

Aldave, A. J., Han, J. and Frausto, R. F. (2013) Genetics of the corneal endothelial dystrophies: an evidence-based review. Clinical Genetics. **84**, 109-119

Aldave, A. J., Yellore, V. S., Bourla, N., Momi, R. S., Khan, M. A., Salem, A. K., Rayner, S. A., Glasgow, B. J. and Kurtz, I. (2007) Autosomal Recessive CHED Associated With Novel Compound Heterozygous Mutations in SLC4A11. Cornea. **26**, 896-900

Alka, K. and Casey, J. R. (2014) Bicarbonate transport in health and disease. IUBMB Life. **66**, 596-615

Alloisio, N., Texier, P., Vallier, A., Ribeiro, M. L., Morle, L., Bozon, M., Bursaux, E., Maillet, P., Goncalves, P., Tanner, M. J., Tamagnini, G. and Delaunay, J. (1997) Modulation of clinical expression and band 3 deficiency in hereditary spherocytosis. Blood. **90**, 414-420

Alper, S. L. (2009) Molecular physiology and genetics of Na^+-independent SLC4 anion exchangers. J Exp Biol. **212**, 1672-1683

Alper, S. L., Kopito, R. R., Libresco, S. M. and Lodish, H. F. (1988) Cloning and characterization of a murine Band 3-related cDNA from kidney and a lymphoid cell line. J. Biol. Chem. **263**, 17092-17099

Alvarez, B. V., Fujinaga, J. and Casey, J. R. (2001) Molecular Basis for angiotensin II-induced increase of chloride/bicarbonate exchange in the myocardium. Circ. Research. **89**, 1246-1253

Alvarez, B. V., Xia, Y., Sowah, D., Soliman, D., Light, P., Karmazyn, M. and Casey, J. R. (2007) A Carbonic Anhydrase Inhibitor Prevents and Reverts Cardiomyocyte Hypertrophy. J. Physiol. **579**, 127-145

Basu, A., Mazor, S. and Casey, J. R. (2010) Measurement of Distances Within a Concatamer of the Plasma Membrane Cl^-/HCO_3^- Exchanger, AE1. Biochemistry. **49**, 9226-9240

Beuerman, R. W. and Pedroza, L. (1996) Ultrastructure of the human cornea. Microscopy Research and Technique. **33**, 320-335

Bevensee, M. O., Schmitt, B. M., Choi, I., Romero, M. F. and Boron, W. F. (2000) An electrogenic Na^+-HCO_3^- cotransporter (NBC) with a novel COOH-terminus, cloned from rat brain. Am. J. Physiol. **278**, C1200-C1211

Biswas, S., Munier, F. L., Yardley, J., Hart-Holden, N., Perveen, R., Cousin, P., Sutphin, J. E., Noble, B., Batterbury, M., Kielty, C., Hackett, A., Bonshek, R., Ridgway, A., McLeod, D., Sheffield, V. C., Stone, E. M., Schorderet, D. F. and Black, G. C. (2001) Missense mutations in COL8A2, the gene encoding the alpha2 chain of type VIII collagen, cause two forms of corneal endothelial dystrophy. Hum. Mol. Genet. **10**, 2415-2423.

Bonanno, J. A. (2003) Identity and regulation of ion transport mechanisms in the corneal endothelium. Prog Retin Eye Res. **22**, 69-94

Bonanno, J. A. (2012) Molecular mechanisms underlying the corneal endothelial pump. Exp Eye Res. **95**, 2-7

Bonar, P. T. and Casey, J. R. (2010) Over-expression and Purification of Functional Human AE1, Expressed in *Saccharomyces cerevisiae* Suitable for Protein Crystallography. Protein Exp. Purif. **74**, 106-115

Bonar, P., Schneider, H.-P., Becker, H. M., Deitmer, J. W. and Casey, J. R. (2013) Three-Dimensional Model for the Human Cl^-/HCO_3^- Exchanger, AE1, by Homology to the *E. coli* ClC Protein. Journal of Molecular Biology. **425**, 2591-2608

Bourne, W. M. (2003) Biology of the corneal endothelium in health and disease. Eye (Lond). **17**, 912-918

Bourne, W. M., Nelson, L. R. and Hodge, D. O. (1997) Central corneal endothelial cell changes over a ten-year period. Investigative Ophthalmology & Visual Science. **38**, 779-782

Brubaker, R. F. (1991) Flow of aqueous humor in humans [The Friedenwald Lecture]. Investigative Ophthalmology & Visual Science. **32**, 3145-3166

Burnham, C. E., Amlal, H., Wang, Z., Shull, G. E. and Soleimani, M. (1997) Cloning and functional expression of a human kidney Na^+:HCO_3^- cotransporter. J. Biol. Chem. **272**, 19111-19114

Casey, J. R. and Reithmeier, R. A. F. (1991) Analysis of the oligomeric state of Band 3, the anion transport protein of the human erythrocyte membrane, by size exclusion high performance liquid chromatography: oligomeric stability and origin of heterogeneity. J. Biol. Chem. **266**, 15726-15737

Chae, H.-J., Kang, J.-S., Byun, J.-O., Han, K.-S., Kim, D.-U., Oh, S.-M., Kim, H.-M., Chae, S.-W. and Kim, H.-R. (2000) Molecular mechanism of staurosporine-induced apoptosis in osteoblasts. Pharmacological Research. **42**, 373-381

Chang, M. H., Dipiero, J., Sonnichsen, F. D. and Romero, M. F. (2008) Entry to "HCO_3^- tunnel" revealed by SLC4A4 human mutation and structural model. J Biol Chem. **283**, 18402-18410

Chen, S., Mienaltowski, M. J. and Birk, D. E. (2015) Regulation of corneal stroma extracellular matrix assembly. Experimental Eye Research. **133**, 69-80

Cheng, S. H., Gregory, R. J., Marshall, J., Paul, S., Souza, D. W., White, G. A., O'Riordan, C. R. and Smith, A. E. (1990) Defective intracellular transport and processing of CFTR is the molecular basis of most cystic fibrosis. Cell. **63**, 827-834.

Choi, I., Aalkjaer, C., Boulpaep, E. L. and Boron, W. F. (2000) An electroneutral sodium/bicarbonate cotransporter NBCn1 and associated sodium channel. Nature. **405**, 571-575

Choi, I., Romero, M. F., Khandoudi, N., Bril, A. and Boron, W. F. (1999) Cloning and characterization of a human electrogenic Na^+-HCO_3^- cotransporter isoform (hhNBC). Am. J. Physiol. **276**, C576-584

Cordat, E. (2006) Unraveling trafficking of the kidney anion exchanger 1 in polarized MDCK epithelial cells. Biochem Cell Biol. **84**, 949-959.

Cordat, E. and Casey, J. R. (2009) Bicarbonate transport in cell physiology and disease. The Biochemical Journal. **417**, 423-439

Cordat, E. and Reithmeier, R. A. F. (2014) Chapter One - Structure, Function, and Trafficking of SLC4 and SLC26 Anion Transporters. In Current Topics in Membranes (Mark, O. B., ed.). pp. 1-67, Academic Press

Cordat, E., Kittanakom, S., Yenchitsomanus, P. T., Li, J., Du, K., Lukacs, G. L. and Reithmeier, R. A. (2006) Dominant and Recessive Distal Renal Tubular Acidosis Mutations of Kidney Anion Exchanger 1 Induce Distinct Trafficking Defects in MDCK Cells. Traffic. **7**, 117-128.

Cuppoletti, J., Goldinger, J., Kang, B., Jo, I., Berenski, C. and Jung, C. Y. (1985) Anion carrier in the human erythrocyte exists as a dimer. J. Biol. Chem. **260**, 15714-15717

Damkier, H. H., Nielsen, S. and Praetorius, J. (2007) Molecular expression of SLC4 derived Na^+ dependent anion transporters in selected human tissues. Am. J Physiol. Regul. Integr. Comp. Physiol. **293**, R2136-2146

DelMonte, D. W. and Kim, T. (2011) Anatomy and physiology of the cornea. Journal of Cataract & Refractive Surgery. **37**, 588-598

Demirci, F. Y., Chang, M. H., Mah, T. S., Romero, M. F. and Gorin, M. B. (2006) Proximal renal tubular acidosis and ocular pathology: a novel missense mutation in the gene (SLC4A4) for sodium bicarbonate cotransporter protein (NBCe1). Mol Vis. **12**, 324-330.

Denning, G. M., Anderson, M. P., Amara, J. F., Marshall, J., Smith, A. E. and Welsh, M. J. (1992) Processing of mutant cystic fibrosis transmembrane conductance regulator is temperature-sensitive. Nature. **358**, 761-764.

Desir, J. and Abramowicz, M. (2008) Congenital hereditary endothelial dystrophy with progressive sensorineural deafness (Harboyan syndrome). Orphanet J Rare Dis. **3**, 28-36

Desir, J., Moya, G., Reish, O., Van Regemorter, N., Deconinck, H., David, K. L., Meire, F. M. and Abramowicz, M. (2007) Borate transporter SLC4A11 mutations cause both Harboyan syndrome and non-syndromic corneal endothelial dystrophy. J. Med. Genet. **44**, 322-326

Dinour, D., Chang, M. H., Satoh, J., Smith, B. L., Angle, N., Knecht, A., Serban, I., Holtzman, E. J. and Romero, M. F. (2004) A novel missense mutation in the

sodium bicarbonate cotransporter (NBCe1/SLC4A4) causes proximal tubular acidosis and glaucoma through ion transport defects. J Biol Chem. **279**, 52238-52246.

Eber, S. a. L., S. E. (2004) Hereditary spherocytosis--defects in proteins that connect the membrane skeleton to the lipid bilayer. Semin Hematol. **41**, 118-141

El Hiani, Y. and Linsdell, P. (2015) Functional Architecture of the Cytoplasmic Entrance to the Cystic Fibrosis Transmembrane Conductance Regulator Chloride Channel Pore. Journal of Biological Chemistry, *in press*

Farjo A, M. M., Soong HK. (2008) Corneal anatomy, physiology, and wound healing. In: Yanoff M, Duker JS, eds, Ophthalmology, 3rd ed. St. Louis, MO, Mosby, 203–208

Fischbarg, J. (2012) Water channels and their roles in some ocular tissues. Molecular Aspects of Medicine. **33**, 638-641

Genetet, S., Ripoche, P., Le Van Kim, C., Colin, Y. and Lopez, C. (2015) Evidence of a Structural and Functional Ammonium Transporter RhBG·Anion Exchanger 1·Ankyrin-G Complex in Kidney Epithelial Cells. Journal of Biological Chemistry. **290**, 6925-6936

Germundsson, J., Karanis, G., Fagerholm, P. and Lagali, N. (2013) Age-Related Thinning of Bowman's Layer in the Human Cornea In VivoAge-Related Thinning of Bowman's Layer. Investigative Ophthalmology & Visual Science. **54**, 6143-6149

Grichtchenko, II, Choi, I., Zhong, X., Bray-Ward, P., Russell, J. M. and Boron, W. F. (2001) Cloning, characterization, and chromosomal mapping of a human electroneutral Na^+-driven Cl^- /HCO_3^- exchanger. J Biol Chem. **276**, 8358-8363

Grinstein, S., Ship, S. and Rothstein, A. (1978) Anion transport in relation to proteolytic dissection of Band 3 protein. Biochim. Biophys. Acta. **507**, 294-304

Groeger, N., Froehlich, H., Maier, H., Olbrich, A., Kostin, S., Braun, T. and Boettger, T. (2010) Slc4a11 prevents osmotic imbalance leading to corneal endothelial dystrophy, deafness, and polyuria. J. Biol. Chem. **285**, 14467-14474

Han, S. B., Ang, H.-P., Poh, R., Chaurasia, S. S., Peh, G., Liu, J., Tan, D. T. H., Vithana, E. N. and Mehta, J. S. (2013) Mice With a Targeted Disruption of Slc4a11 Model

the Progressive Corneal Changes of Congenital Hereditary Endothelial Dystrophy. Investigative Ophthalmology & Visual Science. **54**, 6179-6189

Hassell, J. R. and Birk, D. E. (2010) The molecular basis of corneal transparency. Experimental Eye Research. **91**, 326-335

Hayashi, S., Osawa, T. and Tohyama, K. (2002) Comparative observations on corneas, with special reference to bowman's layer and descemet's membrane in mammals and amphibians. Journal of Morphology. **254**, 247-258

Hemadevi, B., Veitia, R. A., Srinivasan, M., Arunkumar, J., Prajna, N. V., Lesaffre, C. and Sundaresan, P. (2008) Identification of mutations in the SLC4A11 gene in patients with recessive congenital hereditary endothelial dystrophy. Arch Ophthalmol. **126**, 700-708

Horita, S., Yamada, H., Inatomi, J., Moriyama, N., Sekine, T., Igarashi, T., Endo, Y., Dasouki, M., Ekim, M., Al-Gazali, L., Shimadzu, M., Seki, G. and Fujita, T. (2005) Functional analysis of NBC1 mutants associated with proximal renal tubular acidosis and ocular abnormalities. J Am Soc Nephrol. **16**, 2270-2278.

Humphrey, W., Dalke, A. and Schulten, K. (1996) VMD: Visual molecular dynamics. Journal of Molecular Graphics. **14**, 33-38

Igarashi, T., Inatomi, J., Sekine, T., Cha, S. H., Kanai, Y., Kunimi, M., Tsukamoto, K., Satoh, H., Shimadzu, M., Tozawa, F., Mori, T., Shiobara, M., Seki, G. and Endou, H. (1999) Mutations in SLC4A4 cause permanent isolated proximal renal tubular acidosis with ocular abnormalities. Nat. Genet. **23**, 264-266

Igarashi, T., Inatomi, J., Sekine, T., Seki, G., Shimadzu, M., Tozawa, F., Takeshima, Y., Takumi, T., Takahashi, T., Yoshikawa, N., Nakamura, H. and Endou, H. (2001) Novel nonsense mutation in the Na^+/HCO_3^- cotransporter gene (SLC4A4) in a patient with permanent isolated proximal renal tubular acidosis and bilateral glaucoma. J Am Soc Nephrol. **12**, 713-718

Igo, R. P., Jr., Kopplin, L. J., Joseph, P., Truitt, B., Fondran, J., Bardenstein, D., Aldave, A. J., Croasdale, C. R., Price, M. O., Rosenwasser, M., Lass, J. H., Iyengar, S. K. and for the, F. G. M.-c. S. G. (2012) Differing Roles for *TCF4* and *COL8A2* in Central Corneal Thickness and Fuchs Endothelial Corneal Dystrophy. PLoS ONE. **7**, e46742

Ilagan, R. P., Rhoades, E., Gruber, D. F., Kao, H.-T., Pieribone, V. A. and Regan, L. (2010) A new bright green-emitting fluorescent protein – engineered monomeric and dimeric forms. FEBS Journal. **277**, 1967-1978

Iliff, B. W., Riazuddin, S. A. and Gottsch, J. D. (2012) The genetics of Fuchs' corneal dystrophy. Expert Rev Ophthalmol. **7**, 363-375

Inatomi, J., Horita, S., Braverman, N., Sekine, T., Yamada, H., Suzuki, Y., Kawahara, K., Moriyama, N., Kudo, A., Kawakami, H., Shimadzu, M., Endou, H., Fujita, T., Seki, G. and Igarashi, T. (2004) Mutational and functional analysis of SLC4A4 in a patient with proximal renal tubular acidosis. Pflugers Arch. **448**, 438-444

Ishibashi, K., Sasaki, S. and Marumo, F. (1998) Molecular cloning of a new sodium bicarbonate cotransporter cDNA from human retina. Biochem. Biophys. Res. Commun. **246**, 535-538

Jalimarada, S. S., Ogando, D. G., Vithana, E. N. and Bonanno, J. A. (2013) Ion Transport Function of SLC4A11 in Corneal Endothelium. Investigative Ophthalmology & Visual Science. **54**, 4330-4340

Jennings, M. L., Anderson, M. P. and Monaghan, R. (1986) Monoclonal antibodies against human erythrocyte Band 3 protein: localization of proteolytic cleavage sites and stilbenedisulfonate-binding lysine residues. J. Biol. Chem. **261**, 9002-9010

Jiao, X., Sultana, A., Garg, P., Ramamurthy, B., Vemuganti, G. K., Gangopadhyay, N., Hejtmancik, J. F. and Kannabiran, C. (2007) Autosomal recessive corneal endothelial dystrophy (CHED2) is associated with mutations in SLC4A11. J Med Genet. **44**, 64-68.

Johnson, D. E., Ai, H.-W., P., W., Young, J. D., Campbell, R. E. and Casey, J. R. (2009) Red fluorescent protein pH biosensor to detect concentrative nucleoside transport. J. Biol. Chem. **284**, 20499-20511

Kao, L., Azimov, R., Abuladze, N., Newman, D. and Kurtz, I. (2015) Human SLC4A11-C functions as a DIDS-stimulatable $H^+(OH^-)$ permeation pathway: partial correction of R109H mutant transport. American Journal of Physiology - Cell Physiology. **308**, C176-C188

Kelley, L. A. and Sternberg, M. J. E. (2009) Protein structure prediction on the Web: a case study using the Phyre server. Nat. Protocols. **4**, 363-371

Klintworth, G. K. (2009) Corneal dystrophies. Orphanet. J. Rare Dis. **4**, 7

Kodaganur, S. G., Kapoor, S., Veerappa, A. M., Tontanahal, S. J., Sarda, A., Yathish, S., Prakash, D. R. and Kumar, A. (2013) Mutation analysis of the SLC4A11 gene in Indian families with congenital hereditary endothelial dystrophy 2 and a review of the literature. Molecular Vision. **19**, 1694-1706

Kopito, R. R. and Lodish, H. F. (1985) Primary structure and transmembrane orientation of the murine anion exchange protein. Nature. **316**, 234-238

Krepischi, A. C. V., Knijnenburg, J., Bertola, D. R., Kim, C. A., Pearson, P. L., Bijlsma, E., Szuhai, K., Kok, F., Vianna-Morgante, A. M. and Rosenberg, C. (2010) Two distinct regions in 2q24.2-q24.3 associated with idiopathic epilepsy. Epilepsia. **51**, 2457-2460

Kudrycki, K. E., Newman, P. R. and Shull, G. E. (1990) cDNA cloning and tissue distribution of mRNAs for two proteins that are related to the Band 3 Cl^-/HCO_3^- exchanger. J. Biol. Chem. **265**, 462-471

Kulczycki, L. L., Kostuch, M. and Bellanti, J. A. (2003) A clinical perspective of cystic fibrosis and new genetic findings: relationship of CFTR mutations to genotype-phenotype manifestations. Am J Med Genet. **116A**, 262-267

Kumar, A., Bhattacharjee, S., Prakash, D. R. and Sadanand, C. S. (2007) Genetic analysis of two Indian families affected with congenital hereditary endothelial dystrophy: two novel mutations in SLC4A11. Mol Vis. **13**, 39-46.

Laemmli, U. K. (1970) Cleavage of structural proteins during assembly of the head of bacteriophage T4. Nature. **227**, 680-685

Liskova, P., Dudakova, L., Tesar, V., Bednarova, V., Kidorova, J., Jirsova, K., Davidson, A. E. and Hardcastle, A. J. (2015) Detailed Assessment of Renal Function in a Proband with Harboyan Syndrome Caused by a Novel Homozygous SLC4A11 Nonsense Mutation. Ophthalmic Research. **53**, 30-35

Liu, J., Seet, L.-F., Koh, L. W., Venkatraman, A., Venkataraman, D., Mohan, R. R., Praetorius, J., Bonanno, J. A., Aung, T. and Vithana, E. N. (2012) Depletion of SLC4A11 Causes Cell Death by Apoptosis in an Immortalized Human Corneal

Endothelial Cell Line. Investigative Ophthalmology & Visual Science. **53**, 3270-3279

Loganathan, S. K. and Casey, J. R. (2014) Corneal Dystrophy-Causing SLC4A11 Mutants: Suitability for Folding-Correction Therapy. Human Mutation. **35**, 1082-1091

Long, S. B., Campbell, E. B. and Mackinnon, R. (2005) Crystal Structure of a Mammalian Voltage-Dependent Shaker Family K^+ Channel. Science. **309**, 897-903

Long, S. B., Campbell, E. B. and Mackinnon, R. (2005) Voltage sensor of Kv1.2: structural basis of electromechanical coupling. Science. **309**, 903-908

Lopez, I. A., Rosenblatt, M. I., Kim, C., Galbraith, G. G., Jones, S. M., Kao, L., Newman, D., Liu, W., Yeh, S., Pushkin, A., Abuladze, N. and Kurtz, I. (2009) Slc4a11 gene disruption in mice: Cellular targets of sensorineuronal abnormalities. J. Biol. Chem. **28**, 26882-26896

Lukacs, G. L. and Verkman, A. S. (2012) CFTR: folding, misfolding and correcting the ΔF508 conformational defect. Trends in Molecular Medicine. **18**, 81-91

Meek, K. M. and Leonard, D. W. (1993) Ultrastructure of the corneal stroma: a comparative study. Biophysical Journal. **64**, 273-280

Minear, M. A., Li, Y.-J., Rimmler, J., Balajonda, E., Watson, S., Allingham, R. R., Hauser, M. A., Klintworth, G. K., Afshari, N. A. and Gregory, S. G. (2013) Genetic screen of African Americans with Fuchs endothelial corneal dystrophy. Molecular Vision. **19**, 2508-2516

Nigg, E. and Cherry, R. J. (1979) Dimeric association of Band 3 in the erythrocyte membrane demonstrated by protein diffusion measurements. Nature. **277**, 493-494

O'Neill, M. A., Ishii, T., Albersheim, P. and Darvill, A. G. (2004) Rhamnogalacturonan II: structure and function of a borate cross-linked cell wall pectic polysaccharide. Annu. Rev. Plant Biol. **55**, 109-139.

Ogando, D. G., Jalimarada, S. S., Zhang, W., Vithana, E. N. and Bonanno, J. A. (2013) SLC4A11 is an EIPA-sensitive Na^+ permeable pHi regulator. American Journal of Physiology - Cell Physiology. **305**, C716-C727

Paliwal, P., Sharma, A., Tandon, R., Sharma, N., Titiyal, J. S., Sen, S., Nag, T. C. and Vajpayee, R. B. (2010) Congenital hereditary endothelial dystrophy - mutation analysis of SLC4A11 and genotype-phenotype correlation in a North Indian patient cohort. Mol Vis. **16**, 2955-2963

Park, M., Li, Q., Shcheynikov, N., Zeng, W. and Muallem, S. (2004) NaBC1 is a ubiquitous electrogenic Na^+ -coupled borate transporter essential for cellular boron homeostasis and cell growth and proliferation. Mol. Cell. **16**, 331-341

Park, S. H., Jeong, H. J., Kim, M. and Kim, M. S. (2013) A Novel Nonsense Mutation of the SLC4A11 Gene in a Korean Patient With Autosomal Recessive Congenital Hereditary Endothelial Dystrophy. Cornea. **32**, e181-e182

Parker, M. D., Boron, W. F. and Tanner, M. J. (2002) Characterization of human "AE4" as an electroneutral sodium bicarbonate cotransporter. FASEB J. **16**, A796

Parker, M. D., Musa-Aziz, R., Rojas, J. D., Choi, I., Daly, C. M. and Boron, W. F. (2008) Characterization of human SLC4A10 as an electroneutral Na/HCO_3 cotransporter (NBCn2) with Cl^- self-exchange activity. J Biol Chem. **283**, 12777-12788

Parker, M. D., Ourmozdi, E. P. and Tanner, M. J. (2001) Human BTR1, a New Bicarbonate Transporter Superfamily Member and Human AE4 from Kidney. Biochem. Biophys. Res. Commun. **282**, 1103-1109

Pedemonte, N., Lukacs, G. L., Du, K., Caci, E., Zegarra-Moran, O., Galietta, L. J. and Verkman, A. S. (2005) Small-molecule correctors of defective DeltaF508-CFTR cellular processing identified by high-throughput screening. J Clin Invest. **115**, 2564-2571.

Perez, N. G., Alvarez, B. V., Camilion de Hurtado, M. C. and Cingolani, H. E. (1995) pHi regulation in myocardium of the spontaneously hypertensive rat. Compensated enhanced activity of the Na^+-H^+ exchanger. Circ Res. **77**, 1192-1200

Perrotta, S., Borriello, A., Scaloni, A., De Franceschi, L., Brunati, A. M., Turrini, F., Nigro, V., del Giudice, E. M., Nobili, B., Conte, M. L., Rossi, F., Iolascon, A., Donella-Deana, A., Zappia, V., Poggi, V., Anong, W., Low, P., Mohandas, N. and Della Ragione, F. (2005) The N-terminal 11 amino acids of human erythrocyte

band 3 are critical for aldolase binding and protein phosphorylation: implications for band 3 function. Blood. **106**, 4359-4366

Praetorius, J., Kim, Y. H., Bouzinova, E. V., Frische, S., Rojek, A., Aalkjaer, C. and Nielsen, S. (2004) NBCn1 is a basolateral Na^+-HCO_3^- cotransporter in rat kidney inner medullary collecting ducts. Am J Physiol Renal Physiol. **286**, F903-912

Praetorius, J., Nejsum, L. N. and Nielsen, S. (2004) A SLC4A10 gene product maps selectively to the basolateral plasma membrane of choroid plexus epithelial cells. Am J Physiol Cell Physiol. **286**, C601-610

Puangsricharern, V., Yeetong, P., Charumalai, C., Suphapeetiporn, K. and Shotelersuk, V. (2014) Two novel mutations including a large deletion of the SLC4A11 gene causing autosomal recessive hereditary endothelial dystrophy. British Journal of Ophthalmology. **98**, 1460-1462

Pushkin, A., Abuladze, N., Lee, I., Newman, D., Hwang, J. and Kurtz, I. (1999) Cloning, tissue distribution, genomic organization, and functional characterization of NBC3, a new member of the sodium bicarbonate cotransporter family. J. Biol. Chem. **274**, 16569-16575

Pushkin, A., Abuladze, N., Newman, D., Lee, I., Xu, G. and Kurtz, I. (2000) Cloning, characterization and chromosomal assignment of NBC4, a new member of the sodium bicarbonate cotransporter family. Biochim Biophys Acta. **1493**, 215-218

Quilty, J. A., Cordat, E. and Reithmeier, R. A. (2002) Impaired trafficking of human kidney anion exchanger (kAE1) caused by hetero-oligomer formation with a truncated mutant associated with distal renal tubular acidosis. Biochem J. **13**, 895-903

Ramprasad, V. L., Ebenezer, N. D., Aung, T., Rajagopal, R., Yong, V. H., Tuft, S. J., Viswanathan, D., El-Ashry, M. F., Liskova, P., Tan, D. T., Bhattacharya, S. S., Kumaramanickavel, G. and Vithana, E. N. (2007) Novel SLC4A11 mutations in patients with recessive congenital hereditary endothelial dystrophy (CHED2). Mutation in brief #958. Online. Hum. Mutat. **28**, 522-523

Riazuddin, S. A., McGlumphy, E. J., Yeo, W. S., Wang, J., Katsanis, N. and Gottsch, J. D. (2011) Replication of the TCF4 intronic variant in late-onset Fuchs corneal

dystrophy and evidence of independence from the FCD2 locus. Invest. Ophthalmol. Vis. Sci. **52**, 2825-2829

Riazuddin, S. A., Parker, D. S., McGlumphy, E. J., Oh, E. C., Iliff, B. W., Schmedt, T., Jurkunas, U., Schleif, R., Katsanis, N. and Gottsch, J. D. (2012) Mutations in LOXHD1, a recessive-deafness locus, cause dominant late-onset Fuchs corneal dystrophy. Am. J. Hum. Genet. **90**, 533-539

Riazuddin, S. A., Vithana, E. N., Seet, L. F., Liu, Y., Al-Saif, A., Koh, L. W., Heng, Y. M., Aung, T., Meadows, D. N., Eghrari, A. O., Gottsch, J. D. and Katsanis, N. (2010) Missense mutations in the sodium borate co-transporter SLC4A11 cause late onset Fuchs corneal dystrophy. Hum. Mutat. **31**, 1261-1268

Riazuddin, S. A., Zaghloul, N. A., Al-Saif, A., Davey, L., Diplas, B. H., Meadows, D. N., Eghrari, A. O., Minear, M. A., Li, Y. J., Klintworth, G. K., Afshari, N., Gregory, S. G., Gottsch, J. D. and Katsanis, N. (2010) Missense mutations in TCF8 cause late-onset Fuchs corneal dystrophy and interact with FCD4 on chromosome 9p. Am. J. Hum. Genet. **86**, 45-53

Ribeiro, M. L., Alloisio, N., Almeida, H., Gomes, C., Texier, P., Lemos, C., Mimoso, G., Morle, L., Bey-Cabet, F., Rudigoz, R. C., Delaunay, J. and Tamagnini, G. (2000) Severe hereditary spherocytosis and distal renal tubular acidosis associated with the total absence of band 3. Blood. **96**, 1602-1604

Riordan, J. R. (2008) CFTR function and prospects for therapy. Annu Rev Biochem. **77**, 701-726

Riordan, J. R., Rommens, J. M., Kerem, B., Alon, N., Rozmahel, R., Grzelczak, Z., Zielenski, J., Lok, S., Plavsic, N., Chou, J. L., Drumm, M. L., Iannuzzi, M. C., Collins, F. S. and Tsui, L. C. (1989) Identification of the cystic fibrosis gene: cloning and characterization of complementary DNA. Science. **245**, 1066-1073

Robert, R., Carlile, G. W., Liao, J., Balghi, H., Lesimple, P., Liu, N., Kus, B., Rotin, D., Wilke, M., de Jonge, H. R., Scholte, B. J., Thomas, D. Y. and Hanrahan, J. W. (2010) Correction of the Delta phe508 cystic fibrosis transmembrane conductance regulator trafficking defect by the bioavailable compound glafenine. Mol Pharmacol. **77**, 922-930

Romero, M. F., Chen, A.-P., Parker, M. D. and Boron, W. F. (2013) The SLC4 Family of Bicarbonate (HCO_3^-) Transporters. Molecular aspects of medicine. **34**, 159-182

Romero, M. F., Fulton, C. M. and Boron, W. F. (2004) The SLC4 family of HCO_3^- transporters. Pflugers Arch. **447**, 496-509

Romero, M. F., Hediger, M. A., Boulpaep, E. L. and Boron, W. F. (1997) Expression cloning and characterization of a renal electrogenic Na^+/HCO_3^- cotransporter. Nature. **387**, 409-413

Romero, M. F., Henry, D., Nelson, S., Harte, P. J., Dillon, A. K. and Sciortino, C. M. (2000) Cloning and characterization of a Na^+ driven anion exchanger (NDAE1): a new bicarbonate transporter. J. Biol. Chem. **275**, 24552-24559

Ruberti, J. W., Sinha Roy, A. and Roberts, C. J. (2011) Corneal Biomechanics and Biomaterials. Annual Review of Biomedical Engineering. **13**, 269-295

Ruetz, S., Lindsey, A. E., Ward, C. L. and Kopito, R. R. (1993) Functional activation of plasma membrane anion exchangers occurs in a pre-Golgi compartment. J. Cell Biol. **121**, 37-48

Sander, T., Toliat, M. R., Heils, A., Leschik, G., Becker, C., Ruschendorf, F., Rohde, K., Mundlos, S. and Nurnberg, P. (2002) Association of the 867Asp variant of the human anion exchanger 3 gene with common subtypes of idiopathic generalized epilepsy. Epilepsy Res. **51**, 249-255

Sassani, P., Pushkin, A., Gross, E., Gomer, A., Abuladze, N., Dukkipati, R., Carpenito, G. and Kurtz, I. (2002) Functional characterization of NBC4: a new electrogenic sodium-bicarbonate cotransporter. Am J Physiol Cell Physiol. **282**, C408-416

Schey, K. L., Wang, Z., L. Wenke, J. and Qi, Y. (2014) Aquaporins in the eye: Expression, function, and roles in ocular disease. Biochimica et Biophysica Acta (BBA) - General Subjects. **1840**, 1513-1523

Schmedt, T., Silva, M. M., Ziaei, A. and Jurkunas, U. (2012) Molecular bases of corneal endothelial dystrophies. Experimental Eye Research. **95**, 24-34

Scott, R. L. P. and Cannon, B. D. P. (2015) Ophthalmology. Magill's Medical Guide (Online Edition)

Sebat, J., Lakshmi, B., Malhotra, D., Troge, J., Lese-Martin, C., Walsh, T., Yamrom, B., Yoon, S., Krasnitz, A., Kendall, J., Leotta, A., Pai, D., Zhang, R., Lee, Y.-H.,

Hicks, J., Spence, S. J., Lee, A. T., Puura, K., Lehtimäki, T., Ledbetter, D., Gregersen, P. K., Bregman, J., Sutcliffe, J. S., Jobanputra, V., Chung, W., Warburton, D., King, M.-C., Skuse, D., Geschwind, D. H., Gilliam, T. C., Ye, K. and Wigler, M. (2007) Strong Association of De Novo Copy Number Mutations with Autism. Science (New York, N.Y.). **316**, 445-449

Shah, S. S., Al-Rajhi, A., Brandt, J. D., Mannis, M. J., Roos, B., Sheffield, V. C., Syed, N. A., Stone, E. M. and Fingert, J. H. (2008) Mutation in the SLC4A11 gene associated with autosomal recessive congenital hereditary endothelial dystrophy in a large Saudi family. Ophthalmic Genet. **29**, 41-45

Shayakul, C. and Alper, S. L. (2000) Inherited renal tubular acidosis. Current opinion in nephrology and hypertension. **9**, 541-546

Shnitsar, V., Li, J., Li, X., Calmettes, C., Basu, A., Casey, J. R., Moraes, T. F. and Reithmeier, R. A. F. (2013) A Substrate Access Tunnel in the Cytosolic Domain Is Not an Essential Feature of the Solute Carrier 4 (SLC4) Family of Bicarbonate Transporters. Journal of Biological Chemistry. **288**, 33848-33860

Smith, P. K., Krohn, R. I., Hermanson, G. T., Mallia, A. K., Gartner, F. H., Provenzano, M. D., Fujimoto, E. K., Goeke, N. M., Olson, B. J. and Klenk, D. C. (1985) Measurement of protein using bicinchoninic acid. Anal. Biochem. **150**, 76-85

Soumittra, N., Loganathan, S. K., Madhavan, D., Ramprasad, V. L., Arokiasamy, T., Sumathi, S., Karthiyayini, T., Rachapalli, S. R., Kumaramanickavel, G., Casey, J. R. and Rajagopal, R. (2014) Biosynthetic and functional defects in newly identified SLC4A11 mutants and absence of COL8A2 mutations in Fuchs endothelial corneal dystrophy. J Hum Genet. **59**, 444-453

Stehouwer, M., Bijlsma, W. R. and Van der Lelij, A. (2011) Hearing disability in patients with Fuchs' endothelial corneal dystrophy: unrecognized co-pathology? Clin. Ophthalmol. **5**, 1297-1301

Sultana, A., Garg, P., Ramamurthy, B., Vemuganti, G. K. and Kannabiran, C. (2007) Mutational spectrum of the SLC4A11 gene in autosomal recessive congenital hereditary endothelial dystrophy. Mol Vis. **13**, 1327-1332

Sun, X. C. and Bonanno, J. A. (2003) Identification and cloning of the Na/HCO_3^- cotransporter (NBC) in human corneal endothelium. Exp Eye Res. **77**, 287-295

Takano, J., Noguchi, K., Yasumori, M., Kobayashi, M., Gajdos, Z., Miwa, K., Hayashi, H., Yoneyama, T. and Fujiwara, T. (2002) Arabidopsis boron transporter for xylem loading. Nature. **420**, 337-340.

Tan, L., Cai, Z. Q. and Lai, N. S. (2009) Accuracy and sensitivity of the dynamic ocular thermography and inter-subjects ocular surface temperature (OST) in Chinese young adults. Cont Lens Anterior Eye. **32**, 78-83.

Toye, A. M., Williamson, R. C., Khanfar, M., Bader-Meunier, B., Cynober, T., Thibault, M., Tchernia, G., Déchaux, M., Delaunay, J. and Bruce, L. J. (2008) Band 3 Courcouronnes (Ser667Phe): a trafficking mutant differentially rescued by wild-type band 3 and glycophorin A

Tsien, R. Y. (1998) The Green Fluorescent Protein. Annual Review of Biochemistry. **67**, 509-544

Tsuganezawa, H., Kobayashi, K., Iyori, M., Araki, T., Koizumi, A., Watanabe, S. I., Kaneko, A., Fukao, T., Monkawa, T., Yoshida, T., Kim, D. K., Kanai, Y., Endou, H., Hayashi, M. and Saruta, T. (2001) A new member of the HCO_3^- transporter superfamily is an apical anion exchanger of beta-intercalated cells in the kidney. J Biol Chem. **276**, 8180-8189

Tuft, S. J. and Coster, D. J. (1990) The corneal endothelium. Eye. **4**, 389-424

Vilas, G. L., Johnson, D. E., Freund, P. and Casey, J. R. (2009) Characterization of an epilepsy-associated variant of the human Cl^-/HCO_3^- exchanger AE3. American Journal of Physiology. Cell physiology. **297**, C526-536

Vilas, G. L., Loganathan, S. K., Liu, J., Riau, A. K., Young, J. D., Mehta, J. S., Vithana, E. N. and Casey, J. R. (2013) Transmembrane water-flux through SLC4A11: a route defective in genetic corneal diseases. Human Molecular Genetics. **22**, 4579-4590

Vilas, G. L., Loganathan, S., Quon, A., Sundaresan, P., Vithana, E. N. and Casey, J. R. (2012) Oligomerization of SLC4A11 protein and the severity of FECD and CHED2 corneal dystrophies caused by SLC4A11 mutations. Human Mutation. **33**, 419-428

Vilas, G. L., Morgan, P. E., Loganathan, S., Quon, A. and Casey, J. R. (2011) Biochemical Framework for SLC4A11, the Plasma Membrane Protein Defective in Corneal Dystrophies. Biochemistry. **50**, 2157-2169

Vilas, G., Krishnan, D., Loganathan, S. K., Malhotra, D., Liu, L., Beggs, M. R., Gena, P., Calamita, G., Jung, M., Zimmermann, R., Tamma, G., Casey, J. R. and Alexander, R. T. (2015) Increased water flux induced by an aquaporin-1/carbonic anhydrase II interaction. Molecular Biology of the Cell. **26**, 1106-1118

Vincent, A. L. (2014) Corneal dystrophies and genetics in the International Committee for Classification of Corneal Dystrophies era: a review. Clinical & Experimental Ophthalmology. **42**, 4-12

Virkki, L. V., Wilson, D. A., Vaughan-Jones, R. D. and Boron, W. F. (2002) Functional characterization of human NBC4 as an electrogenic Na^+-HCO_3^- cotransporter (NBCe2). Am J Physiol Cell Physiol. **282**, C1278-1289

Vithana, E. N., Morgan, P. E., Ramprasad, V., Tan, D. T., Yong, V. H., Venkataraman, D., Venkatraman, A., Yam, G. H., Nagasamy, S., Law, R. W., Rajagopal, R., Pang, C. P., Kumaramanickevel, G., Casey, J. R. and Aung, T. (2008) SLC4A11 Mutations in Fuchs Endothelial Corneal Dystrophy (FECD). Hum. Mol. Genet. **17**, 656-666

Vithana, E. N., Morgan, P., Sundaresan, P., Ebenezer, N. D., Tan, D. T., Mohamed, M. D., Anand, S., Khine, K. O., Venkataraman, D., Yong, V. H., Salto-Tellez, M., Venkatraman, A., Guo, K., Hemadevi, B., Srinivasan, M., Prajna, V., Khine, M., Casey, J. R., Inglehearn, C. F. and Aung, T. (2006) Mutations in sodium-borate cotransporter SLC4A11 cause recessive congenital hereditary endothelial dystrophy (CHED2). Nature Genetics. **38**, 755-757

Wain, H. M., Lush, M. J., Ducluzeau, F., Khodiyar, V. K. and Povey, S. (2004) Genew: the Human Gene Nomenclature Database, 2004 updates. Nucleic Acids Res. **32**, D255-257

Wang, C. Z., Yano, H., Nagashima, K. and Seino, S. (2000) The Na^+-driven Cl^-/HCO_3^- exchanger: Cloning, tissue distribution, and functional characterization. J Biol Chem. **275**, 35486-35490

Wang, D. N. (1994) Band 3 protein: structure, flexibility and function. FEBS Lett. **346**, 26-31.

Wang, Y., Bartlett, M. C., Loo, T. W. and Clarke, D. M. (2006) Specific rescue of cystic fibrosis transmembrane conductance regulator processing mutants using pharmacological chaperones. Mol Pharmacol. **70**, 297-302.

Wang, Z., Conforti, L., Petrovic, S., Amlal, H., Burnham, C. E. and Soleimani, M. (2001) Mouse Na^+: HCO_3^- cotransporter isoform NBC-3 (kNBC-3): cloning, expression, and renal distribution. Kidney Int. **59**, 1405-1414

White, M. J., DiCaprio, M. J. and Greenberg, D. A. (1996) Assessment of neuronal viability with Alamar blue in cortical and granule cell cultures. Journal of Neuroscience Methods. **70**, 195-200

Whittemore, E. R., Loo, D. T., Watt, J. A. and Cotmans, C. W. (1995) A detailed analysis of hydrogen peroxide-induced cell death in primary neuronal culture. Neuroscience. **67**, 921-932

Wiley, L., SundarRaj, N., Sun, T. T. and Thoft, R. A. (1991) Regional heterogeneity in human corneal and limbal epithelia: an immunohistochemical evaluation. Investigative Ophthalmology & Visual Science. **32**, 594-602

Xu, C., Bailly-Maitre, B. and Reed, J. C. (2005) Endoplasmic reticulum stress: cell life and death decisions. The Journal of Clinical Investigation. **115**, 2656-2664

Xu, J., Wang, Z., Barone, S., Petrovic, M., Amlal, H., Conforti, L., Petrovic, S. and Soleimani, M. (2003) Expression of the Na^+-HCO_3^- cotransporter NBC4 in rat kidney and characterization of a novel NBC4 variant. Am J Physiol Renal Physiol. **284**, F41-50

Zhang, D., Kiyatkin, A., Bolin, J. T. and Low, P. S. (2000) Crystallographic structure and functional interpretation of the cytoplasmic domain of erythrocyte membrane band 3. Blood. **96**, 2925-2933

Zhang, J. and Patel, D. V. (2015) The pathophysiology of Fuchs' endothelial dystrophy – A review of molecular and cellular insights. Experimental Eye Research. **130**, 97-105

Zhang, W., Fujii, N. and Naren, A. P. (2012) Recent advances and new perspectives in targeting CFTR for therapy of cystic fibrosis and enterotoxin-induced secretory diarrheas. Future Medicinal Chemistry. **4**, 329-345